Interpretation of long-term measurements of radiatively active trace gases and ozone depleting substances (Part 1 of 3)

DECC contract numbers: GA1103 and GA0201

Date: March 2011

University of Bristol: Simon O'Doherty, Peter Simmonds, Aoife Grant

Met Office: Alistair J. Manning, Maria Athanassiadou

Contents

1 Introduction

Monitoring of atmospheric concentrations of gases is important in assessing the impact of international policies related to the atmospheric environment. The effects of control measures on chlorofluorocarbons (CFCs), halons and HCFCs introduced under the 'Montreal Protocol of Substances that Deplete the Ozone Layer' are now being observed. Continued monitoring is required to assess the overall success of the Protocol and the implication for atmospheric levels of replacement compounds such as HFCs. Similar analysis of gases regulated by the Kyoto Protocol on greenhouse gases will likewise assist policy makers.

Since 1987, high-frequency, real time measurements of the principal halocarbons and radiatively active trace gases have been made as part of the Global Atmospheric Gases Experiment (GAGE) and Advanced Global Atmospheric Gases Experiment (AGAGE) at Mace Head, County Galway, Ireland. For much of the time, the measurement station, which is situated on the Atlantic coast, monitors clean westerly air that has travelled across the North Atlantic Ocean. However, when the winds have an easterly component, Mace Head receives substantial regional scale pollution in air that has travelled from the industrial regions of Europe. The site is therefore uniquely situated to record trace gas concentrations associated with both the mid-latitude Northern Hemisphere background levels and with the more polluted air arising from Europe.

The Met Office's Lagrangian atmospheric dispersion model, NAME (**N**umerical **A**tmospheric dispersion **M**odelling **E**nvironment), has been run for each 3-hour period of each year from 1989 so as to understand the recent history of the air arriving at Mace Head at the time of each observation. By identifying when the air is unpolluted at Mace Head, i.e. when the air has travelled across the Atlantic and the air concentration reflects the mid-latitude Northern Hemisphere baseline value, the data collected have been used to estimate baseline concentrations, trends and seasonal cycles of a wide range of ozone-depleting and greenhouse gases for the period 1990-2010 inclusive.

By removing the underlying baseline trends from the observations and by modelling the recent history of the air on a regional scale, estimates of UK, Irish and North West European (UK, Ireland, France, Germany, Denmark, the Netherlands, Belgium, Luxembourg) emissions and their geographical distributions have been made using the NAME-Inversion method. The estimates are presented as yearly averages and are compared to UNFCCC and other inventories where available.

The atmospheric measurements and emission estimates of greenhouse gases provide an important cross-check for the emissions inventories submitted to the United Nations Framework Convention on Climate Change (UNFCCC). This verification work is consistent with good practice guidance issued by the Intergovernmental Panel on Climate Change (IPCC).

1.1 Work Programme

1.1.1 Compliance with the Montreal Protocol

a) Analyse and update annually global baseline atmospheric concentration trends and European emissions of the gases controlled by the Montreal Protocol. Comparisons should be made with production and consumption figures provided by industry to the EU if trends are unexpected.

The NAME dispersion model has been used as the primary tool to understand the observations. The latest version of NAME has been run in backwards-in-time mode to understand the history of the air arriving at the Mace Head (and other observation stations) for each three-hour period of observation from Jan. 1989 until Jan. 2011. The geographical domain of these new model runs was extended to include the eastern half of North America to better describe the recent history of the air reaching Mace Head.

The NAME air history maps have been used to estimate the baseline concentrations of each gas measured at Mace Head, where baseline means representative of the mid-latitude Northern Hemisphere well-mixed concentration. The results of this analysis are presented in chapter 3, where the monthly and annual baseline concentrations for each gas are presented along with the time-varying baseline growth rates and average seasonal cycle.

The NAME-Inversion method has been employed to estimate UK, Irish and North West European emissions for each gas measured at Mace Head and the results are presented in chapter 4. Where possible the NAME-Inversion estimates have been compared with UNFCCC and EDGAR emission estimates. The NW European emissions can be scaled up by population to an EU-15 estimate. The countries covered by NW Europe are Ireland, UK, France, Germany, Belgium, Luxembourg, the Netherlands and Denmark and contain 62.8% of the population of the EU-15 countries. The inversion method uses the NAME model in conjunction with the Mace Head measurements and the simulated annealing best-fit technique to derive emission estimates and is explained in chapter 4.

Various aspects of the inversion process have been improved and are described in chapter 4 and [*Manning et al, 2011*]:

- The definition of baseline observations and how they are extrapolated to estimate baseline concentrations and seasonal cycles have been reviewed and improved.
- The method of grouping grid boxes together to assist the inversion process has also undergone significant revision.
- Switching from a normal distribution to a log-normal distribution improved the quantification of uncertainty in the inversion emission estimates. The old method introduced a small positive bias in the emission estimates.

b) Identify departure from expected trends in concentration and emissions of gases controlled by the Montreal Protocol and identify causes of these variations.

The measurement record at Mace Head for some gases is now over 20 years long and so it is possible, using the baseline trends and seasonal cycles estimated for previous years, to recognise departures from what is expected. In chapter 3 the baseline concentrations of each gas are considered separately and any changes from the longer term average are noted and commented on. Similarly in chapter 4 the regional emissions of each gas are considered and discussed. Points of particular note are highlighted.

c) Identify any additional sources of data for monitoring progress under the Montreal Protocol.

Additional observations of some compounds were made at Carnsore Point on the East Coast of Ireland between 2006 and 2010. Additional inversions were performed incorporating these extra data and are presented in chapter 4 together with the Mace Head-only estimates.

1.1.2 Verification of greenhouse gas emissions

d) Assess and report concentrations of direct and indirect greenhouse gases measured at Mace Head and other sites.

The methodology described above in section 1.1.1(a) has been applied to direct and indirect greenhouse gases. In chapter 3, annual and monthly baseline concentrations at Mace Head are presented for each

gas individually. The growth rate and average seasonal cycle of the baseline concentrations are also reported.

e) Identify and assess the reasons for any departure from expected trends in concentrations.

In 2007/08 there was a global rise in methane that is clearly shown in the Mace Head record. The reason for this significant rise is considered to be a combination of increased Arctic emissions in 2007 and increased tropical emissions in 2007/08. In late 2008 the rate of growth in methane baseline concentrations returned to a value close to the decadal average. Nitrous oxide and carbon dioxide baseline levels continue to rise. There were no significant changes to the baseline concentrations of either hydrogen or carbon monoxide. More details of these and other GHGs are presented in chapter 3.

f) Make and update annually estimates of European (EU 15 and, where possible the EU25) and UK emissions of direct and indirect greenhouse gases and provide comparisons with the National Atmospheric Emissions Inventory (NAEI), the UK Greenhouse Gas Inventory (UKGHGI), the European Monitoring and Evaluation Programme (EMEP), the European Environment Agency (EEA) emissions inventories and anything reported to the EU, e.g. under the Emissions Trading Scheme. Any discrepancies with emissions inventories should be highlighted and discussed.

The methodology described above in section 1.1.1(a) has been applied to the direct and indirect greenhouse gases measured at Mace Head. For methane and nitrous oxide, data from other measurement stations have also been used (see chapter 5). Annual UK and NW European emission estimates using Mace Head observations have been presented in chapter 4 for each gas. Where data are available these estimates have been compared to those reported elsewhere, e.g. UNFCCC, EDGAR and EMEP, and any discrepancies have been highlighted and discussed. Due to the significant biogenic emissions and sinks of CO_2, the anthropogenic-only emissions of CO_2 have been estimated using only wintertime observations. To ensure sufficient observations the inversion estimates for CO_2 therefore span five rather than two years.

1.1.3 Other tasks

g) Identify new ozone depleting or global warming substances of potential policy interest, and provide details to Defra.

Under this work programme item, resources have been spent in discussion with the Met Office and the University of Bristol on the identification of new ozone-depleting or global warming substances of potential policy interest from reviewing the available literature. A number of new substances have been identified, as follows:

1. NF_3

This substance is used in semi-conductor manufacture and has a GWP of 17,700.

2. New HFCs: HFC-152, -161, -236cb, -236ea, -245fa, -365mfc, -1234ze.

Several of these novel HFCs are proposed as alternative foam blowing agents.

3. SF_5CF_3, trifluoromethyl sulphur pentaflouride

This is breakdown product of SF_6 from spark discharges in high voltage equipment. It has a GWP of 17,700.

4. Perfluorodecalin

Perfluorodecalin, $C_{10}F_{18}$ is a PFC. It is used as a human blood replacement because of its peculiar property of dissolving oxygen. It has a GWP of 7,500.

5. HFEs (Industrial terminology for new HFCs)

Hydrofluorinated ethers such as HFC-43-10mee are solvents. GWPs for HFEs range from 11 – 14,900.

6. Perfluoropolyethers

Perfluoropoly methyl isopropyl ethers PFPMIE have a GWP of 10,300 and are potential cleaning agents and fire extinguishers.

h) Identify any gaps in existing data from Mace Head and other sites that could potentially be of policy relevance.

Bromoform ($CHBr_3$) and dibromomethane (CH_2Br_2) are now measured at Mace Head and are not reported here for the first time. From preliminary analysis it appears that the dominant sources of emission are along the coast and therefore are most probably naturally occurring emissions from seaweed. This supports our current understanding of these gases.

i) Liaise with Hadley Centre over 3D atmospheric chemistry modelling being carried out at the Hadley Centre and provide data for model validation purposes, if required.

The monthly time-series of baseline concentrations and average seasonal cycles of all of the gases measured at Mace Head have been provided to the Hadley Centre. In the next stage of the contract the annual gradients of baseline concentrations and reported atmospheric lifetimes of some key gases will be used to approximate global emission estimates of each gas.

j) Investigate the use that could be made of new or additional sources of data such as isotope measurements or flux data, in conjunction with data from Mace Head or from any other sites that could potentially be of policy relevance, for verifying GHG emissions.

For methane and nitrous oxide, measurement data have been collected for 2006 and 2007 from up to 11 high-frequency monitoring stations across Europe and have been used to estimate European emissions. This work has been performed in conjunction with the European FP6 project NitroEurope. The results are presented in chapter 5.

k) Investigate the potential and feasibility for further expanding the policy relevance of Mace Head or any other potential sites data, by considering other classes of atmospheric trace gases such as hydrocarbons, oxygenated species, perfluorocarbons, very long lived molecules, and oxygen concentrations.

Resources have been given to the analysis and interpretation of the measurements of a number of hydrocarbon species at Mace Head. The MEDUSA equipment at Mace Head has been altered so that it can record the observations of a number of light hydrocarbons from ethane to the xylenes. Calibration standards have been employed to put the observations onto an absolute scale and data have been collected from 2005 onwards.

Continuous high-frequency in-situ measurements of a range of non-methane hydrocarbons have been made at Mace Head since January 2005. Mace Head is a background Northern Hemispheric site situated on the eastern edge of the Atlantic. Five years of measurements (2005-2009) of eleven non-methane hydrocarbons, namely C2-C5 alkanes, benzene, toluene, ethyl-benzene and the xylenes, have been separated into baseline Northern Hemispheric and European polluted air masses, among other sectors. Seasonal cycles in baseline Northern Hemispheric air masses and European polluted air masses arriving at Mace Head have been studied and reported. Baseline air masses show a broad summer minima between June and September for shorter lived species, longer lived species show summer minima in July/August. All species displayed a winter maxima in February. This seasonal cycle results from the combination of two influences. The main removal process for the VOCs is reaction with hydroxyl OH radicals which is faster in the summer compared with the winter. Also transport times are faster in the winter than in the summer. The combination of this means that Mace Head is more polluted in the winter than in the summer. European air masses showed baseline elevated mole fractions for all non-methane hydrocarbons, largest elevations (of up to 370 ppt) from baseline data were observed in winter maxima, with smaller elevations observed during the summer. Analysis of temporal trends using the Mann-Kendall test showed small (< 6%/year) but statistically significant decreases in the butanes, i-pentane and o-xylene between 2005 and 2009 in European air. Toluene was found to have an increasing trend of 34%/year in European air. No significant trends were found for any species in baseline air. From January to June of 2008 elevations of all C2-C5 non-methane hydrocarbons in baseline air were observed.

The observed seasonal cycles of a selection of reactive hydrocarbons and halocarbons in baseline air masses at Mace Head, Ireland are consistent with a simple picture of largely man-made sources and oxidation by hydroxyl (OH) radicals. As a result, the observed seasonal cycles become more pronounced the more reactive the species are based on their OH-reaction rate coefficients. For the pentanes, the assumption of little wintertime removal breaks down, leading to an apparent dampening of the seasonal cycles relative to ethane, propane and the butanes. A global chemistry-transport model is used to describe the seasonal cycles of the hydrocarbons and halocarbons at Mace Head, based on reasonable estimates of the man-made emission source strengths. The model derived OH concentrations in baseline air masses required to support the observed seasonal cycles of the hydrocarbons and halocarbons averaged 1.38 ± 1.1 x 106 molecule cm-3, with peak daytime levels during summertime of 1.2 x 107 molecule cm-3.

In collaboration with the GKSS Institute in Hamburg, Germany, a study has been made of the concentrations of total gaseous mercury in baseline air masses arriving at Mace Head, Ireland after having traversed the thousands of kilometres uninterrupted fetch of the North Atlantic Ocean. Over a 14-year period, a statistically significant negative (downwards) trend of -0.028 ± 0.01 ng m-3 yr-1, representing a trend of 1.6 – 2.0% per year, has been detected in the total gaseous mercury levels in these baseline air masses. These findings are set in the context of the available literature studies of atmospheric Hg trends.

l) Provide advice, as requested by Defra, on the relative roles of radiatively active trace gases in forcing climate change and, where possible, compute global warming potentials (GWPs) for any new substances identified.

No advice was sought by DECC.

Resources under this programme item have been used to study the seasonal and spatial dependence of the radiative forcing of climate by aircraft NOx emissions.

The global three-dimensional Lagrangian chemistry-transport model STOCHEM has been used to follow changes in the tropospheric distributions of methane CH4 and ozone O3 following the emission of pulses of the oxides of nitrogen NOx from aircraft exhausts. Results were presented from 112 one year integrations of a global chemistry-transport model: a base case, then variants with extra cruise altitude aircraft nitrogen oxide (NOx) emissions added to specific regions in the first month. The NOx stimulates ozone (O3) production and methane (CH4) destruction. The response varies spatially: the most sensitive regions are those with lowest background NOx. Integrated radiative forcings (IRF) over a 100 year time horizon are calculated. Net (O3 + CH4) IRFs are generally negative, although this result is model-dependent. The global average net IRF for aviation NOx, weighted by emissions, is -1.9 mW m-2 yr-1 (Tg NO2)-1. The positive IRF associated with a short-term increase in O3 (4.1 mW m-2 yr-1 (Tg NO2)-1) is more than overwhelmed by effects of the long-term decrease in CH4. Aircraft NOx net IRFs are spatially variable, with local values over the remote Pacific approximately balancing the IRF associated with aviation CO2 emissions (28 mW m-2 yr-1 (Tg NO2)-1). The overall climate impact of global aviation is often represented by a single number, used as a multiplier for CO2 emissions. This is clearly inappropriate.

m) Report on developments in the understanding of anthropogenic and natural sources and sinks of carbon dioxide, methane and nitrous oxide, using seasonal trends in emissions and analysis of annual trends.

Resources under this programme item have been used to develop a simple box model that can be used to derive estimates of methane emissions and hydrogen and ozone uptakes to and from the local peat-bogs around the Mace Head site.

Methane emissions from the peat bogs in Connemara, Ireland have been inferred from the trace gas observations at the Mace Head Atmospheric Research Station using the nocturnal box method. A total of 237 local events, during April to September, over a 12-year period have been studied. Simultaneous emissions of methane, carbon dioxide and chloroform are routinely observed under nocturnal inversions with low wind speeds from the peat bogs proximal to Mace Head. Night-time deposition of ozone and hydrogen occur concurrently with these emissions. Using the temporally correlated methane and ozone data we estimate methane emissions from each event. Simultaneous methane and chloroform emissions, together with ozone and hydrogen deposition have been characterised, leading to the estimation of methane emission rates for each event. The mean methane emission flux was found to be 400 ± 90 ng m^{-2} s^{-1}. A strong seasonal cycle was found in the methane emission fluxes but there was little evidence of a long-term trend in the emissions from the peat bogs in the vicinity of the Mace Head station.

During stable nocturnal inversions with low wind speeds we observed strong depletions of both hydrogen and ozone caused by deposition to the peat bogs in the vicinity of the Mace Head Atmospheric Research Station, Connemara, County Galway, Ireland. From these temporally correlated fluxes and using a simple box model we have estimated the strength of the molecular hydrogen soil sink over a 14-year period (1995-2008). Over this entire period 269 nocturnal deposition events were identified that satisfied the strict selection criteria. The average hydrogen deposition velocity determined from these events was 0.53 mm s^{-1}, covering a range of 0.18-1.29 mm s^{-1}, which is in agreement with the range of deposition velocities reported in the literature for similar peaty biomes. By annually averaging all of the nocturnal inversion events over the most seasonally active period from April-September we reveal a positive correlation with ambient temperature in the relative deposition velocities of hydrogen and ozone, which is not readily apparent in all of the individual events. Furthermore, average hydrogen deposition velocities and accumulated rainfall from 48 hrs before and during each event were to a reasonable extent anti-correlated. However, due to the large uncertainties in determining monthly mean H_2 deposition velocities there is no statistically significant trend in the hydrogen deposition velocities over time.

Simultaneous chloroform ($CHCl_3$) emission and ozone (O_3) deposition are regularly observed under nocturnal inversions during the summer months from and to the peat bogs in the vicinity of the Mace Head Atmospheric Research Station, Connemara, Co Galway, Ireland. Emissions were estimated using the nocturnal box model applied to routine atmospheric observations collected over a 14 year period from 1995-2008. Strict criteria were applied in the selection of events of low wind speed, under a stable night-time inversion layer in baseline air conditions, with no transport from Europe. The mean peatland $CHCl_3$ flux was 2.91 µg m^{-2} hr^{-1} with highly variable fluxes ranging from 0.44-12.94 µg m^{-2} hr^{-1}. These fluxes are generally larger than those reported previously for similar biomes and if correct would make a significant contribution to the global estimated source of $CHCl_3$. Fluxes were not strongly correlated with either atmospheric temperature or the level of precipitation. Over the 14-year period there appears to have been a small increase in overall $CHCl_3$ emissions, although we stress that the nocturnal box model has a number of limitations and assumptions which should be taken into account.

UK and NW European emission estimates have been made using the NAME-inversion method for nitrous oxide and methane for each year 1990-2010. 3D meteorology from the ECMWF re-analysis project has been used from 1990 – 2007 and compared with those estimated using Met Office meteorological data (1995-2008). For the standard inversions ECMWF data are used 1990-2002 and Met Office data used from 2003-2010.

Winter-only emission maps for carbon dioxide have been calculated to estimate the UK and European anthropogenic emissions, see Chapter 4.

n) Compare data from Mace Head and other sites that could potentially be of policy relevance, with data from other national and international studies, where appropriate.

For HFC-125 the NAME-inversion emission estimates for NW Europe, Australia and the USA have been compared to a range of other inventories. The results of this analysis have been published (2009) in a paper led by Dr. Simon O'Doherty of the University of Bristol (O'Doherty S, Cunnold, D.M Miller, B.R., Mühle, J. McCulloch, A. Simmonds, P.G. Manning, A.J. Reimann, S. Vollmer, M.K. Greally, B.R. Prinn, R.G. Fraser, P.J. Steele, L.P. Krummel P.B., Dunse, B.L. Porter, L.W. Lunder, C.R. Schmidbauer, N. Hermansen, O. Salameh, P.K. Harth, C.M. Wang R.H.J. and Weiss R.F., Global and regional emissions of HFC-125 (CHF_2CF_3) from in situ and air archive atmospheric observations at AGAGE and SOGE observatories J. Geophys. Res., J. Geophys. Res., 114, D23304, 2009).

o) Provide assistance and advice to the WMO-UNEP Ozone Layer Assessment Report and to the European Union, as requested by Defra, on validation of European and national-level trace gas emission inventories, and on monitoring compliance with international protocols and agreements or other research conducted for the contract.

Contributions have been provided for the verification chapters of the UK UNFCCC submission 2009, 2010 and 2011. A review of chapter one of the latest WMO-UNEP Ozone Layer Assessment Report was requested by the authors and duly submitted in March 2010. Resources under this work programme item were used to act as a Reviewer for Chapter 5 of the 2010 WMO-UNEP Ozone Layer Assessment Report.

p) Update the Tables: "Equivalent chlorine loadings from ozone depleting substances and greenhouse gases"[1] and “Atmospheric concentrations of major man-made ozone-depleting substances at Mace Head” in Defra’s Digest of Environmental Statistics, on an annual basis. Should any other sites become potentially of policy relevance, similar updated tables shall be produced.

A table with mid-latitude northern hemisphere baseline trace gas concentrations as derived from Mace Head observations and their respective chlorine or bromine contents can be compiled and supplied in the correct format whenever required. The equivalent chlorine loading value per species can also be estimated and submitted to the department in the correct format if required.

q) Ensure information-exchange and coordination with complementary European Union projects on verification of greenhouse gas emissions, for example CarboEurope, NitroEurope, IPCC reports, guidelines or studies, and attend inverse-modelling workshops arranged under the auspices of the EU Monitoring Mechanism.

The Met Office has been an active member of both the NITROEUROPE and EUROHYDROS European funded programmes attending annual meetings in both. The authors have maintained close links with the CarboEurope programme through Met Office and University of Edinburgh involvement. The Met Office has also attended several meetings to discuss new proposals such as ICOS (Integrated Carbon Observing System) and NERC funding of new observations.

r) Make provision for up to 10 days’ ad-hoc policy support to Defra’s Climate, Energy and Ozone: Science and Analysis (CEOSA) Division.

The Met Office attended two ICOS meetings, a workshop on agricultural emissions, two NISC meetings and presented work at a Royal Society event on Greenhouse Gases. Alistair Manning also presented his work at the IPCC workshop on uncertainty in Utrecht, The Netherlands in March.

s) Provide a summary report, as required and not more than once annually, to be included in the (CEOSA) Research Programme Annual Report, of 2-4 pages, summarising work undertaken, main results and policy-relevant conclusions (graphics should be provided in accessible format, to be agreed with (CEOSA) Division).

No activity was required under this work item.

1.2 Publications

O'Doherty, S. and Carpenter, L. J., '*Volatile halogenated compounds' in Koppman R. (ed), Volatile Organic Compounds in the Atmosphere, Blackwell Ltd, London, 2007.*

Miller, B. R., R. F. Weiss, P. K. Salameh, T. Tanhua, B. R. Greally, J. Muhle, P. G. Simmonds, *Medusa: A Sample Preconcentration and GC/MS Detector System for in Situ Measurements of Atmospheric Trace Halocarbons, Hydrocarbons, and Sulfur Compounds, Anal. Chem., ASAP Article; doi: 10.1021/ac702084k, 2008*

Abstract: Significant changes have occurred in the anthropogenic emissions of many compounds related to the Kyoto and Montreal Protocols within the past 20 years and many of their atmospheric abundances have responded dramatically. Additionally, there are a number of related natural compounds with underdetermined source or sink budgets. A new instrument, Medusa, was developed to make the high frequency in situ measurements required for the determination of the atmospheric lifetimes and emissions of these compounds. This automated system measures a wide range of halocarbons, hydrocarbons, and sulfur compounds involved in ozone depletion and/or climate forcing, from the very volatile perfluorocarbons (PFCs, e.g., CF4 and CF3CF3) and hydrofluorocarbons (HFCs, e.g., CH3CF3) to the higher-boiling point solvents (such as CH3CCl3 and CCl2 = CCl2) and CHBr3. A network of Medusa systems worldwide provides 12 in situ ambient air measurements per day of more than 38 compounds of part per trillion mole fractions and precisions up to 0.1% RSD at the five remote field stations operated by the Advanced Global Atmospheric Gases Experiment (AGAGE). Ihis custom system couples gas chromatography/mass spectrometry (GC/MSD) with a novel scheme for cryogen-free low-temperature preconcentration (-165 degrees C) of analytes from 2 L samples in a two-trap process using HayeSep D adsorbent.

Rigby M, R. G. Prinn, P. J. Fraser, P. G. Simmonds, R. L. Langenfelds, J. Huang, D. M. Cunnold, L. P. Steele, P. B. Krummel, R. F. Weiss, S. O'Doherty, P. K. Salameh, H. J. Wang, C. M. Harth, J. Mühle, and L. W. Porter, *Renewed growth of atmospheric methane, Geophys. Res. Lett., 35, L22805, doi:10.1029/2008GL036037, 2008*

Abstract: Following almost a decade with little change in global atmospheric methane mole fraction, we present measurements from the Advanced Global Atmospheric Gases Experiment (AGAGE) and the Australian Commonwealth Scientific and Industrial Research Organisation (CSIRO) networks that show renewed growth starting near the beginning of 2007. Remarkably, a similar growth rate is found at all monitoring locations from this time until the latest measurements. We use these data, along with an inverse method applied to a simple model of atmospheric chemistry and transport, to investigate the possible drivers of the rise. Specifically, the relative roles of an increase in emission rate or a decrease in concentration of the hydroxyl radical, the largest methane sink, are examined. We conclude that: 1) if the annual mean hydroxyl radical concentration did not change, a substantial increase in emissions was required simultaneously in both hemispheres between 2006 and 2007; 2) if a small drop in the hydroxyl radical concentration occurred, consistent with AGAGE methyl chloroform measurements, the emission increase is more strongly biased to the Northern Hemisphere. Citation: Rigby, M., et al. (2008), Renewed growth of atmospheric methane, Geophys. Res. Lett., 35, L22805, doi: 10.1029/2008GL036037.

***Derwent R.G., P.G. Simmonds, A.J. Manning, S. O'Doherty, G. Spain*,** *Methane emissions from peat bogs in the vicinity of the Mace Head Research Station over a 12-year period, Atmospheric Environment, Volume 43, 2328-2335, 2009*

Abstract: Methane emissions from the peat bogs in Connemara, Ireland have been inferred from the trace gas observations at the Mace Head Atmospheric Research Station using the nocturnal box method. A total of 237 local events, mainly during April to September, over a 12-year period have been studied. Simultaneous methane and chloroform emissions, together with ozone and hydrogen deposition have been characterised, leading to the estimation of methane emission rates for each event. The mean methane emission flux was found to be 400 ± 90 ng m-2 s-1. A strong seasonal cycle was found in the methane emission fluxes but there was little evidence of a long-term trend in the emissions from the peat bogs in the vicinity of the Mace Head station.

Stohl A, P. Seibert, J. Arduini, S. Eckhardt, P. Fraser, B. R. Greally, M. Maione, S. O'Doherty, R. G. Prinn, S. Reimann, T. Saito, N. Schmidbauer, P. G. Simmonds, M. K. Vollmer, R. F. Weiss, and Y. Yokouchi, *An analytical inversion method for determining regional and global emissions of greenhouse gases: sensitivity studies and application to halocarbons, Atmos. Chem. Phys., 9, 1597-1620, 2009*

Abstract: A new analytical inversion method has been developed to determine the regional and global emissions of long-lived atmospheric trace gases. It exploits in situ measurement data from three global networks and builds on backward simulations with a Lagrangian particle dispersion model. The emission information is extracted from the observed concentration increases over a baseline that is itself objectively determined by the inversion algorithm. The method was applied to two hydrofluorocarbons (HFC-134a, HFC-152a) and a hydrochlorofluorocarbon (HCFC-22)

for the period January 2005 until March 2007. Detailed sensitivity studies with synthetic as well as with real measurement data were done to quantify the influence on the results of the a priori emissions and their uncertainties as well as of the observation and model errors. It was found that the global a posteriori emissions of HFC-134a, HFC-152a and HCFC-22 all increased from 2005 to 2006. Large increases (21%, 16%, 18%, respectively) from 2005 to 2006 were found for China, whereas the emission changes in North America (-9%, 23%, 17%, respectively) and Europe (11%, 11%,-4%, respectively) were mostly smaller and less systematic. For Europe, the a posteriori emissions of HFC-134a and HFC-152a were slightly higher than the a priori emissions reported to the United Nations Framework Convention on Climate Change (UNFCCC). For HCFC-22, the a posteriori emissions for Europe were substantially (by almost a factor 2) higher than the a priori emissions used, which were based on HCFC consumption data reported to the United Nations Environment Programme (UNEP). Combined with the reported strongly decreasing HCFC consumption in Europe, this suggests a substantial time lag between the reported time of the HCFC-22 consumption and the actual time of the HCFC-22 emission. Conversely, in China where HCFC consumption is increasing rapidly according to the UNEP data, the a posteriori emissions are only about 40% of the a priori emissions. This reveals a substantial storage of HCFC-22 and potential for future emissions in China. Deficiencies in the geographical distribution of stations measuring halocarbons in relation to estimating regional emissions are also discussed in the paper. Applications of the inversion algorithm to other greenhouse gases such as methane, nitrous oxide or carbon dioxide are foreseen for the future.

Mühle, J., J. Huang, R. Weiss, R. Prinn, B. Miller, P. Salameh, C. Harth, P. Fraser, L. Porter, B. Greally, S. O'Doherty and P. Simmonds, *Sulfuryl fluoride in the global atmosphere, J. Geophys. Res., 114, 2009*

Abstract: The first calibrated high-frequency, high-precision, in situ atmospheric and archived air measurements of the fumigant sulfuryl fluoride (SO2F2) have been made as part of the Advanced Global Atmospheric Gas Experiment (AGAGE) program. The global tropospheric background concentration of SO2F2 has increased by 5 +/- 1% per year from similar to 0.3 ppt (parts per trillion, dry air mol fraction) in 1978 to similar to 1.35 ppt in May 2007 in the Southern Hemisphere, and from similar to 1.08 ppt in 1999 to similar to 1.53 ppt in May 2007 in the Northern Hemisphere. The SO2F2 interhemispheric concentration ratio was 1.13 +/- 0.02 from 1999 to 2007. Two-dimensional 12-box model inversions yield global total and global oceanic uptake atmospheric lifetimes of 36 +/- 11 and 40 +/- 13 years, respectively, with hydrolysis in the ocean being the dominant sink, in good agreement with 35 +/- 14 years from a simple oceanic uptake calculation using transfer velocity and solubility. Modeled SO2F2 emissions rose from similar to 0.6 Gg/a in 1978 to similar to 1.9 Gg/a in 2007, but estimated industrial production exceeds these modeled emissions by an average of similar to 50%. This discrepancy cannot be explained with a hypothetical land sink in the model, suggesting that only similar to 2/3 of the manufactured SO2F2 is actually emitted into the atmosphere and that similar to 1/3 may be destroyed during fumigation. With mean SO2F2 tropospheric mixing ratios of similar to 1.4 ppt, its radiative forcing is small and it is probably an insignificant sulfur source to the stratosphere. However, with a high global warming potential similar to CFC-11, and likely increases in its future use, continued atmospheric monitoring of SO2F2 is warranted.

Brooks Ian M, Robert C. Upstill-Goddard, Margaret J. Yelland, Steve Archer, Eric d'Asaro, Philip Balitsky, Rachael Beale, Cory Beatty, Byron Blomquist, A. Anthony Bloom, Barbara J. Brooks, John Cluderay, David Coles, John Dacey, Michael DeGrandpre, Jo Dixon, William Drennan, Joseph Gabriele, Laura Goldson, Nick Hardman-Mountford, Martin K. Hill, Matt Horn, Ping-Chang Hsueh, Barry Huebert, Gerrit de Leeuw, Timothy G. Leighton, Malcolm Liddicoat, Justin J. N. Lingard, Craig McNeil, James B. McQuaid, Ben I. Moat, Gerald Moore, Craig Neill, Philip D. Nightingale, Sarah J. Norris, Simon O'Doherty, Robin W. Pascal, Mike Rebozo, Erik Sahlee, Matt Salter, Ute Schuster, Ingunn Skjelvan, Hans Slagter, Michael H. Smith, Paul D. Smith, Meric Srokosz, John A. Stephens, Peter K. Taylor, Maciek Telszewski, Roisin Walsh, Brian Ward, David K. Woolf, Dickon Young, Henk Zemmelink, *Physical Exchanges at the Air-Sea Interface UK-SOLAS Field Measurements,* Bulletin of the American meteorological Society, 90(5), 629-644, 2009

Abstract: As part of the UK contribution to the international Surface Ocean – Lower Atmosphere Study a series of three related projects – DOGEE, SEASAW, and HiWASE –undertook experimental studies of the processes controlling the physical exchange of gases and seaspray aerosol at the sea surface. The studies share a common goal: to reduce the high degree of uncertainty in current parameterization schemes. The wide variety of measurements made during the studies, which incorporated tracer and surfactant release experiments, included direct eddy correlation fluxes, detailed wave spectra, wind history, photographic retrievals of whitecap fraction, aerosol size spectra and composition, surfactant concentration, and bubble populations in the ocean mixed layer. Measurements were made during three cruises in the NE Atlantic on the RRS Discovery during 2006 and 2007; a fourth campaign has been making continuous measurements on the Norwegian weather ship Polarfront since September 2006. This paper provides an overview of the three projects and some of the highlights of the measurement campaigns.

Patra P.K, Masayuki Takigawa, Kentaro Ishijima, Byoung-Choel Choi, Derek Cunnold, Edward J. Dlugokencky, Paul Fraser, Angel J. Gomez-Pelaez, Tae-Young Goo, Jeong-Sik Kim, Paul Krummel, Ray Langenfelds, Frank Meinhardt, Hitoshi Mukai, Simon O'Doherty, Ronald G. Prinn, Peter Simmonds, Paul Steele, Yasunori Tohjima, Kazuhiro Tsuboi, Karin Uhse, Ray Weiss, Doug Worthy And Takakiyo Nakazawa,

Growth rate, seasonal, synoptic and diurnal variations in lower atmospheric methane, J. Meteorol. Society of Japan, Vol. 87, No. 4, 635-663, 2009

Abstract: We have used an AGCM (atmospheric general circulation model)-based Chemistry Transport Model (ACTM) for the simulation of methane (CH4) in the height range of earth's surface to about 90 kin. The model simulations are compared with measurements at hourly, daily, monthly and interannual time scales by filtering or averaging all the timeseries appropriately. From this model-observation comparison, we conclude that the recent (1990-2006) trends in growth rate and seasonal cycle at most measurement sites can be fairly successfully modeled by using existing knowledge of CH4 flux trends and seasonality. A large part of the interannual variability (IAV) in CH4 growth rate is apparently controlled by IAV in atmospheric dynamics at the tropical sites and forest fires in the high latitude sites. The flux amplitudes are optimized with respect to the available hydroxyl radical (OH) distribution and model transport for successful reproduction of latitudinal and longitudinal distribution of observed CH4 mixing ratio at the earth's surface. Estimated atmospheric CH4 lifetime in this setup is 8.6 years. We found a small impact (less than 0.5 ppb integrated over 1 year) of OH diurnal variation, due to temperature dependence of reaction rate coefficient, on CH4 simulation compared to the transport related variability (order of +/-15 ppb at interannual timescales). Model-observation comparisons of seasonal cycles, synoptic variations and diurnal cycles are shown to be useful for validating regional flux distribution patterns and strengths. Our results, based on two emission scenarios, Suggest reduced emissions from temperate and tropical Asia region (by 13, 5, 3 Tg-CH4 for India, China and Indonesia, respectively), and compensating increase (by 9, 9, 3 Tg-CH4 for Russia, United States and Canada, respectively) in the boreal Northern Hemisphere (NH) are required for improved model-observation agreement.

O'Doherty S, Cunnold, D.M Miller, B.R., Mühle, J. McCulloch, A. Simmonds, P.G. Manning, A.J. Reimann, S. Vollmer, M.K. Greally, B.R. Prinn, R.G. Fraser, P.J. Steele, L.P. Krummel P.B., Dunse, B.L. Porter, L.W. Lunder, C.R. Schmidbauer, N. Hermansen, O. Salameh, P.K. Harth, C.M. Wang R.H.J. and Weiss R.F., *Global and regional emissions of HFC-125 (CHF2CF3) from in situ and air archive atmospheric observations at AGAGE and SOGE observatories,* J. Geophys. Res., J. Geophys. Res., 114, D23304, 2009.

Abstract: High-frequency, in situ observations from the Advanced Global Atmospheric Gases Experiment (AGAGE) and System for Observation of halogenated Greenhouse gases in Europe (SOGE) networks for the period 1998 to 2008, combined with archive flask measurements dating back to 1978, have been used to capture the rapid growth of HFC-125 (CHF2CF3) in the atmosphere. HFC-125 is the fifth most abundant HFC, and it currently makes the third largest contribution of the HFCs to atmospheric radiative forcing. At the beginning of 2008 the global average was 5.6 ppt in the lower troposphere and the growth rate was 16% yr(-1). The extensive observations have been combined with a range of modeling techniques to derive global emission estimates in a top-down approach. It is estimated that 21 kt were emitted globally in 2007, and the emissions are estimated to have increased 15% yr(-1) since 2000. These estimates agree within approximately 20% with values reported to the United Nations Framework Convention on Climate Change (UNFCCC) provided that estimated emissions from East Asia are included. Observations of regionally polluted air masses at individual AGAGE sites have been used to produce emission estimates for Europe (the EU-15 countries), the United States, and Australia. Comparisons between these top-down estimates and bottom-up estimates based on reports by individual countries to the UNFCCC show a range of approximately four in the differences. This process of independent verification of emissions, and an understanding of the differences, is vital for assessing the effectiveness of international treaties, such as the Kyoto Protocol.

Bergamaschi P, M. Krol, J. F. Meirink, F. Dentener, A. Segers, J. van Aardenne, S. Monni, A. T. Vermeulen, M. Schmidt, M. Ramonet, C. Yver, F. Meinhardt, E. G. Nisbet, R. E. Fisher, S. O'Doherty, and E. J. Dlugokencky, *Inverse modelling of European CH4 emissions 2001-2006,* Geophys. Res., 115, D22309, doi:10.1029/2010JD014180, 2010

Abstract: European CH4 emissions are estimated for the period 2001-2006 using a four-dimensional variational (4DVAR) inverse modeling system, based on the atmospheric zoom model TM5. Continuous observations are used from various European monitoring stations, complemented by European and global flask samples from the NOAA/ESRL network. The available observations mainly provide information on the emissions from northwest Europe (NWE), including the UK, Ireland, the BENELUX countries, France and Germany. The inverse modeling estimates for the total anthropogenic emissions from NWE are 21% higher compared to the EDGARv4.0 emission inventory and 40% higher than values reported to U.N. Framework Convention on Climate Change. Assuming overall uncertainties on the order of 30% for both bottom-up and top-down estimates, all three estimates can be still considered to be consistent with each other. However, the uncertainties in the uncertainty estimates prevent us from verifying (or falsifying) the bottom-up inventories in a strict sense. Sensitivity studies show some dependence of the derived spatial emission patterns on the set of atmospheric monitoring stations used, but the total emissions for the NWE countries appear to be relatively robust. While the standard inversions include a priori information on the spatial and temporal emission patterns from bottom-up inventories, a further sensitivity inversion without this a priori information results in very similar NWE country totals, demonstrating that the available observations provide significant constraints on the emissions from the NWE countries independent from bottom-up inventories.

Xiao X, R. G. Prinn, P. J. Fraser, P. G. Simmonds, R. F. Weiss, S. O'Doherty, B.R. Miller, P. Salameh, C. Harth, L. W. Porter, P. B. Krummel, J.Muhle, D. Cunnold, R.Wang, S. A. Montzka, J. W. Elkins, G. S. Dutton, T. M. Thompson, J. H. Butler, B. D. Hall, S. Reimann, M. K. Vollmer, F. Stordal, C. Lunder, M. Maione, and Y. Yokouchi, *Optimal Estimation of the Surface Fluxes of Methyl Chloride using a 3-D Global Chemical Transport Model,* Atmos. Chem. Phys.,10 5515-5530, 2010

Abstract. Methyl chloride (CH3Cl) is a chlorine-containing trace gas in the atmosphere contributing significantly to stratospheric ozone depletion. Large uncertainties in estimates of its source and sink magnitudes and temporal and spatial variations currently exist. GEIA inventories and other bottom-up emission estimates are used to construct a priori maps of the surface fluxes of CH3Cl. The Model of Atmospheric Transport and Chemistry (MATCH), driven by NCEP interannually varying meteorological data, is then used to simulate CH3Cl mole fractions and quantify the time series of sensitivities of the mole fractions at each measurement site to the surface fluxes of various regional and global sources and sinks. We then implement the Kalman filter (with the unit pulse response method) to estimate the surface fluxes on regional/global scales with monthly resolution from January 2000 to December 2004. High frequency observations from the AGAGE, SOGE, NIES, and NOAA/ESRL HATS in situ networks and low frequency observations from the NOAA/ESRL HATS flask network are used to constrain the source and sink magnitudes. The inversion results indicate global total emissions around 4100±470 Gg yr-1 with very large emissions of 2200±390 Gg yr-1 from tropical plants, which turn out to be the largest single source in the CH3Cl budget. Relative to their a priori annual estimates, the inversion increases global annual fungal and tropical emissions, and reduces the global oceanic source. The inversion implies greater seasonal and interannual oscillations of the natural sources and sink of CH3Cl compared to the a priori. The inversion also reflects the strong effects of the 2002/2003 globally widespread heat waves and droughts on global emissions from tropical plants, biomass burning and salt marshes, and on the soil sink.

Lee J.D, G. McFiggans, J. D. Allan, A. R. Baker, S. M. Ball, A. K. Benton, L. J. Carpenter, R. Commane, B. D. Finley, M. Evans, E. Fuentes, K. Furneaux, A. Goddard, N. Good, J. F. Hamilton, D. E. Heard, H. Herrmann, A. Hollingsworth, J. R. Hopkins, T. Ingham, M. Irwin, C. E. Jones, R. L. Jones, W. C. Keene, M. J. Lawler, S. Lehmann, A. C. Lewis, M. S. Long, A. Mahajan, J. Methven, S. J. Moller, K. Müller, T. Müller, N. Niedermeier, S. O'Doherty, H. Oetjen, J. M. C. Plane, A. A. P. Pszenny, K. A. Read, A. Saiz-Lopez, E. S. Saltzman, R. Sander, R. von Glasow, L. Whalley, A. Wiedensohler, and D. Young, *Reactive Halogens in the Marine Boundary Layer (RHaMBLe): the tropical North Atlantic experiments*, Atmos. Chem. Phys., 10, 1031-1055, 2010.

Abstract. The NERC UK SOLAS-funded Reactive Halogens in the Marine Boundary Layer (RHaMBLe) programme comprised three field experiments. This manuscript presents an overview of the measurements made within the two simultaneous remote experiments conducted in the tropical North Atlantic in May and June 2007. Measurements were made from two mobile and one ground-based platforms. The heavily instrumented cruise D319 on the RRS Discovery from Lisbon, Portugal to São Vicente, Cape Verde and back to Falmouth, UK was used to characterise the spatial distribution of boundary layer components likely to play a role in reactive halogen chemistry. Measurements onboard the ARSF Dornier aircraft were used to allow the observations to be interpreted in the context of their vertical distribution and to confirm the interpretation of atmospheric structure in the vicinity of the Cape Verde islands. Long-term ground-based measurements at the Cape Verde Atmospheric Observatory (CVAO) on São Vicente were supplemented by long-term measurements of reactive halogen species and characterisation of additional trace gas and aerosol species during the intensive experimental period. This paper presents a summary of the measurements made within the RHaMBLe remote experiments and discusses them in their meteorological and chemical context as determined from these three platforms and from additional meteorological analyses. Air always arrived at the CVAO from the North East with a range of air mass origins (European, Atlantic and North American continental). Trace gases were present at stable and fairly low concentrations with the exception of a slight increase in some anthropogenic components in air of North American origin, though NOx mixing ratios during this period remained below 20 pptv (note the non-IUPAC adoption in this manuscript of pptv and ppbv, equivalent to pmol mol-1 and nmol mol-1 to reflect common practice). Consistency with these air mass classifications is observed in the time series of soluble gas and aerosol composition measurements, with additional identification of periods of slightly elevated dust concentrations consistent with the trajectories passing over the African continent. The CVAO is shown to be broadly representative of the wider North Atlantic marine boundary layer; measurements of NO, O3 and black carbon from the ship are consistent with a clean Northern Hemisphere marine background. Aerosol composition measurements do not indicate elevated organic material associated with clean marine air. Closer to the African coast, black carbon and NO levels start to increase, indicating greater anthropogenic influence. Lower ozone in this region is possibly associated with the increased levels of measured halocarbons, associated with the nutrient rich waters of the Mauritanian upwelling. Bromide and chloride deficits in coarse mode aerosol at both the CVAO and on D319 and the continuous abundance of inorganic gaseous halogen species at CVAO indicate significant reactive cycling of halogens. Aircraft measurements of O3 and CO show that surface measurements are representative of the entire boundary layer in the vicinity both in diurnal variability and absolute levels. Above the inversion layer similar diurnal behaviour in O3 and CO is observed at lower mixing ratios in the air that had originated from south of Cape Verde, possibly from within the ITCZ. ECMWF calculations on two days indicate

very different boundary layer depths and aircraft flights over the ship replicate this, giving confidence in the calculated boundary layer depth.

Stohl A, Kim J, Li S, O'Doherty S, Salameh P.K, Saito T, Vollmer M.K, Wan D, Yao B, Yokouchi Y and Zhou L.Z, *Hydrochlorofluorocarbon and hydrofluorocarbons emissions in East Asia determined by inverse modelling,* Atmos. Chem. Phys., 10, 3545- 3560, 2010

Abstract. The emissions of three hydrochlorofluorocarbons, HCFC-22 (CHClF2), HCFC-141b (CH3CCl2F) and HCFC-142b (CH3CClF2) and three hydrofluorocarbons, HFC-23 (CHF3), HFC-134a (CH2FCF3) and HFC-152a (CH3CHF2) from five East Asian countries for the year 2008 are determined by inverse modeling. The inverse modeling is based on in-situ measurements of these halocarbons at the Japanese stations Cape Ochi-ishi and Hateruma, the Chinese station Shangdianzi and the South Korean station Gosan. For every station and every 3 h, 20-day backward calculations were made with the Lagrangian particle dispersion model FLEXPART. The model output, the measurement data, bottom-up emission information and corresponding uncertainties were fed into an inversion algorithm to determine the regional emission fluxes. The model captures the observed variation of halocarbon mixing ratios very well for the two Japanese stations but has difficulties explaining the large observed variability at Shangdianzi, which is partly caused by small-scale transport from Beijing that is not adequately captured by the model. Based on HFC-23 measurements, the inversion algorithm could successfully identify the locations of factories known to produce HCFC-22 and emit HFC-23 as an unintentional byproduct. This lends substantial credibility to the inversion method. We report national emissions for China, North Korea, South Korea and Japan, as well as emissions for the Taiwan region. Halocarbon emissions in China are much larger than the emissions in the other countries together and contribute a substantial fraction to the global emissions. Our estimates of Chinese emissions for the year 2008 are 65.3±6.6 kt/yr for HCFC-22 (17% of global emissions extrapolated from Montzka et al., 2009), 12.1±1.6 kt/yr for HCFC-141b (22%), 7.3±0.7 kt/yr for HCFC-142b (17%), 6.2±0.7 kt/yr for HFC-23 (>50%), 12.9±1.7 kt/yr for HFC-134a (9% of global emissions estimated from Velders et al., 2009) and 3.4±0.5 kt/yr for HFC-152a (7%).

Grant A, C. S. Witham, P. G. Simmonds, A. J. Manning, and S. O'Doherty*, A 15 year record of high-frequency, in situ measurements of hydrogen at Mace Head, Ireland,* Atmos. Chem. Phys., 10, 1203-1214, 2010

Abstract. Continuous high-frequency measurements of atmospheric molecular hydrogen have been made at Mace Head atmospheric research station on the west coast of Ireland from March 1994 to December 2008. The presented data provides a wealth of information on long term trends and seasonal cycles of hydrogen in background northern hemispheric air. Individual measurements have been sorted using a Lagrangian dispersion model to separate clean background air from regionally polluted European air masses and those transported from southerly latitudes. No significant trend was observed in background northern hemispheric air over the 15 year record, elevations in yearly means were accounted for from large scale biomass burning events. Seasonal cycles show the expected pattern with maxima in spring and minima in late autumn. The mean hydrogen mole fraction in baseline northern hemispheric air was found to be 500.1 ppb. Air transported from southerly latitudes showed an elevation from baseline mean of 11.0 ppb, reflecting both the latitudinal gradient of hydrogen, with higher concentrations in the southern hemisphere, and the large photochemical source of hydrogen from southerly latitudes. European polluted air masses arriving at Mace Head showed mean elevation of 5.3 ppb from baseline air masses, reflecting hydrogen's source from primary emissions like fossil fuel combustion. Forward modelling of transport of hydrogen to Mace Head suggests that the ratio of hydrogen to carbon monoxide in primary emissions is considerably less in non-traffic sources than traffic sources.

Grant A, K. F. Stanley, S. J. Henshaw, D.E. Shallcross and S. O'Doherty, *High-frequency urban measurements of hydrogen and carbon monoxide,* Atmos. Chem. Phy., 10, 4715-4724, 2010

Abstract. High-frequency measurements of atmospheric hydrogen (H2) and carbon monoxide (CO) were made at an urban site in the UK from mid-December 2008 until early March 2009. Very few measurements of these trace gases exist in the urban environment, particularly within the United Kingdom, but are an essential component in the assessment of anthropogenic emissions of H2 and CO. These data provide detailed information on urban time-series, diurnal cycles as well as sources and sinks of both H2 and CO at urban locations. High-frequency data were found to be strongly influenced by local meteorological conditions of wind speed and temperature. Diurnal cycles were found to follow transport frequency very closely due to the sites proximity to major carriageways, consequently a strong correlation was found between H2 and CO mole fractions. Background subtracted mean and rush hour H2/CO emission ratios of 0.50 and 0.53 were calculated, the scatter plot of which displayed an unusual two population pattern, the source of which could not be elucidated. H2 emissions from transport in the UK were estimated at 175 Gg/yr, with 7.8 Tg/yr of H2 produced from vehicle emissions globally. H2 and CO deposition velocities were calculated over stable periods when a clear decay of both species was observed. CO was found to have a much higher deposition velocity than H2, 1.3×10-3 and 2.2×10-4 m s-1, respectively, going against the law of molecular diffusivity. The source of this unusual result was investigated, however no conclusive evidence was found for increased loss of CO over H2 during stable night time inversion events.

Mühle J, A. L. Ganesan, B. R. Miller, P. K. Salameh, C. M. Harth, B. R. Greally, M. Rigby, L. W. Porter, L. P. Steele, C. M. Trudinger, P. B. Krummel, S. O'Doherty, P. J. Fraser, P. G. Simmonds, R. G. Prinn, and R. F. Weiss, *Perfluorocarbons in the global atmosphere: tetrafluoromethane, hexafluoroethane, and octafluoropropane*, Atmos. Chem. Phys., 10, 5145-5164, 2010

Abstract. We present atmospheric baseline growth rates from the 1970s to the present for the long-lived, strongly infrared-absorbing perfluorocarbons (PFCs) tetrafluoromethane (CF4), hexafluoroethane (C2F6), and octafluoropropane (C3F8) in both hemispheres, measured with improved accuracies (~1–2%) and improved precisions (<0.3%, or <0.2 ppt (parts-per-trillion), for CF4; <1.5%, or <0.06 ppt, for C2F6; <4.5%, or <0.02 ppt, for C3F8) within the Advanced Global Atmospheric Gases Experiment (AGAGE). Pre-industrial background values of 34.7±0.2 ppt CF4 and 0.1±0.02 ppt C2F6 were measured in air extracted from Greenland ice and Antarctic firn. Anthropogenic sources are thought to be primary aluminum production (CF4, C2F6, C3F8), semiconductor production (C2F6, CF4, C3F8) and refrigeration use (C3F8). Global emissions calculated with the AGAGE 2-D 12-box model are significantly higher than most previous emission estimates. The sum of CF4 and C2F6 emissions estimated from aluminum production and non-metal production are lower than observed global top-down emissions, with gaps of ~6.4–7.6 Gg/yr CF4 in recent years. The significant discrepancies between previous CF4, C2F6, and C3F8 emission estimates and observed global top-down emissions estimated from AGAGE measurements emphasize the need for more accurate, transparent, and complete emission reporting, and for verification with atmospheric measurements to assess the emission sources of these long-lived and potent greenhouse gases, which alter the radiative budget of the atmosphere essentially permanently once emitted.

Yates E, R.G. Derwent, P. G. Simmonds, B.R. Greally, S. O'Doherty, D. E. Shallcross, *The seasonal cycles and photochemistry of C2 - C5 alkanes at Mace Head*, Atmos. Environ., Volume 44, 2705-2713, 2010

Abstract. Continuous in-situ measurements of NMHCs at Mace Head, Ireland during two full annual cycles from January 2005 to January 2007 were used to investigate NMHC emission sources and transport including dilution and photochemical oxidation. The Mace Head research station is ideally located to sample a wide range of air masses including polluted European transport, clean North Atlantic and Arctic air masses and the ultra-clean, Southern Atlantic air masses. The variety in air mass sampling is used to investigate interaction of emissions, transport, dilution and photochemistry. Variability of long-lived hydrocarbon ratios is used to assess and estimate typical transport times from emission source to the Mace Head receptor. Seasonality in the ratios of isomeric alkane pairs (for butane and pentanes) are used to assess the effects of atmospheric transport and photochemical ageing. Finally, the natural logarithms of NMHC ratios are used to assess photochemical oxidation.

Xiao X, R. G. Prinn, R. F. Weiss, P. G. Simmonds, P. J. Fraser, S. O'Doherty, B. R. Miller, P. K. Salameh, C. M. Harth, P. B. Krummel, A. Golombek, L. W. Porter, J. W. Elkins, G. S. Dutton, B. D. Hall, S. A. Montzka, R. H. J. Wang and D. M. Cunnold,. *Three Dimensional Inverse Modeling of Regional Industrial Emissions and Global Oceanic Uptake of Carbon Tetrachloride*, Atmos. Chem. Phys., 10, 10421-10434, 2010

Abstract. Carbon tetrachloride (CCl4) has substantial stratospheric ozone depletion potential and its consumption is controlled under the Montreal Protocol and its amendments. We implement a Kalman filter using atmospheric CC14 measurements and a 3-dimensional chemical transport model to estimate the interannual regional industrial emissions and seasonal global oceanic uptake of CCl4 for the period of 1996–2004. The Model of Atmospheric Transport and Chemistry (MATCH), driven by offline National Center for Environmental Prediction (NCEP) reanalysis meteorological fields, is used to simulate CCl4 mole fractions and calculate their sensitivities to regional sources and sinks using a finite difference approach. High frequency observations from the Advanced Global Atmospheric Gases Experiment (AGAGE) and NOAA Earth System Research Laboratory (ESRL) and low frequency flask observations are together used to constrain the source and sink magnitudes, estimated as factors that multiply the a priori fluxes. Although industry data imply that the global industrial emissions were substantially declining with large interannual variations, the optimized results show only small interannual variations and a small decreasing trend. The global surface CCl4 mole fractions were declining in this period because the CCl4 oceanic and stratospheric sinks exceeded the industrial emissions. Compared to the a priori values, the inversion results indicate substantial increases in industrial emissions originating from the South Asian/Indian and Southeast Asian regions, and significant decreases in emissions from the European and North American regions.

Rigby M, J. Mühle, B. Miller, R. Prinn, P. Fraser, P. Krummel, P. Steele, N. Derek, R. Weiss, P. Salameh, C. Harth, S. O'Doherty, P. Simmonds, M. Vollmer, S. Reimann, J. Kim, R. Wang, E. Dlugokencky, and G. Dutton, *History of atmospheric SF6 mole fractions and emissions from 1973 to 2008*, Atmos. Chem. Phys. Discuss., 10, 13519-13555, 2010

Abstract. We present atmospheric sulfur hexafluoride (SF6) mole fractions and emissions estimates from the 1970s to 2008. Measurements were made of archived air samples starting from 1973 in the Northern Hemisphere and from 1978 in the Southern Hemisphere, using the Advanced Global Atmospheric Gases Experiment (AGAGE) gas chromatographic–mass spectrometric (GC-MS) systems. These measurements were combined with modern high-frequency GC-MS and GC-electron capture detection (ECD) data from AGAGE monitoring sites, to produce a

unique air history of this potent greenhouse gas. Atmospheric mole fractions were found to have increased by more than an order of magnitude between 1973 and 2008. The 2008 growth rate was found to be the highest recorded, at 0.29 ± 0.02 pmol mol-1 yr-1. A three-dimensional chemical transport model and a minimum variance Bayesian inverse method was used to estimate annual emission rates using the measurements. Consistent with the mole fraction growth rate maximum, global emissions during 2008 were also found to be highest in the 1973–2008 period, reaching 7.5 ± 0.4 Ggyr-1 and surpassing the previous maximum in 1995. The 2008 values follow an increase in emissions of 50 ± 25% since 2000. A second global inversion which also incorporated National Oceanic and Atmospheric Administration (NOAA) flask measurements and in situ monitoring site data was found to agree well with the emissions derived using AGAGE measurements alone. By estimating continent-scale emissions using all available AGAGE and NOAA surface measurements covering the period 2004–2008, we find that it is likely that much of the global emissions rise during this five-year period originated primarily from Asian countries that do not report emissions to the United Nations Framework Convention on Climate Change (UNFCCC). We also find it likely that SF6 emissions reported to the UNFCCC were underestimated between at least 2004 and 2007.

Miller B.R, M. Rigby, L. J. M. Kuijpers, P. B. Krummel, L. P. Steele, M. Leist, P. J. Fraser, A. McCulloch, C. Harth, P. Salameh, J. Mühle, R. F. Weiss, R. G. Prinn, R. H. J. Wang, S. O'Doherty, B. Greally, and P. G. Simmonds, *CHF_3 (HFC-23) emission trend response to $CHClF_2$ (HCFC-22) production and recent CHF_3 emission abatement measures,* Atmos. Chem. Phys. Discuss., 10, 13179-13217, 2010

Abstract. HFC-23 (also known as CHF3, fluoroform or trifluoromethane) is a potent greenhouse gas (GHG), with a global warming potential (GWP) of 14 800 for a 100-year time horizon. It is an unavoidable by-product of HCFC-22 (CHClF2, chlorodifluoromethane) production. HCFC-22, an ozone depleting substance (ODS), is used extensively in commercial refrigeration and air conditioning, in the extruded polystyrene (XPS) foam industries (dispersive applications) and also as a feedstock in fluoropolymer manufacture (a non-dispersive use). Aside from small markets in specialty uses, HFC-23 has historically been considered a waste gas that was, and often still is, simply vented to the atmosphere. Efforts have been made in the past two decades to reduce HFC-23 emissions, including destruction (incineration) in facilities in developing countries under the United Nations Framework Convention on Climate Change's (UNFCCC) Clean Development Mechanism (CDM), and by process optimization and/or voluntary incineration by most producers in developed countries. We present observations of lower-tropospheric mole fractions of HFC-23 measured by "Medusa" GC/MSD instruments from ambient air sampled in situ at the Advanced Global Atmospheric Gases Experiment (AGAGE) network of five remote sites and in Cape Grim air archive (CGAA) samples (1978–2009) from Tasmania, Australia. These observations are used with the AGAGE 2-D atmospheric 12-box model and an inverse method to produce model mole fractions and a "top-down" HFC-23 emission history. The model 2009 annual mean global lower-tropospheric background abundance is 22.8 (±0.2) pmol mol-1. The derived HFC-23 emissions show a "plateau" during 1997–2003, followed by a rapid ~50% increase to a peak of 15.0 (+1.3/-1.2) Gg/yr in 2006. Following this peak, emissions of HFC-23 declined rapidly to 8.6 (+0.9/-1.0) Gg/yr in 2009, the lowest annual emission of the past 15 years. We derive a 1990–2008 "bottom-up" HFC-23 emission history using data from the United Nations Environment Programme and the UNFCCC. Comparison with the top-down HFC-23 emission history shows agreement within the stated uncertainties. In the 1990s, HFC-23 emissions from developed countries dominated all other sources, then began to decline and eventually became fairly constant during 2003–2008. From the beginning of that plateau, the major factor determining the annual dynamics of global HFC-23 emissions became the historical rise of HCFC-22 production for dispersive uses in developing countries to a peak in 2007. Thereafter in 2007–2009, incineration through CDM projects became a larger factor, reducing global HFC-23 emissions despite rapidly rising HCFC-22 feedstock production in developing countries.

Simmonds P.G, R.G. Derwent, A.J. Manning, S. O'Doherty and G. Spain, *Estimation of hydrogen deposition velocities from 1995-2008 at Mace Head, Ireland using a simple box model and concurrent ozone depositions,* Tellus series B-chemical and physical meteorology, Volume 63, Issue 1, 40-51, 2010

Abstract: During stable nocturnal inversions with low wind speeds, we observed strong depletions of both hydrogen and ozone caused by deposition to the peat bogs in the vicinity of the Mace Head Atmospheric Research Station, Connemara, County Galway, Ireland. From these temporally correlated fluxes and using a simple box model, we have estimated the strength of the molecular hydrogen soil sink over a 14-yr period (1995-2008). Over this entire period 269 nocturnal deposition events were identified that satisfied the strict selection criteria. The average hydrogen deposition velocity determined from these events was 0.53 mm s-1, covering a range of 0.18-1.29 mm s-1, which is in agreement with the range of deposition velocities reported in the literature for similar peaty biomes. By annually averaging all of the nocturnal inversion events over the most seasonally active period from April-September we reveal a positive correlation with ambient temperature in the relative deposition velocities of hydrogen and ozone, which is not readily apparent in all of the individual events. Furthermore, average hydrogen deposition velocities and accumulated rainfall from 48 h before and during each event were to a reasonable extent anti-correlated. However, due to the large uncertainties in determining monthly mean H2 deposition velocities there is no statistically significant trend in the hydrogen deposition velocities over time.

Simmonds P.G, R.G. Derwent, A.J. Manning, S. O'Doherty and G. Spain, *Natural chloroform emissions from the blanket peat bogs in the vicinity of Mace Head, Ireland over a 14-year period,* Atmospheric Environment, Volume 44, Issue 10, 1284-1291, 2010

Abstract: Simultaneous chloroform (CHCl3) emission and ozone (O-3) deposition are regularly observed under nocturnal inversions during the summer months from and to the peat bogs in the vicinity of the Mace Head Atmospheric Research Station, Connemara, Co Galway, Ireland. Emissions were estimated using the nocturnal box model applied to routine atmospheric observations collected over a 14-year period from 1995 to 2008. Strict criteria were applied in the selection of events of low wind speed, under a stable night-time inversion layer in baseline air conditions, with no transport from Europe. The mean peatland CHCl3 flux was 2.91 mu g m(-2) h(-1) with highly variable fluxes ranging from 0.44 to 12.94 mu g m(-2) h(-1). These fluxes are generally larger than those reported previously for similar biomes and if representative would make a significant contribution to the global estimated source of CHCl3. Fluxes were not strongly correlated with either atmospheric temperature or the level of precipitation. Over the 14-year period there appears to have been a small increase in overall CHCl3 emissions, although we stress that the nocturnal box model has a number of limitations and assumptions which should be taken into account.

Tripathi O, S. G. Jennings, C. D. O'Dowd, L. Coleman, S. Leinert, E. Moran, S.J. O'Doherty, T.G. Spain, *Statistical Analysis of Eight Surface Ozone Measurement Series for various sites in Ireland,* J. Geophys. Res., 115, D19302, doi:10.1029/2010JD014040, 2010

Abstract: Data from various stations having different measurement record periods between 1988 and 2007 are analyzed to investigate the surface ozone concentration, long-term trends, and seasonal changes in and around Ireland. Time series statistical analysis is performed on the monthly mean data using seasonal and trend decomposition procedures and the Box-Jenkins approach (autoregressive integrated moving average). In general, ozone concentrations in the Irish region are found to have a negative trend at all sites except at the coastal sites of Mace Head and Valentia. Data from the most polluted Dublin city site have shown a very strong negative trend of -0.33 ppb/yr with a 95% confidence limit of 0.17 ppb/yr (i.e., -0.33 +/- 0.17) for the period 2002-2007, and for the site near the city of Cork, the trend is found to be -0.20 +/- 0.11 ppb/yr over the same period. The negative trend for other sites is more pronounced when the data span is considered from around the year 2000 to 2007. Rural sites of Wexford and Monaghan have also shown a very strong negative trend of -0.99 +/- 0.13 and -0.58 +/- 0.12, respectively, for the period 2000-2007. Mace Head, a site that is representative of ozone changes in the air advected from the Atlantic to Europe in the marine planetary boundary layer, has shown a positive trend of about +0.16 +/- 0.04 ppb per annum over the entire period 1988-2007, but this positive trend has reduced during recent years (e. g., in the period 2001-2007). Cluster analysis for back trajectories are performed for the stations having a long record of data, Mace Head and Lough Navar. For Mace Head, the northern and western clean air sectors have shown a similar positive trend (+0.17 +/- 0.02 ppb/yr for the northern sector and +0.18 +/- 0.02 ppb/yr for the western sector) for the whole period, but partial analysis for the clean western sector at Mace Head shows different trends during different time periods with a decrease in the positive trend since 1988 indicating a deceleration in the ozone trend for Atlantic air masses entering Europe.

Manning A, S. O'Doherty, A. R. Jones, P. G. Simmonds, and R. G. Derwent, *Estimating UK methane and nitrous oxide emissions from 1990 to 2007 using an inversion modeling approach*, J. Geophys. Res., 116, D0230, doi:10.1029/2010JD014763, 2011

Abstract: Methane (CH4) and nitrous oxide (N2O) have strong radiative properties in the Earth's atmosphere and both are regulated through the United Nations Framework Convention on Climate Change. Through this convention the United Kingdom is obliged to report an inventory of annual emission estimates from 1990. This paper describes a methodology that estimates emissions of CH4 and N2O completely independent of the inventory values. Emissions have been estimated for each year 1990-2007 for the United Kingdom and for NW Europe. The methodology combines high-frequency observations from Mace Head, a monitoring site on the west coast of Ireland, with an atmospheric dispersion model and an inversion system. The sensitivities of the inversion method to the modeling assumptions are reported. The 20 year Northern Hemisphere midlatitude baseline mixing ratios, growth rates, and seasonal cycles of both gases are also presented. The results indicate reasonable agreement between the inventory and inversion results for the United Kingdom for N2O over the entire period. For CH4 the agreement is poor in the 1990s but good in the 2000s. The UK CH4 inventory reported reduction from 1990-1992 to 2005-2007 (over 50%) is dominated by changes to landfill and coal mine emissions and is more than double the corresponding drop in the inversion estimated emissions (24%). The inversion results suggest that the United Kingdom has met its Kyoto commitment (-12.5%) but by a smaller margin (-14.3%) than reported (-17.3%). The results for NW Europe with the United Kingdom removed show reasonable agreement in trend, on average the inversion results for N2O are 25% lower and for CH4 21% higher.

Messager, C., Schmidt, M., Ramonet, M., Bousquet, P., Simmonds, P., Manning, A.J., Kazan, V., Spain, G., Jennings, S.G., Ciais, P. *Ten years of CO_2, CH_4, CO, N_2O fluxes over western Europe inferred from atmospheric measurements at Mace Head, Ireland.* Atmos. Chem. Phys. Discussions, 8, pp. 1191-1237 (2008)

We estimated CO2, CH4, CO and N2O emission fluxes over the British Isles and Western Europe using atmospheric radon observations and concentrations recorded at the Mace Head Atmospheric Research Station between 1996 and 2005. We classified hourly concentration data into either long-range European or regional sources from Ireland and UK, by using local wind speed data in conjunction with 222Rn and 212Pb threshold criteria. This leads to the selection of about 7% of the total data for both sectors. We then used continuous 222Rn measurements and assumptions on the surface emissions of 222Rn to deduce the unknown fluxes of CO2, CH4, CO and N2O. Our results have been compared to the UNFCCC, EMEP and EDGAR statistical inventories and to inversion results for CH4. For Western Europe, we found yearly mean fluxes of 4.1±1.5 106 kgCO2 km−2 yr−1 , 11.9±2.0 103 kgCH4 km−2 yr−1, 12.8±4.2 103 kgCOkm−2 yr−1 and 520.2±129.2 kgN2Okm−2 yr−1, respectively, for CO2, CH4, CO and N2O over the period 1996–2005. The method based upon 222Rn to 15 infer emissions has many sources of systematic errors, in particular its poorly known and variable footprint, uncertainties in 222Rn soil fluxes and in atmospheric mixing of air masses with background air. However, these biases are likely to remain constant in the long-term, which makes the method quite efficient to detect trends in fluxes. Over the last ten years period, the decrease of the anthropogenic CH4, CO and N2O 20 emissions in Europe estimated by inventories (respectively −30%, −35% and −23%) is confirmed by the Mace Head data within 2%. Therefore, the 222Rn method provides an independent way of verification of changes in national emissions derived from inventories. Using European-wide estimates of the CO/CO2 emission ratio, we also found that it is possible to separate the fossil fuel CO2 emissions contribution from the one of 25 total CO2 fluxes. The fossil fuel CO2 emissions and their trends derived in that manner agree very well with inventories.

Pyle, J. A., M. J. Ashfold, N. R. P. Harris, A. D. Robinson, N. J. Warwick, G. D. Carver, B. Gostlow, L. M. O'Brien, A. J. Manning, S. M. Phang, S. E. Yong, K. P. Leong, E. H. Ung, S. Ong (2011), Bromoform in the tropical boundary layer of the maritime continent during OP3. *Atmos. Chem. Phys.,* 11, pp. 529-542, doi:10.5194/acp-11-529-2011.

We report measurements of bromoform made by gas chromatography during the OP3 campaign in 2008. Measurements were made simultaneously for a few days at the World Meteorological Organization (WMO) Global Atmospheric Watch (GAW) site in the Danum Valley, a rainforest location in Sabah, Borneo, and at a nearby coastal site at Kunak. Background values at Kunak were higher than those measured in the rainforest (2–5 ppt compared with 1 ppt) and excursions away from the background were very much higher, reaching 10 s of ppt. Measurements of C2Cl4, an industrial tracer, showed no significant difference in background at the two sites. Modelling using two different models can reproduce a number of the observed features. The data are consistent with a strong, local coastal source of bromoform in eastern Sabah and can be used to infer the strength of the source of bromoform in South East Asia. However, they provide only a very weak constraint on global emissions. The global model results highlight the difficulty for short-lived species of extrapolating limited duration, local measurements to a global source.

Polson, D., D. Fowler, E. Nemitz, U. Skiba, A. McDonald, D. Famulari, C. Di Marco, I. Simmons, K. Weston, R. Purvis, H. Coe, A. J. Manning, H. Webster, M Harrison, D O'Sullivan, C Reeves, D Oram., Estimation of spatial apportionment of greenhouse gas emissions for the UK using boundary layer measurements and inverse modelling technique (2011), *Atmospheric Environment*, 45, 4, pp. 1042-1049. doi:10.1016/j.atmosenv.2010.10.011

A technique is described to independently validate the national emission inventories produced using the methodology of the Intergovernmental Panel on Climate Change (IPCC). A boundary layer budget approach is applied to the United Kingdom and an inverse modelling technique is used to derive total and spatial apportionment of emissions for CO, CO2, CH4, N2O, HFC-134a, HCFC-141b, HCFC-142b and HCFC-22. During the summer of 2005 and September 2006 an aircraft circumnavigating the UK was used to collect data upwind and downwind of the UK coast. The concentration measurements were inverted to produce mapped emissions of the UK. The modelled overall CO flux (2900 ± 107 kt yr-1) and spatial apportionment throughout the UK are remarkably consistent with the official UK NAEI (National Atmospheric Emission Inventory) inventory. The CO2 total emissions (620 ± 105 Mt yr-1) and spatial apportionment are also close to the NAEI. However for N2O and CH4, the estimated annual fluxes, 500 ± 370 kt yr-1 and 3500 (range 0 – 8000 kt yr-1) respectively, are larger than the NAEI albeit with significant uncertainty. Emissions of four halocarbon compounds were also calculated with total emissions of 3.1 ± 0.4 kt yr-1 for HFC-134a, 0.9 ± 0.6 kt yr-1 for HCFC-141b, 0.56 ± 0.2 kt yr-1 for HCFC-142b and 3.8 ± 1.0 kt yr-1 for HCFC-22 consistent with other published data.

Ebinghaus, R., , S.G. Jennings, H.H. Kock , R.G. Derwent, A.J. Manning, T.G. Spain, Decreasing trends in total gaseous mercury observations in baseline air at Mace head, Ireland from 1996 to 2009. In press Atmospheric Environment, Jan 2011.

In this study, the concentrations are reported of total gaseous mercury in baseline air masses arriving at Mace Head, Ireland after having traversed the thousands of kilometres uninterrupted fetch of the North Atlantic Ocean. Over a 14-year period, a statistically significant negative (downwards) trend of -0.028 ± 0.01 ng m-3 yr-1, representing a trend of – (1.6 – 2.0) % per year, has been detected in the total gaseous mercury levels in these baseline air masses. These findings are set in the context of the available literature studies of atmospheric Hg trends.

Pyle, J. A., N. J. Warwick, N. R. P. Harris, Alex Archibald, M. J. Ashfold, K. Ashworth, M. P. Barkley, G. D. Carver, K. Chance, J. Dorsey, D. Fowler, S. Gonzi, B. Gostlow, N. Hewitt, T. P. Kurosu, J. D. Lee, S. B. Langford, G. Mills, S. Moller, A.R. MacKenzie, A. J. Manning, P. Misztal, M. S. M. Nadzir, E. Nemitz, H. Newton, L. M. O'Brien, S. Ong, D. Oram, P. I. Palmer, L. K. Peng, S. M. Phang, R. Pike, T. Pugh, A. D. Robinson, A. A. Samah, U. Skiba, H. E. Ung, S. E. Yong, P. Young, The impact of local surface processes in Borneo on atmospheric composition at wider spatial scales: coastal processes, land use change and air quality. In Press, Atmos. Chem. Phys., 2011

We present some results from the OP3 campaign in Sabah during 2008 that allow us to study the impact of local changes over Borneo at the regional and wider scale. Model studies of land-use change confirm the earlier study of Hewitt et al. (2009). Further changes to an intensive oil palm agriculture In South East Asia, and the tropics in general, could have important impacts on air quality, with the biggest factor being the concomitant changes in NOx emissions. With the scenarios used here, local increase in ozone of around 50% could occur. We also report measurements of short-lived brominated compounds around Sabah suggesting the importance of oceanic (and, especially, coastal) sources. High concentrations were frequently measured when the local atmospheric circulation, over regions of high potential emissions, confined air in the local boundary layer, allowing concentrations to build up with time. Based on the background values, total short-lived bromine concentrations measured at the surface during OP3 amount to about 7 ppt, putting some constraint the amount of these species that can reach the lower stratosphere.

Manning, A.J.,The challenge of estimating regional trace gas emissions from atmospheric observations. In press, Special issue of Philosophical Transactions, 2011

This paper discusses some of the major issues that surround estimating regional emissions of trace gases from atmospheric observations through inversion modelling. Inversion methods use modelled knowledge of how emissions dilute in the atmosphere as they travel from their source to an observation point, together with the observations, to calculate a grid of emissions. The problem is one of minimising the mismatch between a modelled and observed time-series of concentration. There are many methods of comparing time-series, some involving a priori knowledge others without. The location, terrain and height of the observation station can also be very significant in determining how well a model can represent the dilution from emission source to receptor. The inversion solution (emission map) will assign some of the sources incorrectly for a variety of reasons e.g. local sources, intermittent releases, errors in the modelled transport or observation, and the choice of the spatial and temporal resolution of the emission map. The reasons for uncertainty in the modelled emissions are discussed along with suggestions as to how some of these can be minimized. Using multiple stations to further constrain the inversion should reduce the uncertainty however care is needed if the potential improvements can be realised.

Derwent, R.G., D.S. Stevenson, R.M. Doherty, W.J. Collins, M.G. Sanderson, C.E. Johnson, (2008). Radiative forcing from surface NOx emissions: Spatial and seasonal variations. Climatic Change 88, 385-401.

Derwent, R.G., D.S. Stevenson, R.M. Doherty, W.J. Collins, M.G. Sanderson, (2008). How is surface ozone in Europe linked to Asian and North American NOx emissions? Atmospheric Environment 42, 7412-7422.

Stevenson, D.S., R.G. Derwent, (2009). How does the location of aircraft nitrogen oxide emissions affect their climate impact? Geophysical Research Letters 36, L17810, doi:10.1029/2009GL039422.

PRESENTATIONS

- Understanding the annual and seasonal trends in observations from Mace Head, Ireland, using an atmospheric transport model, Geophysical Research Abstracts, Vol. 9, 03821, EGU General Assembly 2007, Vienna, Austria, April 2007.
- Selected results from trace gas inter-comparisons between AGAGE in situ and NOAA flask data, NOAA ESRL global monitoring annual conference, May 15-15th, 2008
- Advanced Global Atmospheric Gases Experiment (AGAGE) and associated networks, 7th Ozone Research Managers' Meeting, Geneva, Switzerland, 19th-21st May, 2008
- AGAGE measurements of Carbon Monoxide at Mace Head, ICOS meeting, LSCE, Gif-sur-Yvette, France, 17-18th November 2008
- Quantifying Regional GHG Emissions of HFC-134a from Atmospheric Measurements at Trinidad Head (California), Cape Grim (Australia) and Mace Head (Ireland), AGU fall meeting, San Fransisco, December 2008
- Chemical, physical and biological influences on trace gases in the tropics: First two years of results from the Cape Verde Atmospheric Observatory, AGU fall meeting, San Francisco, December 2008

- Nitrogen trifluoride and sulfuryl fluoride: Two new greenhouse gases, Cape Grim baseline air pollution station, Annual science meeting, Australia, 2008
- Growth of HFC-125 in the atmosphere determined from in situ observations at AGAGE and SOGE observatories, EGU meeting, Vienna, April 2009
- EuroHydros - A European Network for Atmospheric Hydrogen observations and studies. The observational network, EGU meeting, Vienna, April 2009
- Chemical, physical and biological influences on trace gases in the tropics: First two years of results from the Cape Verde Atmospheric Observatory, EGU meeting, Vienna, April 2009
- AGAGE and CSIRO Measurements of Recent Global Methane Growth, NOAA ESRL 2009 Global Monitoring Annual Conference, May 13-14th, 2009
- Growth of HFC-125 in the Atmosphere measured at AGAGE and SOGE observatories, Fifth International Symposium on Non-CO2 Greenhouse Gases (NCGG-5) Science, Reduction Policy and Implementation, Wageningen, The Netherlands, June 30 - July 3, 2009
- Global and regional emission estimations using halocarbon measurements at background sites, Fifth International Symposium on Non-CO2 Greenhouse Gases (NCGG-5) Science, Reduction Policy and Implementation, Wageningen, The Netherlands, June 30 - July 3, 2009
- Overview of comparisons of non-CO2 trace gas measurements between AGAGE and NOAA at common sites, 15th WMO CO2 experts meeting, Jena, September 2009
- Simulation of maturity and decay of methyl chloroform (MCF; CH3CCl3) in the atmosphere, AGU fall meeting, San Francisco, December 2009
- Halogenated greenhouse gas emissions over Central Europe inferred from ambient air measurements and 222-Rn activity, EGU meeting, Vienna, May 2010
- CHF_3 (HFC-23) emission trend response to $CHClF_2$ (HCFC-22) production and recent emission abatement measure, NOAA ESRL 2009 Global Monitoring Annual Conference, May 18-19th, 2010
- Top-down Validation of European Halocarbon Emission Inventories, NOAA ESRL 2009 Global Monitoring Annual Conference, May 18-19th, 2010

POSTERS
- Tetrafluoromethane in the Global Atmosphere, AGU fall meeting, San Francisco, December 2008
- The International Halocarbons in Air Comparison Experiment: First Results, AGU fall meeting, San Francisco, December 2008
- Long term continuous measurements of OVOCs at Mace Head, Ireland, RSC meeting, 2009
- Tetrafluoromethane in the Global Atmosphere, NOAA ESRL 2009 Global Monitoring Annual Conference, May 13-14th, 2009
- New Estimates of Global Sulfur Hexafluoride Emissions using AGAGE and NOAA data, NOAA ESRL 2009 Global Monitoring Annual Conference, May 13-14th, 2009
- Long term continuous measurements of OVOCs at Mace Head, Ireland, Royal Society of Chemistry meeting, 2009
- Evaluation of the Picarro G1301 and deployment at three Irish sites, 15th WMO CO2 experts meeting in Jena, September 2009
- Perfluorocarbons in the global atmosphere: a) Measurements of tetrafluoromethane, hexafluoroethane, and octafluoropropane, AGU fall meeting, San Francisco, December 2009
- Atmospheric Sulphur Hexafluoride: Measurements and Emission Estimates from 1970 – 2008, AGU fall meeting, San Francisco, December 2009
- Perfluorocarbons in the global atmosphere: b) Emission estimates using inversions of atmospheric observations of tetrafluoromethane, hexafluoroethane, and octafluoropropane, AGU fall meeting, San Francisco, December 2009
- Simulation of maturity and decay of methyl chloroform (CH3CCl3) in the atmosphere, AGU fall meeting, San Francisco, December 2009
- Inverse modelling European CH_4 and N_2O emissions, NitroEurope Open Science Conference, Solothurn, February 2010
- Growth of HFC-143a (CH_3CF_3) in the atmosphere determined from in situ observations at AGAGE observatories, EGU meeting, Vienna, May 2010

1.3 Meetings

DEFRA kick-off meeting, London (March 2008). Presented methodology.
AGAGE 37, Grindelwald, Switzerland (June 2008). Presented baseline concentration methodology and results.
Co-ordination meeting with Bristol University, Met Office (Sept. 2008).
EUROHYDROS annual meeting, Bologna, Italy (Sept. 2008). Presented work related to hydrogen baseline concentration and issues with estimating emissions.
6-month review meeting with DEFRA, London (Oct. 2008). Presented emission estimate results.
Co-ordination meeting with Edinburgh University (Nov. 2008)
AGU annual meeting, San Francisco, USA (Dec. 2008). Gave oral presentation. Compared baseline concentrations of HFC-134a at Mace Head (Ireland), Cape Grim (Australia) and Trinidad Head (USA) and presented regional emission estimates for NW Europe, Australia and USA.
Co-ordination meeting with Bristol University, University of Bristol (Jan. 2009)
NITROEUROPE annual meeting, Gothenburg, Sweden (Jan 2009). Presented results of multi-site inversion for methane over Europe for 2006.
LULUCF sponsored meeting discussing inversion methodologies and additional UK observations linked to Integrated Carbon Observing System (ICOS), University of Edinburgh (Feb 2009).
NERC QUEST Science Liaison Group, London (Feb 2009). Discussed benefits of additional UK observations and how to fund them.
Co-ordination meeting with Leicester University, Met Office (Feb 2009). Discussed progress of work to use satellite observations to infer emissions.
DECC review meetings April and October 2009.
Attended the Weybourne Advsory Group (May 2009) to discuss the use and future of observations at the UEA Weybourne station.
Co-ordination meeting with Bristol University, Prof. Derwent and Prof. Simmonds. (July and Dec. 2009).
ICOS meeting in London (July 2009).
Attended the UK-EOF meeting in Reading about the use of observations (July 2009).
NISC meeting in London (Sept 2009).
Visited Cambridge University to give a seminar about inversion modelling (Sept 2009).
NITROEUROPE modellers' meeting (Oct 2009) and full annual meeting (Feb 2010).
Defra sponsored workshop on GHG emissions from agriculture (Nov 2009).
Attended MethaneNet kick-off meeting in Milton Keynes (Jan 2010).
Presented inversion work to the Royal Society (Feb 2010).
Presented inversion work to the IPCC workshop on uncertainty in emission estimates (Mar 2010).
AGAGE meeting – China (May 2010), presented CH_4/N_2O work.
AGAGE meeting – Australia (Nov 2010), presented emission estimates from Gosan data.

1.4 Abbreviations

Table of Abbreviations and Definitions

AGAGE	Advanced Global Atmospheric Gases Experiment
AGU	American Geophysical Union
CEOSA	Climate, Energy and Ozone: Science and Analysis Division
CFC	Chlorofluorocarbon
DECC	Department of Energy and Climate Change
DEFRA	Department for Environment, Food and Rural Affairs
ECD	Electron Capture Detector
ECMWF	European Centre for Medium-Range Weather Forecasts
eCO_2	CO_2 equivalent
EDGAR	Emissions Database for Global Atmospheric Research
EEA	European Environment Agency
EMEP	European Monitoring and Evaluation Programme
EMPA	Swiss Federal Laboratories for Materials Science and Technology
ESRL	Earth System Research Laboratory
FID	Flame Ionisation Detector
GAGE	Global Atmospheric Gases Experiment
GC	Gas Chromatograph
GHG	Greenhouse Gas
GMD	Global Monitoring Division
GWP	Global Warming Potential
HCFC	Hydrochlorofluorocarbon
HED	High Energy Dinode
HFC	Hydrofluorocarbon
HFE	Hydrofluoroether
HFO	Hydrofluoroolefin
ICOS	Integrated Carbon Observation System
IPCC	Intergovernmental Panel on Climate Change
IRF	Integrated Radiative Forcings
MD	Multi-Detector
MS	Mass Spectrometer
NAEI	National Atmospheric Emissions Inventory
NAME	Numerical Atmospheric dispersion Modelling Environment
NERC	Natural Environment Research Council
NMHC	Non-Methane Hydrocabon
NOAA	National Oceanic and Atmospheric Administration
ODP	Ozone Depletion Potential
OVOC	Oxygenated Volatile Organic Compound
PFC	Perfluorocarbon
ppb	Part Per Billion
ppm	Part Per Million
ppt	Part Per Trillion
RGA	Reduction Gas Analyser
UEA	University of East Anglia
UKGHGI	UK Greenhouse Gas Inventory
UNEP	United Nations Environment Programme
UNFCCC	United Nations Framework Convention on Climate Change
WMO	World Meteorological Organization

2 Instrumental Performance

2.1 Summary of Gases measured

AGAGE measured species. Medusa in Blue; GC-MD: Green; Both: Red.

Compound	~NH (2009) (ppt)	Typical % precision	Compound	~NH (2009) (ppt)	Typical % precision
CF_4	78.1	0.15	H-1211	4.34	0.4
CHF_3	23.1	0.7	H-1301	3.27	1.7
C_2F_6	4.07	1	H-2402	0.474	2
C_3F_8	0.53	3	CH_3Cl	537	0.2
c-C_4F_8	1.25	1.5	CH_3Br	8.0	0.6
CH_2F_2	6.1	3	CH_3I	0.8	2
SF_6	6.91	0.6	CH_2Cl_2	37	0.5
SO_2F_2	1.64	2	CH_2Br_2	1.4	1.5
HFC-134a	58.0	0.5	$CHCl_3$	11	0.4
HFC-152a	9.0	1.4	$CHBr_3$	3	0.6
HFC-125	8.0	0.7	CCl_4	85	1
HFC-143a	10.7	1	CH_3CCl_3	9.2	0.7
HFC-227ea	0.56	2.2	$CHCl=CCl_2$	0.5	3
HFC-236fa	0.072	10	$CCl_2=CCl_2$	3	0.5
HFC-245fa	1.19	3	COS	370-570	0.5
HFC-365mfc	0.59	5	C_2H_2	10-200	0.5
HFC-43-10mee	0.18	3	C_2H_4	50-500	2
HCFC-22	212	0.3	C_2H_6	500-2000	0.3
HCFC-141b	21.3	0.5	C_6H_6	10-100	0.3
HCFC-142b	21.3	0.4	C_7H_8	0.1-2	0.6
HCFC-124	1.56	2			
CFC-11	243	0.2	**GC-MD Only**	**(ppb)**	
CFC-12	537	0.1			
CFC-13	2.90	2	**CH_4**	1835-1880	**0.2**
CFC-113	76.0	0.2	**N_2O**	322.8	**0.05**
CFC-114	16.57	0.3	**CO**	86-140	**0.2**
CFC-115	8.40	0.7	**H_2**	480-514	**0.6**

(ppt = parts per trillion, ppb = parts per billion)

2.2 GC-MD

2007 (July – Dec). An important change in air sampling occurred in May 2007, the metal bellows pump traditionally used by the MD for air sampling was removed and was replaced by a tee from the Medusa air sample module. This air sample module now supplies both the GC-MD and Medusa-MS. However there are a number of outstanding data issues relating to drift and jumps in the principal CFCs and CCl_4.

2008. There were very few mechanical failures of the Mace Head GC-MD instrument during 2008. Unfortunately an attempt to improve the resolution of CFC-113 and methyl iodide (CH_3I) by increasing the phase loading on the GC column was not successful. It will require further research to see if a different phase could improve this resolution problem without compromising other species. The interference of CH_3I with the CFC-113 peak is predominately a summertime problem when large ocean emissions of CH_3I (produced by macroalgae in the ocean surface layers) are observed at Mace Head. The hydrogen data has been more noisy and erratic than the historical record, mainly caused by problems with the hydrogen generator. There has been a big improvement in the frequency of power outages after installation of standby generator.

A Mace Head calibration tank was measured at EMPA, Switzerland using an aerolaser prior to arriving at Mace Head. This independent check of the carbon monoxide concentration contained in the calibration tank is a vital check of the calibration scale employed at Mace Head. It is envisaged that a selection future "tertiary" calibration gases will undergo this type of comparison in the future. Similarly a Mace Head calibration tank was measured against the new calibration scale for hydrogen developed at Max Planck-Institute for Biogeochemistry, Jena. This independent check of the hydrogen concentration contained in the calibration tank is a vital check of the calibration scale employed at Mace Head. It is envisaged that a new calibration gas will be purchased for Mace Head and undergo this type of comparison on a regular basis (annually) in the future

2009. Overall there were no mechanical failures of the Mace Head GC-MD instrument during 2009, although the RGA3, which measures CO and H_2, was troublesome with periodic noisy baselines. There were a larger number than usual standard tank comparisons which may have contributed to some of this instability. Even with the standby generator there were still a few power outages due to tripping of the circuit breakers. A contaminated cylinder of argon-methane (P5) carrier gas contributed to noisy data with large offsets in the baseline effecting CFC-11, CFC-113, $CHCl_3$, CH_3CCl_3, CCl_4 between 17th January 2009 and 12th February 2009. Frequent trap bake-out cycles to clean up the carrier gas supply were unable to cure this problem. The data quality improved once the impure carrier gas was removed and the clean-up traps baked and cleaned.

2010. During 2010 there was only one mechanical failure of the Mace Head GC-MD instrument, although the RGA3, which measures CO and H_2, has been troublesome with periodic noisy baselines. There have been a larger number than usual of standard tank comparisons which may have contributed to some of this instability. We have just received a new style lamp and power unit tested by the University of Heidelberg. It is hoped that this change will stabilise the RGA3 performance. Even with the standby generator there have still been a few power outages due to tripping of the circuit breakers. Channel 2 columns (Silicone columns) were changed on 3rd June 2009 with no significant change in precisions for any species. However, several species had improved precisions prior to the column change – possibly due to changes in column flow. The only mechanical failure to report was that of the valve 6 actuator (channel 2, backflush valve). It was noted from variations in channel 2 peak retention times that the backflush valve switched intermittently (3rd March 2010). The valve was manually set and disabled in the backflush position until a replacement electric actuator could be sent from Scripps Institution of Oceanography (SIO). The replacement actuator was fitted on 26th April 2010.

2.3 Medusa GC-MS

2007 (July – Dec). There were a number of changes to the Medusa system: A new hard disc drive was installed on agage3 computer (2nd May 07), at this time the new configuration for air sample module was implemented. This resulted in the module supplying ambient air to both the Medusa and the GC-MD. This option was chosen due to the high failure rate of metal bellows pumps that had historically been used to supply the MD. Having said this - we did not experience many failure of this type of pump at Mace Head. It was thought that running air sample module in continuous mode might improve the potential CHF_3 contamination experienced using the air sample module, the unit was run in this mode between 3rd – 16th July 07, however, this mode of operation caused problems with a range of other compounds, so we switched back to non-continuous mode (KNF being switch on prior to each sample acquisition). The sampling protocol was adjusted to allow sampling of the laboratory air (21st August 07) once per week. Results from the first analysis exhibited very high values for certain species, notably HCFC-142b – Gerry Spain removed possible source of HCFC-142b (foam) from lab. In subsequent weeks the levels of this compound in the lab have dropped dramatically. As might be expected certain hydrocarbon species (benzene, toluene, xylenes) are also very high because they are laboratory reagents and used in many applications that can out-gas these compounds.

In October 2007 the KNF air pump with viton diaphragm was replaced with a new pump containing a neoprene diaphragm. This pump ran for 2 days before stopping mid run, it was determined that the pump motor was overheating; the motor was replaced with the motor from the pump that had been removed. A site visit was carried out from 24th-26th October 2007. The PoraBOND-Q main column was replaced, in order to re-establish peak resolution which had deteriorated over time with the old column. In December 2007 it was noted that the chromatographic baseline was "wandering" and degradation in the precision of the ambient air analysis was occurring. The degradation was worse of some compounds than others. After many tests were carried out on-site at Mace Head, an air leak was found at the head of the chromatographic column. Whilst tightening the nut to fix the leak, the fitting broke. The GCMS was shutdown whilst the broken fittings were replaced (13th December 2007).

After restarting the GCMS the issue of the air leak was resolved however the baseline oscillation persisted. It was decided that the most likely cause of the problem has been ingess of air from the leak oxidising the new chromatographic column which has been in use since October 24th, a replacement column was ordered and installed on December 18th. Initially it appeared that the oscillation had been resolved, however, inspection of the data after the Christmas break indicated the oscillation had reoccurred.

2008. In an attempt to determine if the problem was column related the original column (pre-October and pre-oscillation) was reinstalled (January 2nd) to determine if the oscillation persisted, it did, thus ruling out the column as the source of the problem? A series of test were devised to isolate potential components of the sampling system as a source of the oscillation (valves were realigned, valves were switch around, the Agilent auxiliary units, used to supply and control the gas pressures were swapped around, the helium cylinder fittings and all lines were extensively leak checked, the regulators were pressure pulsed), all without success. A less likely but possible source of the problem was the mass spectrometer itself. After discussions with service engineers at Agilent a series of tests and procedures for cleaning components within the mass spectrometer were formulated. One of the first tests was to blow out the interior of the ion-source and quadrupole housing with clean air to remove and dust/particles that might be contained (10^{th} January 2008). This procedure resolved the oscillation, the hypothesis being that the particle(s) contained within the chamber were becoming charged and causing the compound ions (mass fragments) to be deflected from the HED. This deflection caused a drop in the ion abundance reaching the detector and hence a drop in signal. This persisted until the charged particle became unstable and discharged and the ion abundance was re-established, this charge/discharge process continued continuously causing an oscillation in the sample baseline. On the 7^{th} July 2008 it was noted that the counter-purge flow was not at the correct flow rate (250ml/min), the only way to achieve this flow was to increase the supply pressure to the nafion dryer from the recommended 7psig to 30 psig. After a number of experiments it was determined that a blockage had developed in the tubing connecting the outlet from nafion 1 to the inlet of nafion 2. The tubing was replaced on 11^{th} July 2008 and the correct counter-purge flow (250ml/min) was achieved with a pressure setting of 7 psig. The precision of the standards and the general stability of ambient measurements measured using the Medusa continued improved and the instrument continued to run well.

2009. The Medusa GC-MS ran exceptionally well during 2009. Following problem with noisy data in Jan 2009, the MS was shutdown and filaments were changed. The Varian solenoid fuse associated with the Varian valve and Medusa vacuum shell failed on a number of occasions with the loss of data for CF_4. Simon O'Doherty carried out a site visit from 23^{rd} – 27^{th} January 2009, during this visit the ion-source was changed. The MS was shutdown on 2^{nd} July 2009 to change the ion-source, when restarted the ion-source temperature was apparently at 510ºC. All connections were ok and the problem was resolved by replacing the source heater block. On June 11^{th} it was noted that the Medusa sample module heater fan had seized. The fan was replaced on the 17^{th} June. A power cut on 29^{th} June caused the Medusa to shutdown. After power was restored the Cryotiger would not cool below 40ºC. Cooling was restored after running the "baseplate warm-up procedure" and sampling was restarted on 2^{nd} July. Staff at Scripps Institution of Oceanography upgraded the GCWerks software on 2nd July. On 7th July the Porabond-Q column was replaced with an AGAGE batch produced column, the heated Valco helium purifier was also installed.

2010. The Medusa GC-MS performed well in 2010 with only one major instrumental problem. This instrumental problem occurred during a period with no cover at the Mace Head site (Staff were on holiday after the AGAGE meeting in La Jolla). On 31st October 2010 the instrument device drivers lost communication and trap 2 heated to 100 °C and remained at this temperature until 9th November 2010. When the device drivers were restarted trap 2 remained at 100 °C, it transpired that the trap set-point had changed to 100°C from -200 °C, once this parameter was reset the trap cooled. As a consequence of the prolonged heat input from trap 2, the baseplate minimum temperature rose from -176 °C to -169 °C and the trap 2 minimum temperature rose from to -169 °C to -148 °C. The initial concern was that the baseplate and/or trap 2 had been permanently damaged. After restarting the instrument in an exploratory exercise, the chromatographic resolution was shown to be unaffected. However, the differential temperature between trap 2 and the baseplate was larger than usual -21 °C instead of -16 °C. This temperature differential showed signs of returning to normal as the trap and baseplate slowly reached lower temperatures. It was decided to continue sampling until a service visit could be scheduled to examine the trap and baseplate. The scheduled service visit had to be postponed, by this time the recovery of the minimum temperature and precision of the data was such that it was decided that to remove the baseplate and trap 2 was unnecessary and could potentially introduce more problems than it would solve. The consequence of this problem resulted in a loss of all Medusa data between 31^{st} October and 9^{th} November 2010, followed by a continued loss of CF_4 data until the 28^{th} November when the baseplate/trap 2 temperature dropped low enough to allow quantitative trapping of this very volatile compound.

Compound	Data Recovery (%)		
	2008	2009	2010
CH_4	86	94	84
N_2O	82	88	81
CFC-12	84	88	81
CFC-11	83	86	82
CFC-113	82	88	84
$CHCl_3$	85	88	85
CH_3CCl_3	83	88	85
CCl_4	85	90	85
CO	82	92	88
H_2	84	91	87

Table 1. Illustrating the percentage data recovery achieved using the AGAGE-MD

Compound	Data Recovery (%)		
	2008	2009	2010
HFC-23	82	76	80
HFC-125	84	75	82
HFC-143a	84	76	82
HFC-134a	83	75	83
HFC-152a	84	75	82
HFC-227ea	85	76	83
HFC-236fa	65	65	70
HFC-245fa	52	73	68
HFC-365mfc	83	77	81
HCFC-22	82	75	81
HCFC-142b	83	75	82
HFCF-141b	84	75	82
SF6	83	74	83
PFC-14	79	69	76
PFC-116	84	76	83
PFC-218	84	77	83
Halon-1211	84	75	83
Halon-1301	84	76	82
Halon-2402	84	74	82
CH_3Cl	78	73	80
CH_3Br	83	76	81
CH_3I	84	76	82
CH_2Cl_2	84	75	83

Table 2. Illustrating the percentage data recovery achieved using the AGAGE-Medusa

2.4 INTERCOMPARISONS AND INTERCALIBRATIONS

On-going inter-comparisons of AGAGE data with independent data collected at common sites are useful as they are sensitive diagnostic tests of data quality for the laboratories involved and they enable data sets to be merged more accurately for use by AGAGE scientists and other researchers (e.g. by modellers). At Mace Head, inter-comparisons have been carried out between AGAGE in situ data and flask data collected by laboratories such as NOAA/ ESRL /GMD (USA).
An example of the comparisons carried out between AGAGE *in situ* GC-multi-detector CH_4 data and other laboratory data (flask) is shown in Figure 1. In situ AGAGE data, that are compared to flask data, were selected within a window of 1-3 hours either side of the time of collection of the flask data.

The flask *in-situ* comparisons for each species consist of 3-panel figures. The 3-panels consist of: Panel (1) shows both of the full data sets as time series. Panel (2) shows only the matched data points as time series. Panel (3) shows the differences between the data sets as a function of time, and includes the mean difference and the standard deviation of the mean difference. The difference data have also been 2-sigma clipped about a running mean to remove outliers (the running mean width in points is indicated on the plot). The clipped data are shown in orange and the final running mean line is shown in green. All

points marked as orange in all the other panels correspond to the clipped values. NOTE: the running mean width is reduced at the beginning and end of the data in the following manner: the initial part of the smoothed line is given by $\Delta Conc\_avg(i)=\Sigma(\Delta Conc(1:i+(n-1)/2+1))/(i+(n-1)/2+1)$ until the full smoothing width (n) is achieved (at i=(n-1)/2+1). These comparisons are carried out for all species that are measured at Mace Head and NOAA/ESRL/GMD (USA).

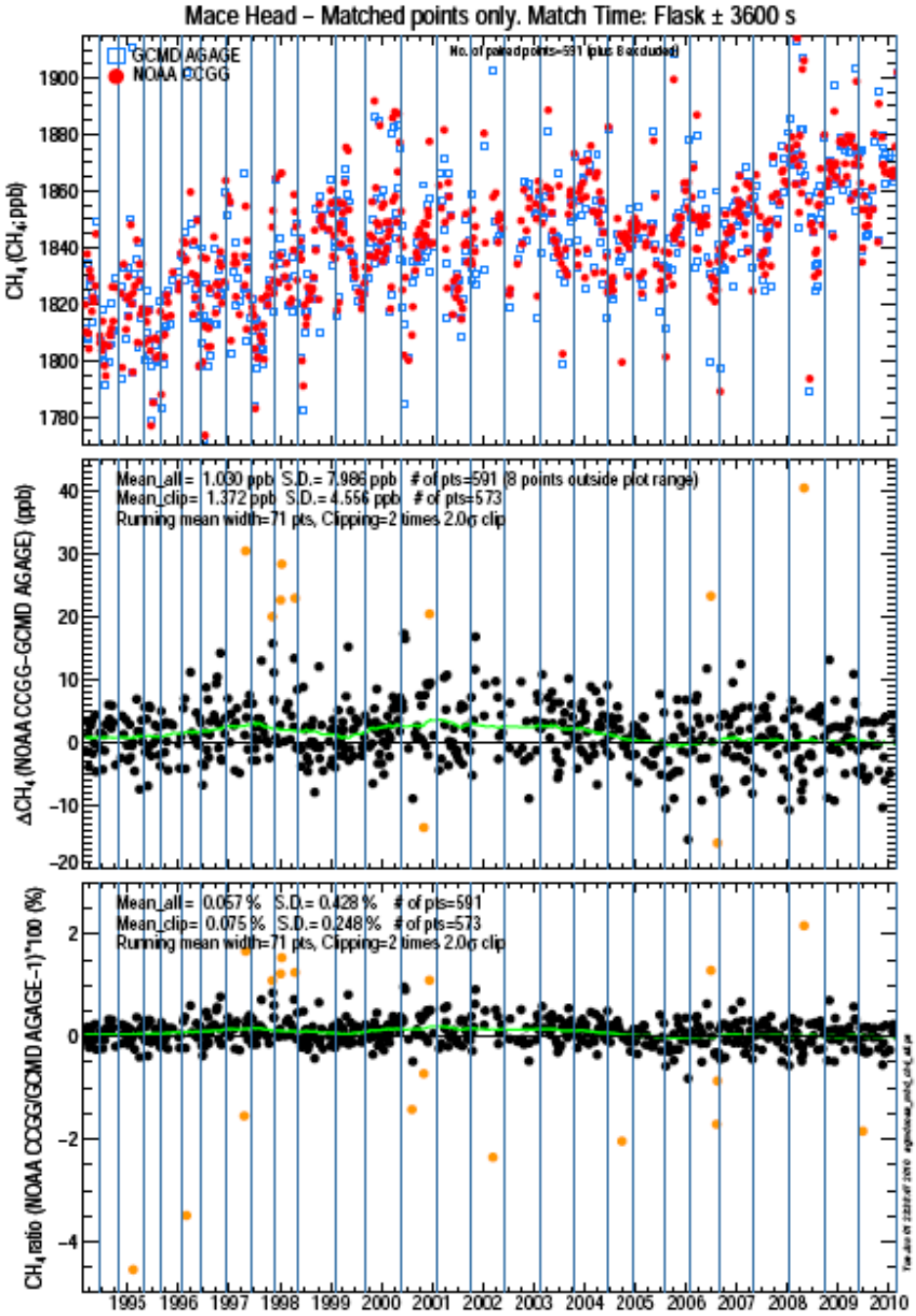

Figure 1. Example of inter-comparison plots for AGAGE Mace Head in CH_4 in-situ data and NOAA CH_4 flask data.

3 Baseline analysis of Mace Head observations

2.1. Introduction
2.2. Methodology
2.3. Baseline concentrations
2.3.1. CFC
2.3.2. HCFC
2.3.3. HFC
2.3.4. Fluorine compounds (PFC)
2.3.5. Chlorine compounds
2.3.6. Bromine compounds
2.3.7. Hydrocarbons
2.3.8. Oxides of carbon, nitrous oxide, ozone and hydrogen

3.1 Introduction

This section presents the baseline concentrations estimated from the Mace Head observations for the years 1990-2010 inclusive. Baseline concentrations are defined here as those that have not been influenced by significant emissions within ten days of the travel, i.e. those that are well mixed and are representative of the mid-latitude Northern Hemisphere background concentrations.

The observations at Mace Head from February 1989 to December 2010 have been analysed for each gas measured. The principle tool used to estimate the trends in baseline concentration for each gas is the NAME dispersion model. The methodology used is presented first followed by the analysis of each individual gas. The analysis considers the long term trend of the monthly and annual baseline concentrations, their rate of growth and their seasonal cycle.

3.2 Methodology

This section describes in detail how the monthly baseline concentrations for each gas observed at Mace Head were derived. There are several specific stages to the process and the section is broken down into these segments with examples were possible.

The NAME model is run backwards-in-time to estimate the recent history (12 days) of the air en-route to Mace Head. Air history maps, such as those shown in Fig.2, has been calculated for each 3-hour period from 1995-2010 using UM meteorology and from 1989-2008 using ERA-Interim meteorology, amounting to more than 90000 air history maps. The model output estimates the 12-day time-integrated air concentration (dosage) at each grid box (40km horizontal resolution and 0-100m above ground level) from a release of 1 g/s at Mace Head (the receptor). The 3-D nature of the NAME model ensures that it is not just surface transport that is modelled, an air parcel can travel from the surface to a high altitude and then back to the surface but only those times when the air parcel is within the lowest 100m above the ground will it be recorded in the maps. The computational domain covers 100^{o}W to 45.125^{o}E longitude and 10^{o}N to 80.125^{o}N latitude and extends to more than 10km vertically (actual height varies depending on version of meteorology used). For each 3-hour period 33,000 inert model particles were released and followed, sufficient to describe the dispersion over 12 days. No chemical or deposition processes were modelled, this is realistic given the long atmospheric lifetimes of the vast majority of gases considered.

By dividing the dosage [gs/m^3] by the total mass emitted [3600s/hr x 3hr x 1g/s] and multiplying by the geographical area of each grid box [m^2], the model output is converted into a dilution matrix [s/m]. Each element of this matrix *D* dilutes a continuous emission (*e*) of 1 g/m^{2}s from a given grid box over the previous 12 days to an air concentration [g/m^3] at the receptor (*o*) during a 3-hour period.

$$D\,\underline{e} = \underline{o} \qquad \ldots 1$$

Baseline concentrations are defined here as those that have not been influenced by significant emissions within the previous twelve days of travel en-route to Mace Head, i.e. those that are well mixed and are representative of the mid-latitude Northern Hemisphere background concentrations.

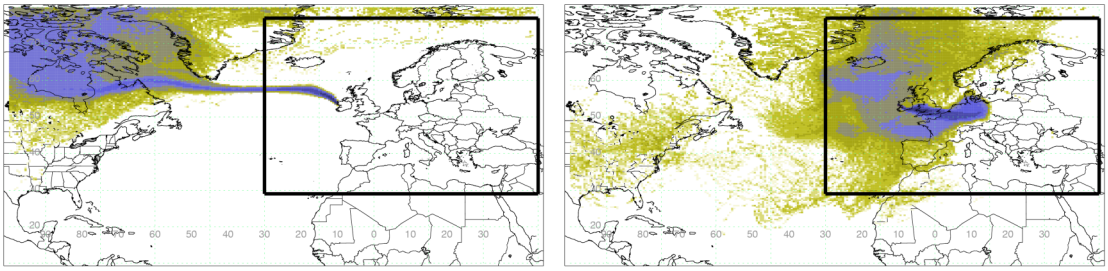

(a) (b)

Figure 2: Examples of 3-hour air history maps derived from NAME (a) baseline period (b) regionally polluted period. The air-history maps describe which surface areas in the previous 12-days impact the observation point at a particular time.

A three-hour period is classed as 'baseline' if it meets the following criteria:

- The total air concentration from the nine grid boxes centred on and surrounding Mace Head is less than ten times the *dilution sensitivity limit* (defined below) i.e. local emissions do not significantly contribute.
- The total air concentration contribution from the European land mass is less than five times the *dilution sensitivity limit* i.e. European emissions do not significantly contribute.
- The contribution from the southerly latitudes is less than twice the *dilution sensitivity limit* indicating that southerly latitude air is not significantly present.

In order to define a *dilution sensitivity limit* it is necessary to arbitrarily decide on a level of emission that would produce an agreed response at the observation point. In this study we chose an emission of 100 kt CH_4 /yr/grid to produce a 10 ppb impact. As shown later, 10 ppb is approximately the noise found in the baseline signal for methane and an emission of 100 kt/year is about 4% of the estimated UK release of methane in 2006. At a standard temperature and pressure of 273.15 K and 1000 mb respectively, 10 ppb CH_4 is equivalent to ~7 ug/m3. Assuming a horizontal grid resolution of 40 km at a latitude of 50^o N, 100 kt CH_4 /yr/grid is approximately ~2 ug/m^2/s, thus the *dilution sensitivity limit* is calculated, using equation 1, to be 3.4 s/m.

The *dilution sensitivity limit* is attempting to define a threshold above which an emission source would generate a concentration at Mace Head that would be discernible above the baseline noise. The same limit value is used for all of the gases analysed. Although the chosen limit value is somewhat arbitrary the impact of doubling it is small.

Figure 3 shows a three month extract of the methane observations measured at Mace Head. The observations have been colour coded to indicate whether, using the above classification, the air mass they were sampled from was considered baseline. For the baseline analysis all non-baseline observations are removed.

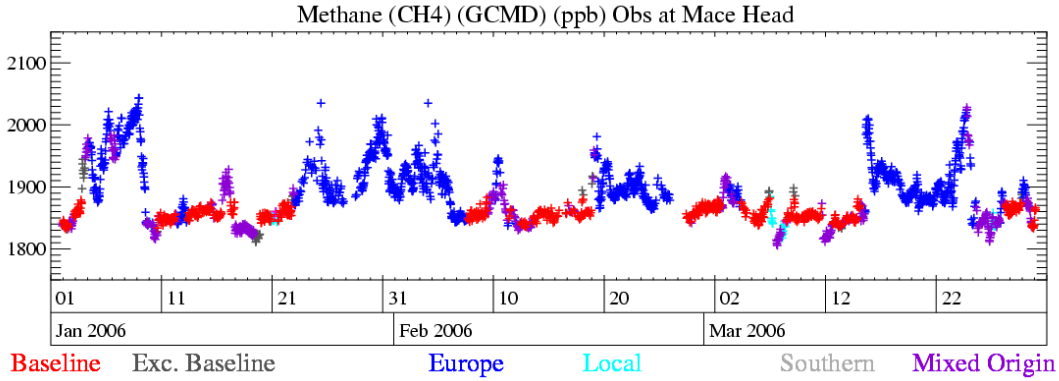

Figure 3: 3-month time-series of Mace Head methane observations showing the impact of the baseline and non-baseline classification. The baseline observations are shown in red.

The points defined as baseline using the above methodology still have a certain level of noise. The principle reasons for this are; emissions from the populated regions of the USA and Canada, unexpected emissions for instance forest fires in Canada or from shipping, local emissions that are not identified using the above criteria above, incorrectly modelled meteorology or transport, i.e. European air defined as baseline by error.

Irrespective of the methodology used to identify these events some will inevitably be classed as baseline when it is inappropriate to do so. To capture such events the baseline data are statistically filtered to isolate and remove these non-baseline observations. For each baseline point in turn, the baseline points in a 40-day window surrounding this central value are considered and, provided that there are sufficient points (>8 with at least 3 in each third of the window), a quadratic is fitted to these values. The standard deviation of the actual points and the fitted curve is calculated (*std*) and if the current baseline value is more than *x std* away from the fitted value it is marked for exclusion from the baseline observations. After all baseline points have been considered, those to be excluded are removed. The process is repeated nine times, each time the value for *x* is gradually reduced from 6 to 2, thus ensuring that those points statistically far from the fitted baseline do not unduly affect the points to be excluded by skewing the fitted curve. If there are fewer than 9 baseline points in a 40 day window none are excluded. The observations removed through this statistical filter are shown in black in figure 3.

For each hour in the time-series the baseline points in a running 40-day window are fitted using a quadratic function and the value extracted for the current hour in question. The process is then advanced by an hour and repeated. If there are insufficient baseline points (fewer than 30) well spaced within the window (at least 10 in each third) it is gradually extended up to 150-days.

For each hour within the observation time record a smoothed baseline concentration is estimated by taking the median of all fitted baseline values within a 20-day time window. If there are fewer than 120 baseline values in the time window then the window is steadily increased up to a maximum of 40 days. If there are still insufficient points then no smoothed baseline concentration is estimated for that hour.

The noise or potential error in the smoothed baseline concentration is estimated to be the standard deviation of the difference between the observations classed as baseline and the smoothed baseline concentrations at the corresponding times. Figure 4 shows, on a much expanded y-axis compared to Figure 3, the typical spread of baseline observations about the smoothed continuous baseline estimate. For methane the baseline noise over 1989-2008 using ECMWF meteorology is 8.7 ppb and over 1995-2010 using UM meteorology is 8.3 ppb, the values for nitrous oxide are 0.25 ppb and 0.19 ppb respectively. The reduction in the standard deviation magnitude from using ECMWF meteorology to using Met Office meteorology is thought to be largely attributed to the improved accuracy of the observations from 1994 onwards rather than due to the different meteorology.

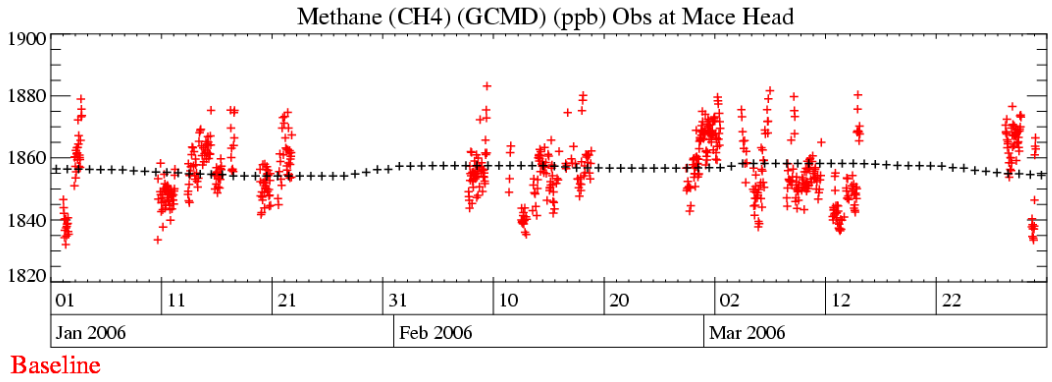

Figure 4: Observations of methane at Mace Head within a 3-month period classed as baseline (red) with the estimated daily baseline concentrations for the same period (black). Note: the y-axis has been expanded compared to Figure 3.

Monthly and annual baseline concentrations are estimated by averaging all of the hourly baseline values within the appropriate time window. A monthly value is estimated if there are at least 504 hourly values (21 days) within the month, this ensures a good representation of the whole month.

The baseline analysis has been conducted with both sets of meteorology (ECMWF and Met Office) for both methane and nitrous oxide. The differences in the estimated monthly baseline concentrations are small, the mean difference in monthly baseline for methane is 0.1 ppb (std = 0.93 ppb) and for nitrous oxide is 0.01 ppb (std = 0.01 ppb), in both cases the baseline derived using ECMWF is, on average, marginally higher. The monthly baseline concentrations from both analyses are shown in figure 5.

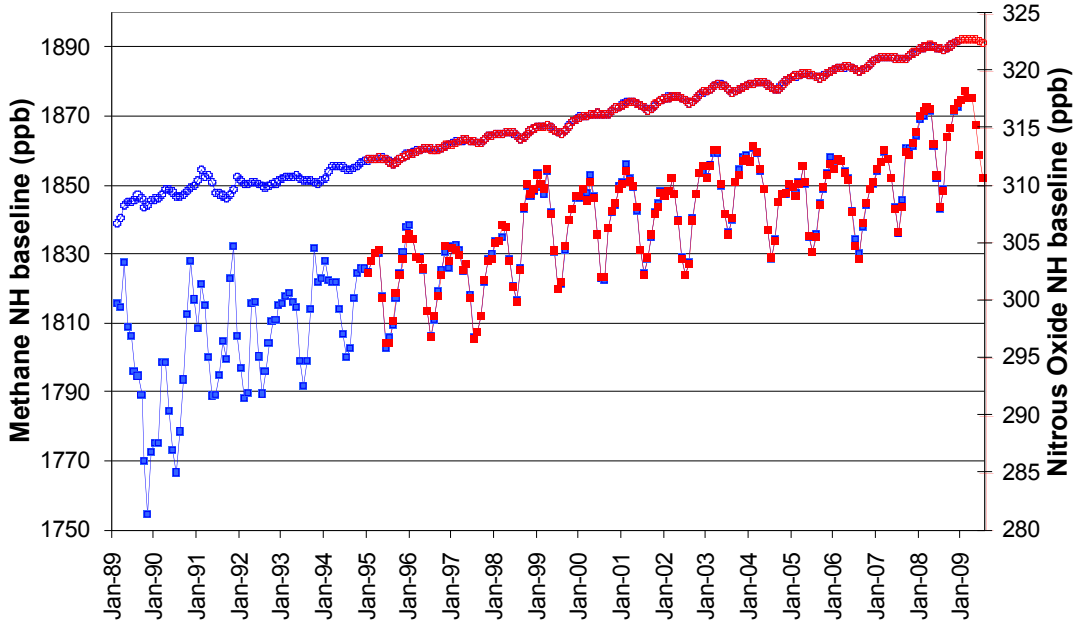

Figure 5: Northern Hemisphere monthly baseline concentrations for methane (solid squares) (left axis) and nitrous oxide (open circles) (right axis). The baseline derived using ECMWF meteorology is shown in blue and using Met Office meteorology in red.

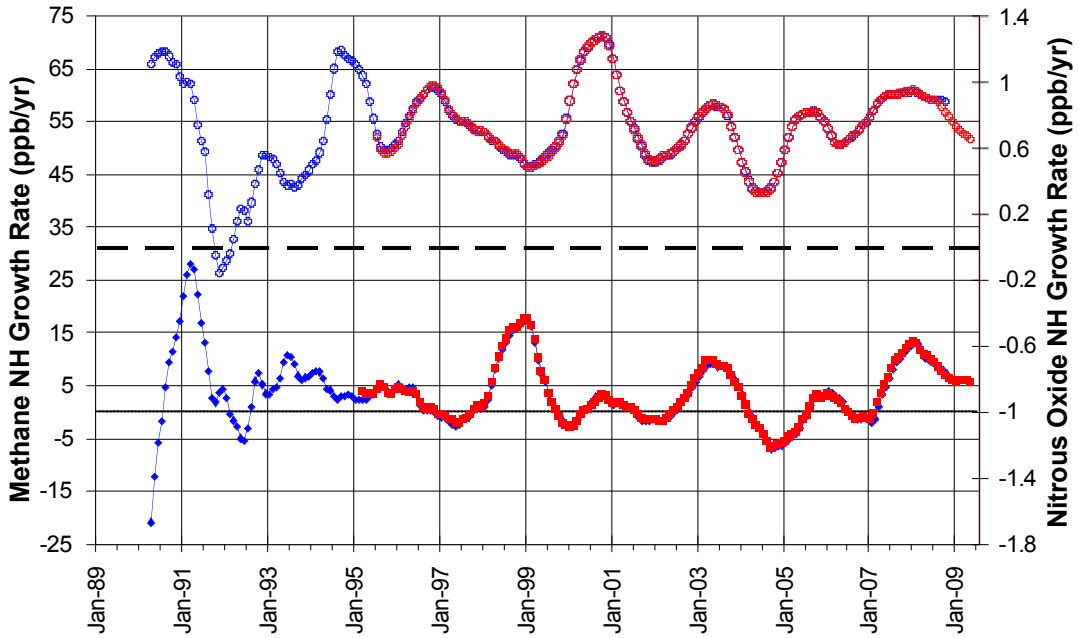

Figure 6: Northern Hemisphere monthly growth rates for methane (solid squares) (left axis) and nitrous oxide (open circles) (right axis). The growth rates derived using ECMWF meteorology is shown in blue and using Met Office meteorology in red. The solid black line and dashed line indicate the zero growth level for methane and nitrous oxide respectively.

The annual growth rate on a particular day is defined as the current daily baseline value minus the previous year's value on the same day, e.g. Growth rate for 14th Jan 1996 = (Daily baseline for 14th Jan 1996) – (Daily baseline for 14th Jan 1995). By averaging the annual growth rate values (one per day) within a running 12-month period (6 months either side of the day), a smoothed annual growth rate per day is estimated. Monthly averages of these growth rates for methane and nitrous oxide are shown in Figure 6.

The monthly baseline concentrations were de-trended to produce perturbation values (S_i) for each month and year using equation (**2**):

$$S_i = C_i - a_i \qquad \ldots 2$$

Where C_i is a monthly mean baseline concentration and a_i is the annual average baseline for month i. a_i is calculated by fitting a quadratic function to five consecutive annual averages (a_1 to a_5) centred on the current month of interest and extracting the appropriate value from the quadratic fit. The de-trended perturbation values (S_i) are averaged for each month over the data period studied to produce the mean values shown in Fig. 7 - 55. The range of values for each month is also shown on the plots.

3.3 Baseline Concentrations

For each gas observed at Mace Head a baseline analysis has been performed. ECMWF meteorology is used from 1989 – 2002 inclusive and Met Office meteorology from 2003-2010 inclusive. The figures that follow illustrate for each gas the monthly and annual baselines, the changing baseline growth rates and the average seasonal cycle seen within the observations. The gases are grouped into similar chemical families; CFC, HCFC, HFC, fluorine compounds (PFCs), chlorine compounds, bromine compounds (halons), hydrocarbons, oxides of carbon and finally nitrous oxide, ozone and hydrogen. Table 1 summaries the annual baseline mass mixing ratios within the observation period for each of the gases considered.

Gas	1990	1991	1992	1993	1994	1995	1996	1997	1998	1999
CFC-11 (GCMD)	264	267	268	269	268	267	266	264	263	261
CFC-12 (GCMD)	496	506	516	522	529	533	537	540	542	544
CFC-13										
CFC-113 (GCMD)	75.5	81.2	84.2	85	84.6	84.6	84.3	83.8	83.2	82.7
CFC-113										
CFC-114										
CFC-115										8
HCFC-124										1.3
HCFC-141b						5.1	7.3	9.7	11.3	13.3
HCFC-142b						8	9.3	10.7	11.4	12.4
HCFC-22										145
HFC-125										1.3
HFC-134a						2.3	4.3	6.3	9.6	13.4
HFC-143a										
HFC-152a						1.2	1.2	1.4	1.9	2.2
HFC-23										
HFC-32										
HFC-227ea										
HFC-236fa										
HFC-245fa										
HFC-365mfc										
PFC-14										
PFC-116										
PFC-216										
SF6										
SO2F2										
CH3Cl										536
CH2Cl2							36.7	36.9	34.9	32
CHCl3 (GCMD)						12.3	12.6	12	12.2	11.6
CHCl3							12.9	12.4	12.8	13.1
CH3CCl3 (GCMD)	151	153	150	139	125	111	95	80	66	55
CH3CCl3										
CCl4 (GCMD)			105	104	103	102	101	100	99	98
CHClCCl2										
CCl2CCl2										
CH3Br										11
CH2Br2										
CHBr3										
Halon-1211						3.5	3.6		4	4.2
Halon-1301										2.8
Halon-2402										
CH3I										
CH4 (ppb)	1792	1808	1803	1812	1817	1821	1824	1822	1835	1839
CO (ppb)						118	129	118	147	124
CO2 (ppm)						360	363	364	367	369
C2H6										
C6H6										
C7H8										
COS										
N2O (ppb)	309	310	310	310	312	312	313	314	314	315
O3 (ppb)	34.6	36.1	35.4	35	36.4	35.1	37.3	37	40.6	41.4
H2 (ppb)						496	502	494	506	508

Table 1a: Summary of annual baseline mass mixing ratios (ppt unless specified) at Mace Head (1990-1999)

Gas	2000	2001	2002	2003	2004	2005	2006	2007	2008	2009	2010	Growth
CFC-11 (GCMD)	260	259	256	255	253	250	248	246	244	243	241	-1.03
CFC-12 (GCMD)	546	546	546	546	545	544	543	541	539	536	534	2.18
CFC-13					2.8	2.8	2.9	2.9	2.9	2.9	2.9	0.02
CFC-113 (GCMD)	82.2	81.5	80.6	79.9	79.3	78.7	77.8	77.1	76.6	76	75.3	0.1
CFC-113						78.8	77.9		76.7	76	75.2	-0.62
CFC-114					16.6	16.6	16.6	16.5	16.5	16.5	16.4	-0.04
CFC-115	8.1	8.2	8.1	8.2	8.4	8.4	8.4	8.3	8.4	8.4	8.4	0.04
HCFC-124	1.4	1.6	1.6	1.6	1.6	1.6	1.6	1.6	1.6	1.6	1.5	0.03
HCFC-141b	15.1	16.3	17.6	18.6	19.1	19.1	19.6	20.4	21	21.3	22	1.11
HCFC-142b	13.6	14.6	15	15.5	16.2	16.9	18.1	19.3	20.6	21.4	21.9	0.93
HCFC-22	151	158	164	169	175	180	187	195	204	212	219	6.8
HFC-125	1.6	2.1	2.4	3.1	3.7	4.3	5	5.8	6.9	7.9	9.2	0.67
HFC-134a	17.1	20.7	24.9	29.6	34.6	39.3	43.7	48	53.3	58	63.2	4.05
HFC-143a					5.5	6.4	7.4	8.4	9.6	10.7	11.9	1.07
HFC-152a	2.5	2.9	3.5	4.2	4.8	5.6	6.8	8	8.9	9	9.4	0.56
HFC-23									22.5	23.1	23.7	0.54
HFC-32					1.1	1.6	2.1	2.7	3.4	4.1	5.2	0.66
HFC-227ea								0.4	0.5	0.6	0.6	0.07
HFC-236fa								0.1	0.1	0.1	0.1	0.01
HFC-245fa								0.9	1.1	1.2	1.3	0.13
HFC-365mfc					0.2	0.3	0.4	0.5	0.5	0.6	0.6	0.08
PFC-14					74.9	75.5	76.2	76.9	77.7	78.1	78.7	0.64
PFC-116					3.7	3.7	3.8	3.9	4	4.1	4.1	0.08
PFC-216					0.4	0.5	0.5	0.5	0.5	0.5	0.6	0.02
SF6					5.6	5.8	6.1	6.3	6.6	6.9	7.2	0.27
SO2F2						1.5	1.5	1.6	1.6	1.7	1.7	0.05
CH3Cl	518	513	513	525	520	527	520	528	533	531	529	-1.65
CH2Cl2	30.3	29.3	29.5	31.1	31	30.7	32.2	34.4	36.1	36.7	39.9	0.15
CHCl3 (GCMD)	11	10.9	11	11.2	11.2	11.1	11.3	11.2	11.6	11	11.6	-0.08
CHCl3	11.7	11.2	10.6	11.3	11	11.1	11.2	10.6	10.5	10.2	11.1	-0.16
CH3CCl3 (GCMD)	47	39	32	27	23	19	16	13	11	9	8	-7.02
CH3CCl3		39.2	31.1	26.8	23	18.8	15.7	13.1	11	9.3	7.9	-3.46
CCl4 (GCMD)	97	96	95	94	93	92	91	90	89	88	87	-1.03
CHClCCl2		1.4	1.1	1.1	1.3	1	1	1.3	0.8	0.6	0.5	-0.1
CCl2CCl2		5.1	4.8	4.8	4.7	3.9	3.8	3.6	3.4	3	3	-0.25
CH3Br	10.5	9.9	9.1	8.9	9.1	10.3	9.5	9.1	9.2	8.6	8.3	-0.23
CH2Br2							1.6	1.7	1.6	1.6	1.8	0.02
CHBr3						5.5	5.9	4.6	4.7	4.8	5.5	-0.11
Halon-1211	4.3	4.4	4.4	4.4	4.5	4.5	4.5	4.4	4.4	4.3	4.3	0.04
Halon-1301	3	3	3.1	3.1	3.1	3.2	3.2	3.2	3.3	3.3	3.3	0.05
Halon-2402						0.5	0.5	0.5	0.5	0.5	0.5	-0.01
CH3I		1.6	1.7	1.8	2	2	1.4	1.6	1.4	0.9	0.9	-0.09
CH4 (ppb)	1842	1842	1842	1851	1847	1846	1846	1854	1864	1868	1869	4.03
CO (ppb)	119	117	126	137	123	123	123	120	120	115		-0.07
CO2 (ppm)	369	371	373	376	378	379	382	384	386	387	390	1.90
C2H6						1287	1321	1337	1353	1066	1068	-48.67
C6H6						66.9	63.9	62.0	67.5	61.9	60.6	-0.71
C7H8						15.8	12.9	14.9	22.6	30.4		3.93
COS								531	486	469	494	-16.75
N2O (ppb)	316	317	318	318	319	320	320	321	322	323	323	0.71
O3 (ppb)	40.9	39.1	40	41.1	40.6	40	41.1	39.8	40.6	40.6		0.28
H2 (ppb)	499	496	497	500	497	500	503	499	501	498		0.09

Table 1b: Summary of annual baseline mass mixing ratios (ppt unless specified) at Mace Head (2000-2010)

Gas	Growth	Growth
CFC-11 (GCMD)	-1.03	-1.75
CFC-12 (GCMD)	2.18	-2.56
CFC-13	0.02	0.02
CFC-113 (GCMD)	0.1	-0.71
CFC-113	-0.62	
CFC-114	-0.04	-0.09
CFC-115	0.04	0.01
HCFC-124	0.03	-0.06
HCFC-141b	1.11	0.47
HCFC-142b	0.93	0.53
HCFC-22	6.8	7.52
HFC-125	0.67	1.15
HFC-134a	4.05	4.10
HFC-143a	1.07	1.18
HFC-152a	0.56	0.13
HFC-23	0.54	0.56
HFC-32	0.66	
HFC-227ea	0.07	0.08
HFC-236fa	0.01	0.01
HFC-245fa	0.13	0.10
HFC-365mfc	0.08	0.03
PFC-14	0.64	0.49
PFC-116	0.08	0.06
PFC-216	0.02	
SF6	0.27	0.28
SO2F2	0.05	0.07
CH3Cl	-1.65	-3.27
CH2Cl2	0.15	2.24
CHCl3 (GCMD)	-0.08	0.07
CHCl3	-0.16	0.43
CH3CCl3 (GCMD)	-7.02	-1.49
CH3CCl3	-3.46	-1.49
CCl4 (GCMD)	-1.03	-1.16
CHClCCl2	-0.1	-0.69
CCl2CCl2	-0.25	-0.21
CH3Br	-0.23	-0.46
CH2Br2	0.02	0.08
CHBr3	-0.11	0.48
Halon-1211	0.04	-0.07
Halon-1301	0.05	0.01
Halon-2402	-0.01	0.01
CH3I	-0.09	-0.25
CH4 (ppb)	4.03	1.25
CO (ppb)	-0.07	0.05
CO2 (ppm)	1.90	1.6
C2H6	-48.67	-146.
C6H6	-0.71	-1.26
C7H8	3.93	
COS	-16.75	7.58
N2O (ppb)	0.71	0.60
O3 (ppb)	0.28	0.57
H2 (ppb)	0.09	-2.38

Table 1c: Summary of average growth rates from entire record and 2010 only (ppt/yr unless specified) at Mace Head.

3.3.1 CFCs

The time series of baseline selected (i.e. minus pollution events) monthly means for atmospheric chloro-flouro-carbons are shown; CFC-11 (Figure 7), CFC-12 (Figure 8), CFC-13 (Figure 9), CFC-113 (Figure 10), CFC-114 (Figure 11) and CFC-115 (Figure 12).

The emissions of all of the CFC compounds have decreased substantially in response to the Montreal Protocol on Substances that Deplete the Ozone Layer, the rate of removal of these compounds by their sinks is limited by their long atmospheric lifetimes. CFC-12, which has a 100 year lifetime, has declined linearly at a rate of 2.6 ppt/yr over the 6-month period (2010) reaching a mixing ratio in December 2010 of 532.7 ppt, as is shown in Figure 8.

Similarly CFC-11 (45 year lifetime) has also declined over the same period at a rate of 1.7 ppt/yr where its mixing ratio at Mace Head is 239.9 ppt in December 2010 (Figure 7). As shown in Figure 10, CFC-113 (85 year lifetime) has declined at a rate of 0.7 ppt/yr over the 6-month period (January-June 2010) to 75.1 ppt in December, 2010.

3.3.1.1 CFC-11

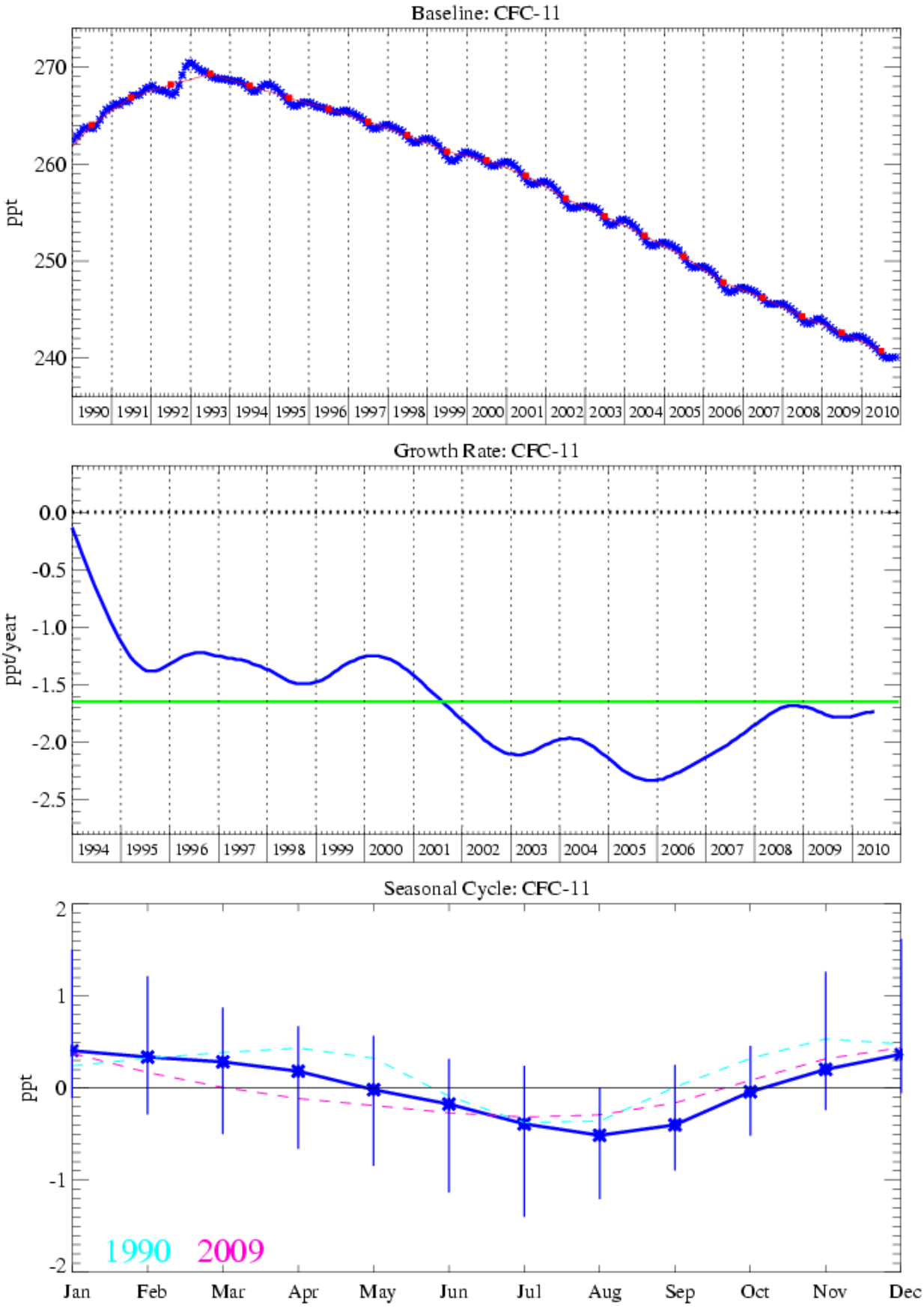

Figure 7: CFC-11: Monthly (blue) and annual (red) baseline (top plot). Annual (blue) and overall average growth rate (green) (middle plot). Seasonal cycle (de-trended) with year to year variability (lower plot).

3.3.1.2 CFC-12

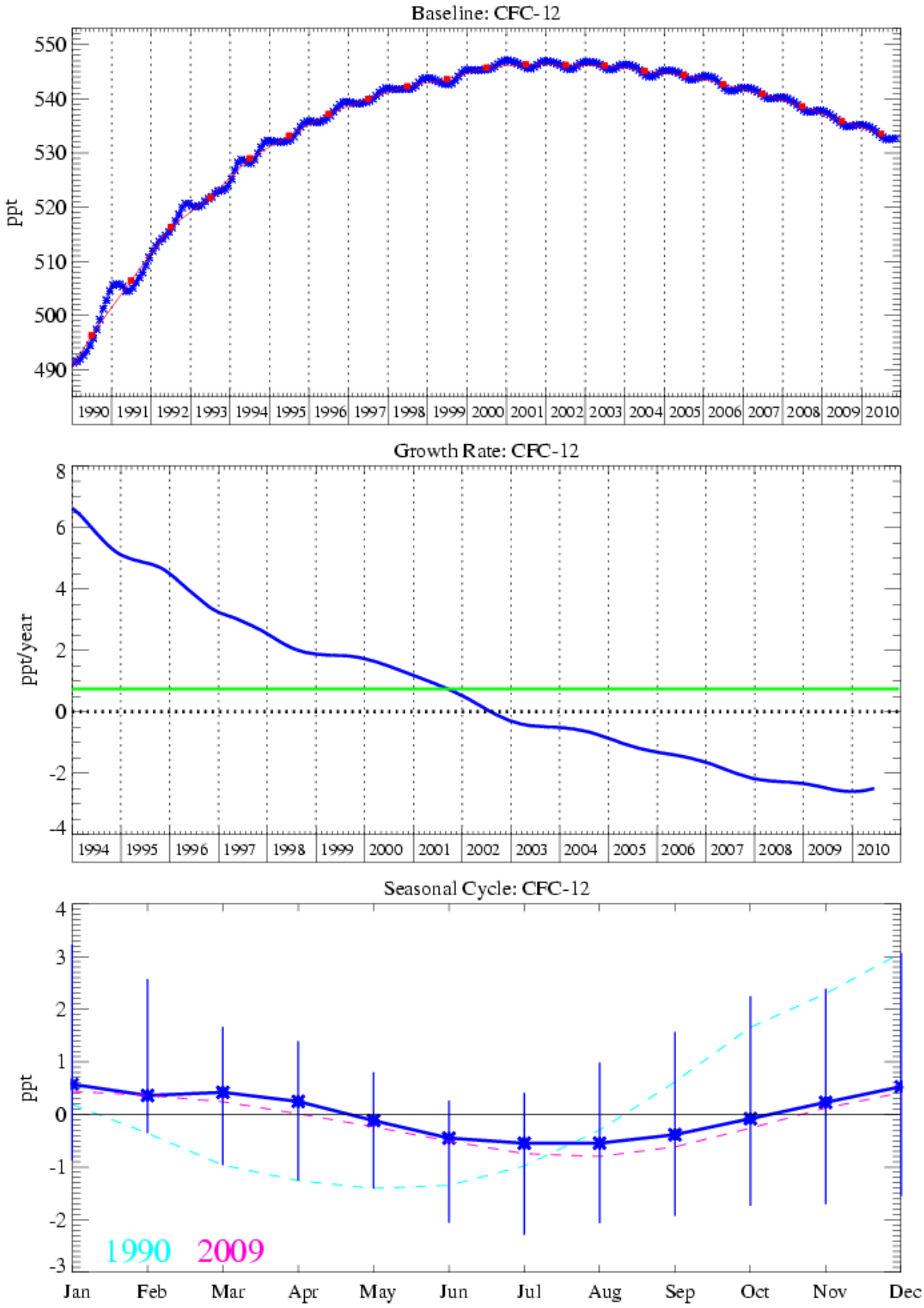

Figure 8: CFC-12: Monthly (blue) and annual (red) baseline (top plot). Annual (blue) and overall average growth rate (green) (middle plot). Seasonal cycle (de-trended) with year to year variability (lower plot).

3.3.1.3 CFC-13

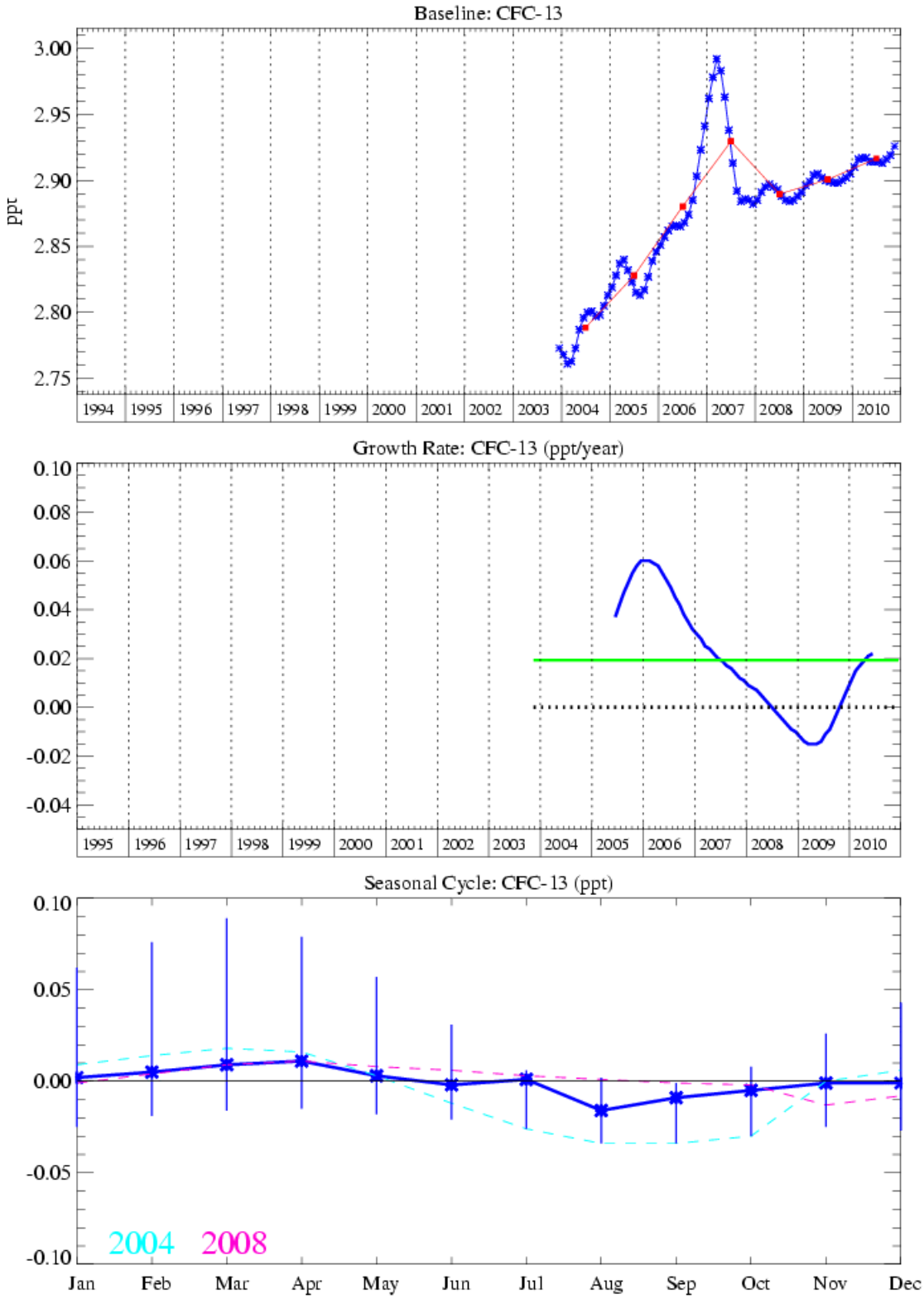

Figure 9: CFC-13: Monthly (blue) and annual (red) baseline concentrations (top plot). Annual (blue) and overall average growth rate (green) (middle plot). Seasonal cycle (de-trended) with year to year variability (lower plot).

3.3.1.4 CFC-113

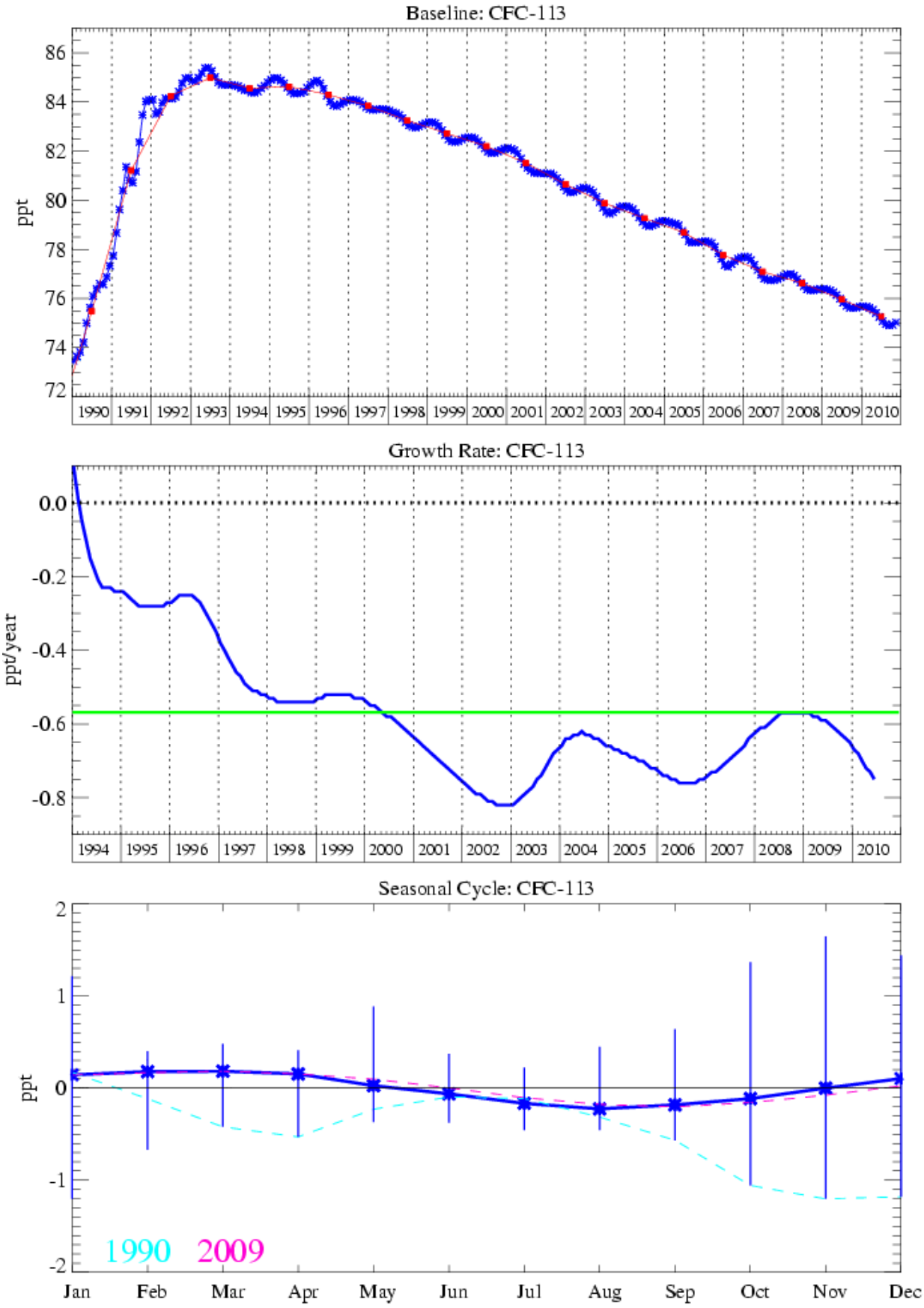

Figure 10: CFC-113: Monthly (blue) and annual (red) baseline concentrations (top plot). Annual (blue) and overall average growth rate (green) (middle plot). Seasonal cycle (de-trended) with year to year variability (lower plot).

3.3.1.5 CFC-114

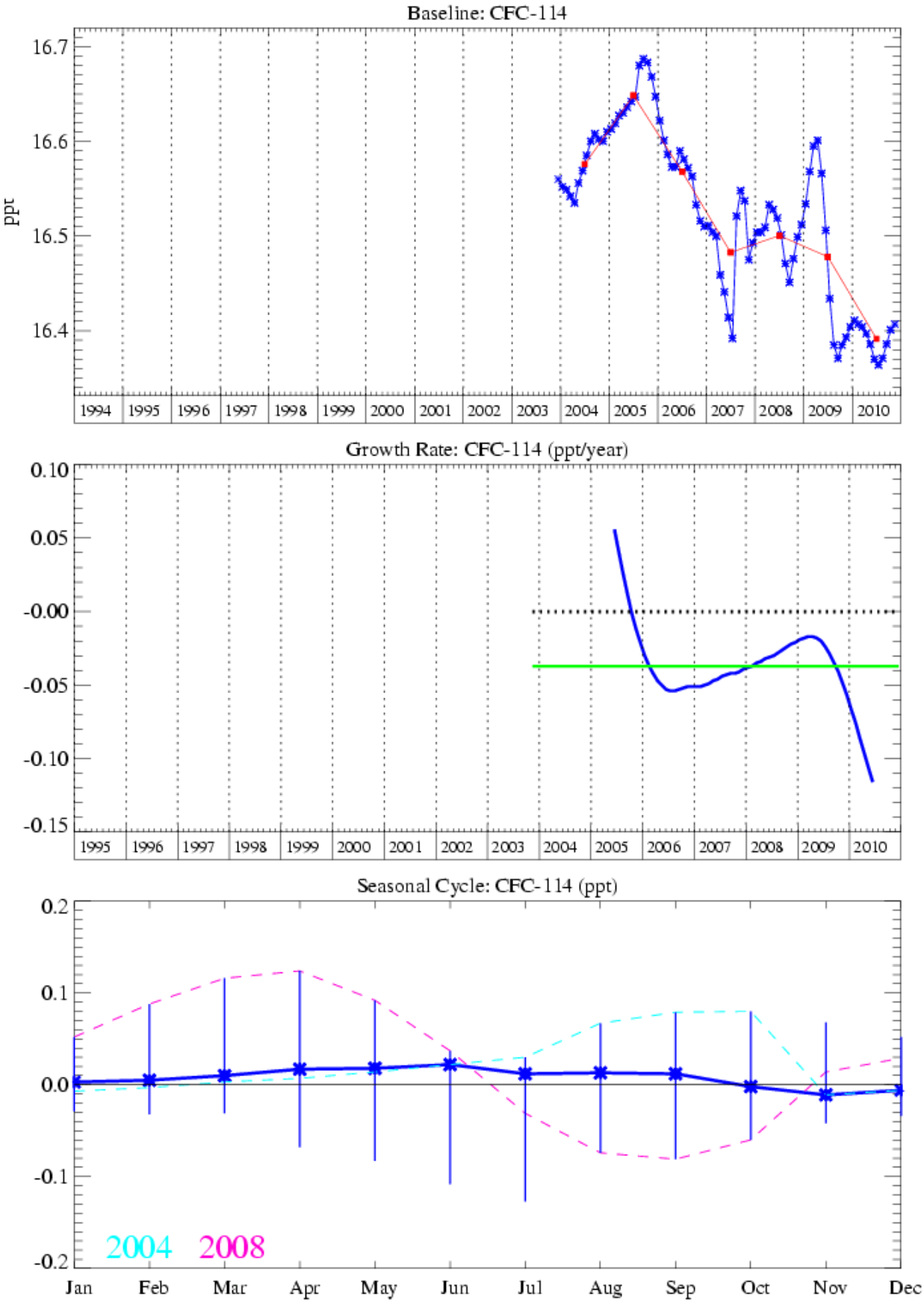

Figure 11: CFC-114: Monthly (blue) and annual (red) baseline concentrations (top plot). Annual (blue) and overall average growth rate (green) (middle plot). Seasonal cycle (de-trended) with year to year variability (lower plot).

3.3.1.6 CFC-115

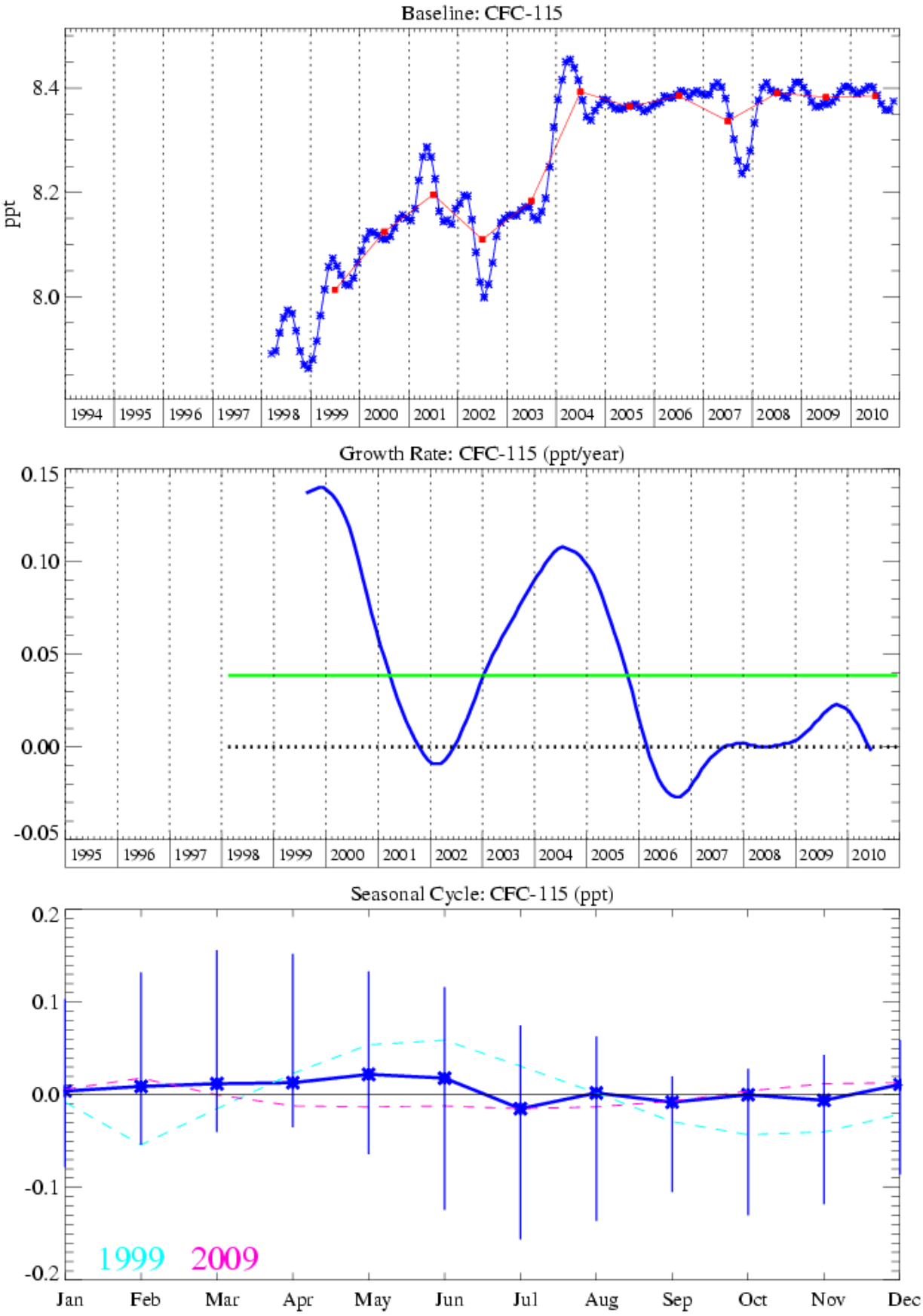

Figure 12: CFC-115: Monthly (blue) and annual (red) baseline concentrations (top plot). Annual (blue) and overall average growth rate (green) (middle plot). Seasonal cycle (de-trended) with year to year variability (lower plot).

3.3.2 HCFCs

Over the past 12-months HCFC-22, the dominant globally produced HCFC compound, has grown steadily at a rate of 7.5 ppt/yr and has currently reached a level at Mace Head of approximately 223.8 ppt (December 2010). HCFC-142b and HCFC-141b have also continued to grow in the atmosphere at increased rates since 2003 and 2005 respectively. Prior to these dates HCFC-142b and HFCF-141b showed decreased growth in the atmosphere in line with their expected phase-out. Analysis of the HCFC content of regionally-polluted air arriving at Mace Head from the European continent shows that European emissions reached a peak during 2000-2001 and have subsequently declined following the phase-out in their usage. The reductions are consistent with the phase-out of HCFC production and use from the year 2001 onwards mandated by European regulations designed to exceed the requirements of the Montreal Protocol. In the US implementation of HCFC phase-out through the Clean Air Act Regulations, 2004 resulted in no production or importation of HCFC-141b since 2003, these restriction do not apply to HCFC-142b until 2010. Increasing evidence indicates that increased emissions of these compounds from Asia, in particular China are now offsetting the phase-out in developed countries. The growth rates of HCFC-141b and 142b (January-June 2010) are 0.5 ppt/yr. The growth rates of these compounds, calculated from the baseline monthly mean mixing ratios shown in Figures 14 and 15, are also presented in Table1c.

3.3.2.1 HCFC-124

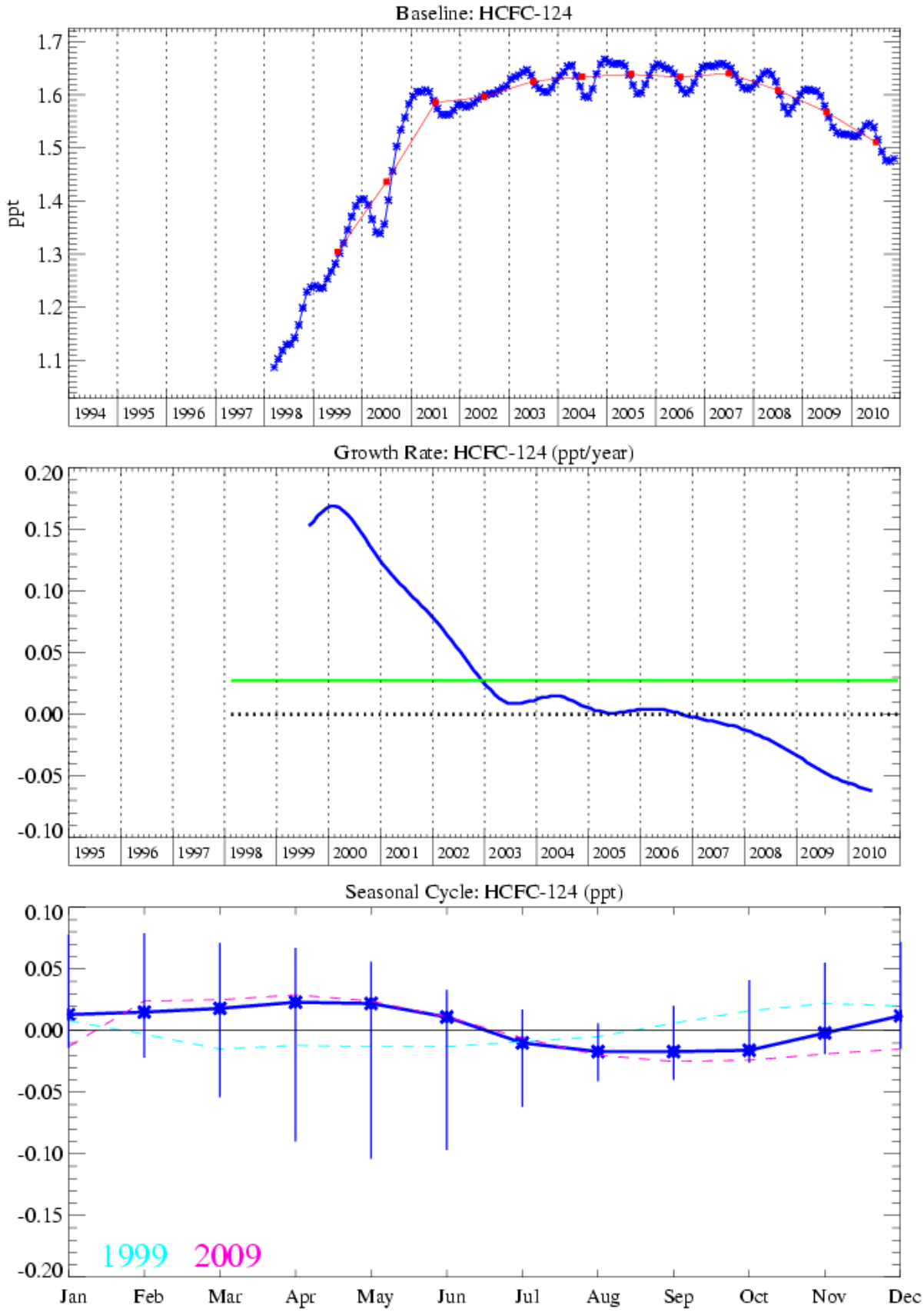

Figure 13: HCFC-124: Monthly (blue) and annual (red) baseline concentrations (top plot). Annual (blue) and overall average growth rate (green) (middle plot). Seasonal cycle (de-trended) with year to year variability (lower plot).

3.3.2.2 HCFC-141b

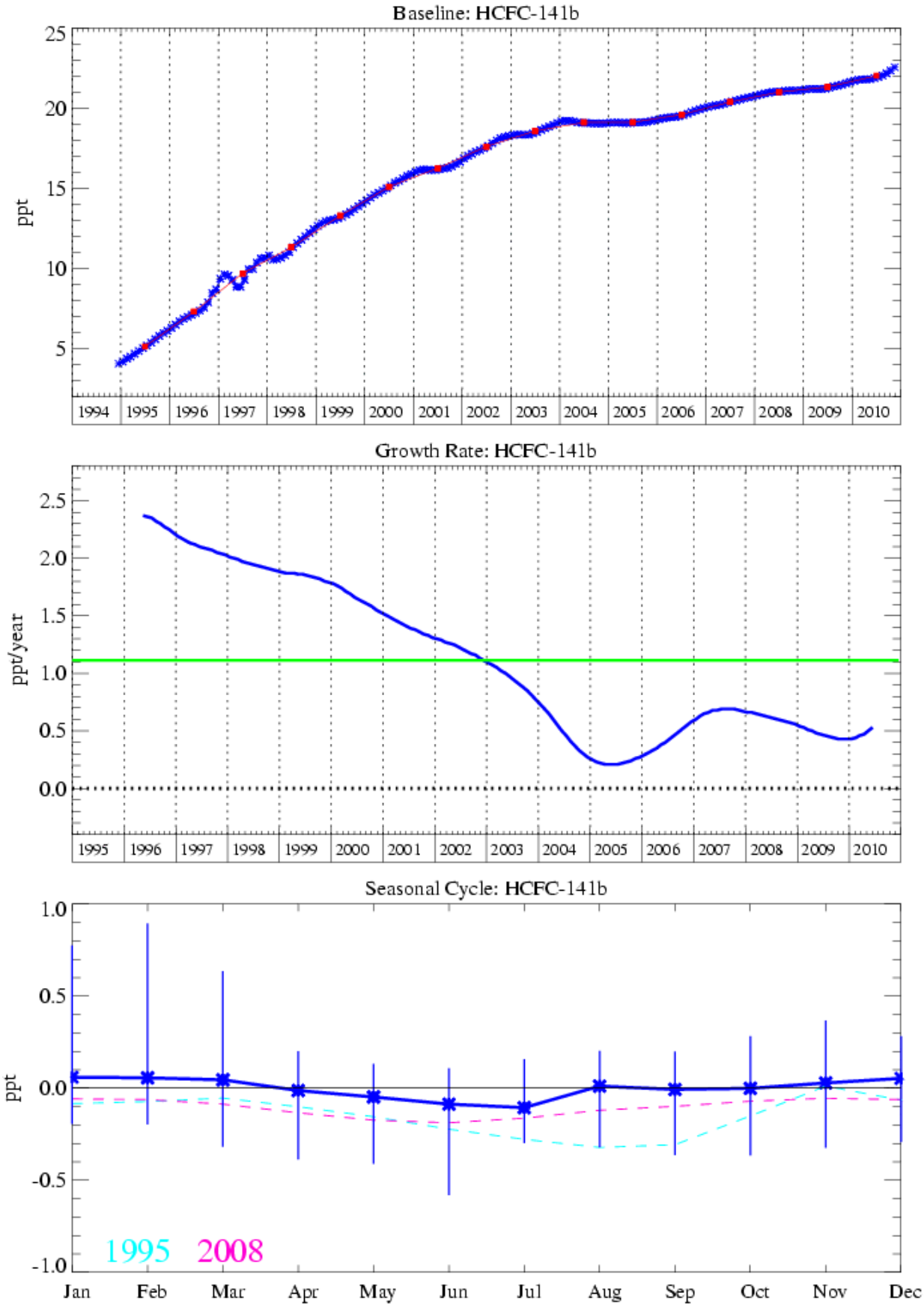

Figure 14: HCFC-141b: Monthly (blue) and annual (red) baseline concentrations (top plot). Annual (blue) and overall average growth rate (green) (middle plot). Seasonal cycle (de-trended) with year to year variability (lower plot).

3.3.2.3 HCFC-142b

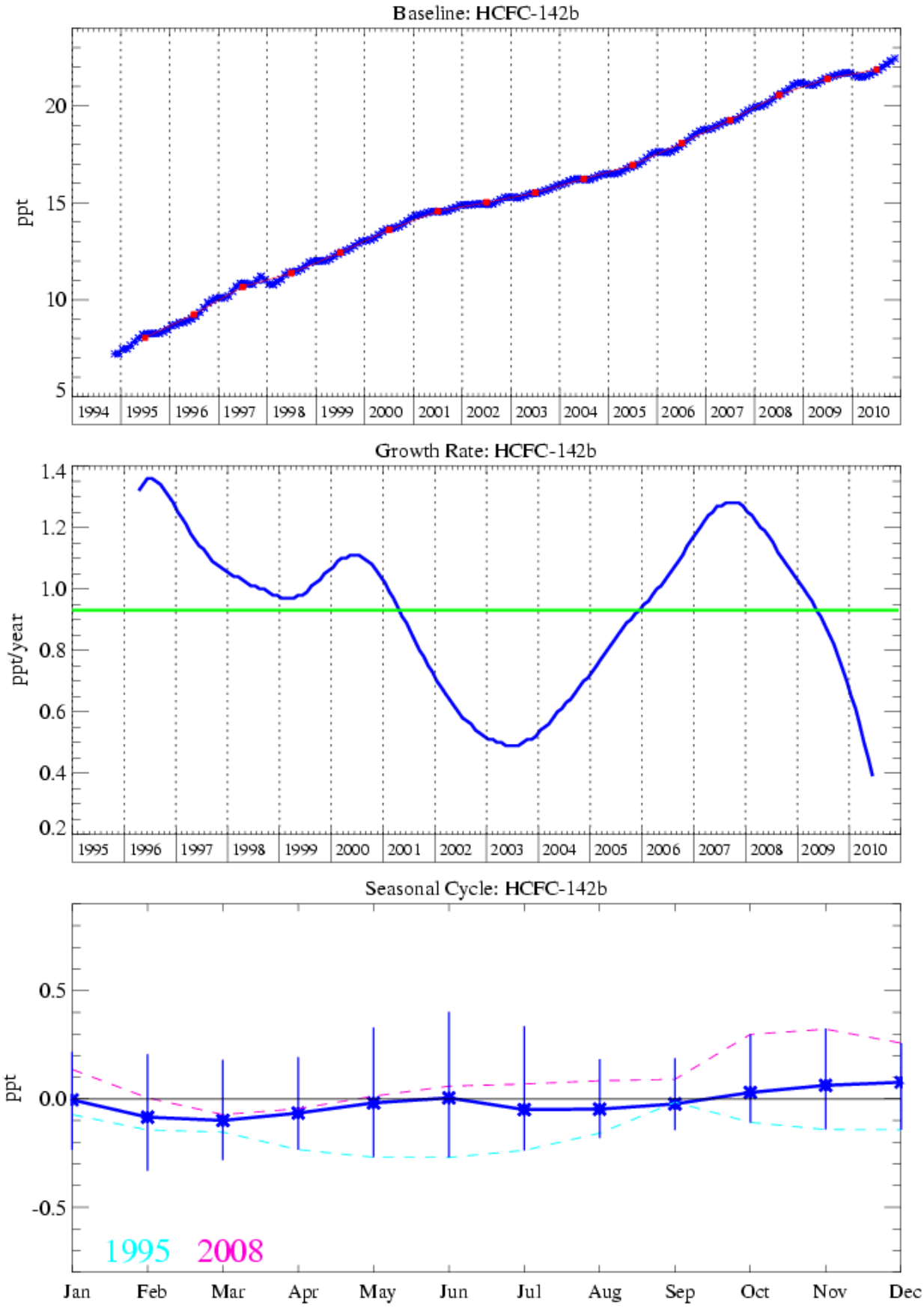

Figure 15: HCFC-142b: Monthly (blue) and annual (red) baseline concentrations (top plot). Annual (blue) and overall average growth rate (green) (middle plot). Seasonal cycle (de-trended) with year to year variability (lower plot).

3.3.2.4 HCFC-22

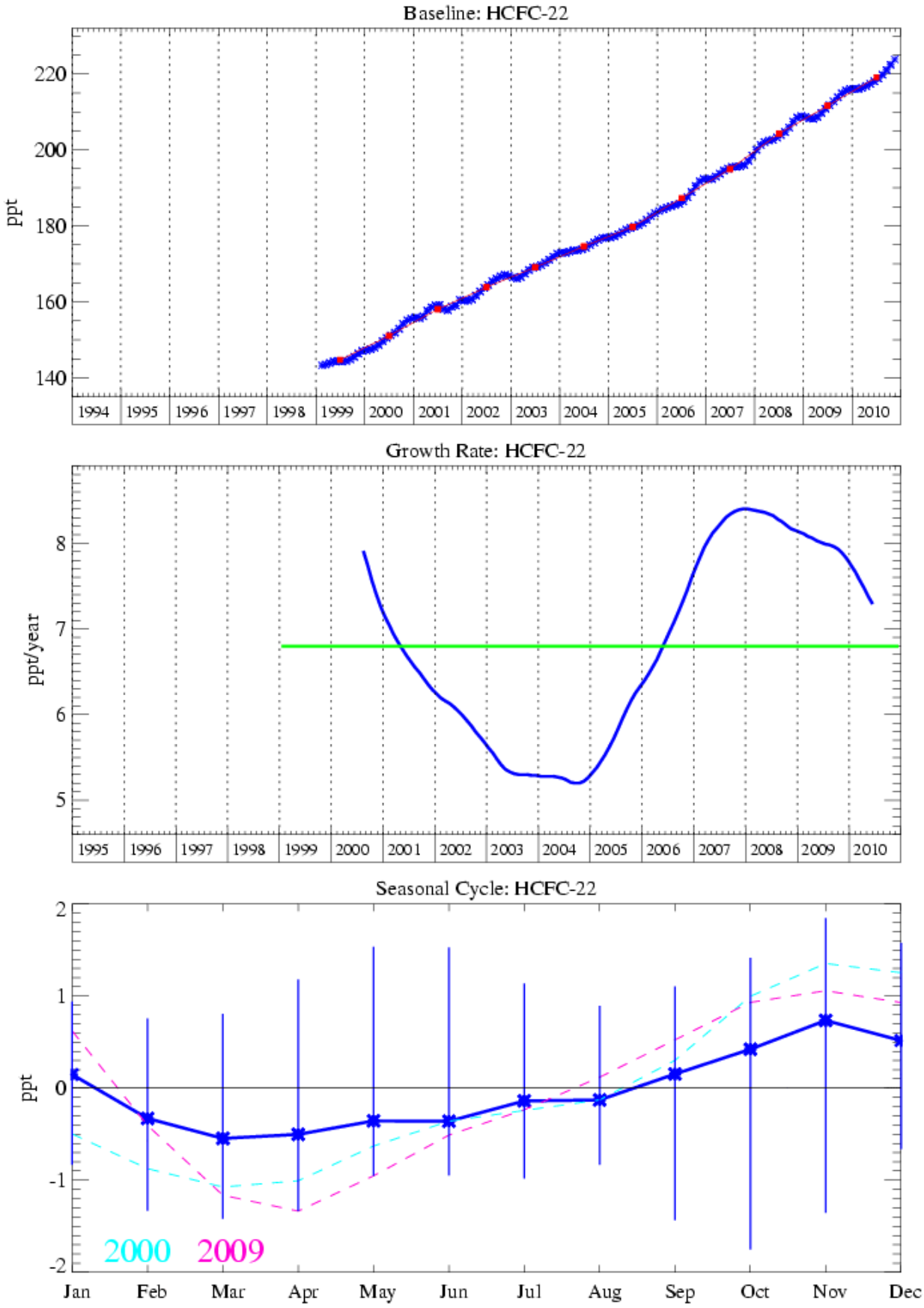

Figure 16: HCFC-22: Monthly (blue) and annual (red) baseline concentrations (top plot). Annual (blue) and overall average growth rate (green) (middle plot). Seasonal cycle (de-trended) with year to year variability (lower plot).

3.3.3 HFCs

The most recent measurements of the HFCs at Mace Head indicate that the mixing ratios of all HFC compounds continue to grow, as is consistent with sustained emissions of these replacement compounds into the atmosphere. As of December 2010 the atmospheric mole fractions of HFC-125 (10.0 ppt), 134a (66.6 ppt), 143a (12.6 ppt), 152a (9.9 ppt), and 365mfc (0.7 ppt). Their growth rates for January-June 2010 are 1.1, 5.0, 1.2, 0.1, and 0.02 ppt/yr respectively. Globally, HFC-134a is the most abundant HFC present in the atmosphere. Due to its long lifetime and relatively high GWP100 (Forster et al., 2007) the use of HFC-134a (and any other HFCs with a GWP100 >150) will be phased out in Europe between 2011 and 2017. In developing countries the potential for growth of HFC-134a is still large (Velders et al., 2009).The baseline monthly mean, mixing ratios for all the HFCs are shown in Figure 17-26, and the growth rates of these compounds, calculated from the data are presented in Table1c.

Three new HFC compounds have now successfully been added to the Medusa analysis (since 11 January 2008). The atmospheric mole fraction of HFC-245fa is 1.4 ppt and it is growing at a rate of 0.1 ppt/yr. This compounds is used as a foam blowing agent for polyurethane (PUR) foams (atmospheric lifetime 7.6 years and GWP (100 year time horizon) of 1020). HFC-227ea is used as a propellant for medical aerosols and a fire fighting agent (atmospheric lifetime 34.2 years and GWP (100 year time horizon) of 3140). It is has reached a mole fraction of 0.7 ppt with a growth rate of 0.08 ppt/yr. Finally, HFC-236fa, used as a fire fighting agent (atmospheric lifetime 240 years and GWP (100 year time horizon) of 9500) has reached a mixing ratio of 0.08 ppt and is growing at a rate of 0.006 ppt/yr.

3.3.3.1 HFC-125

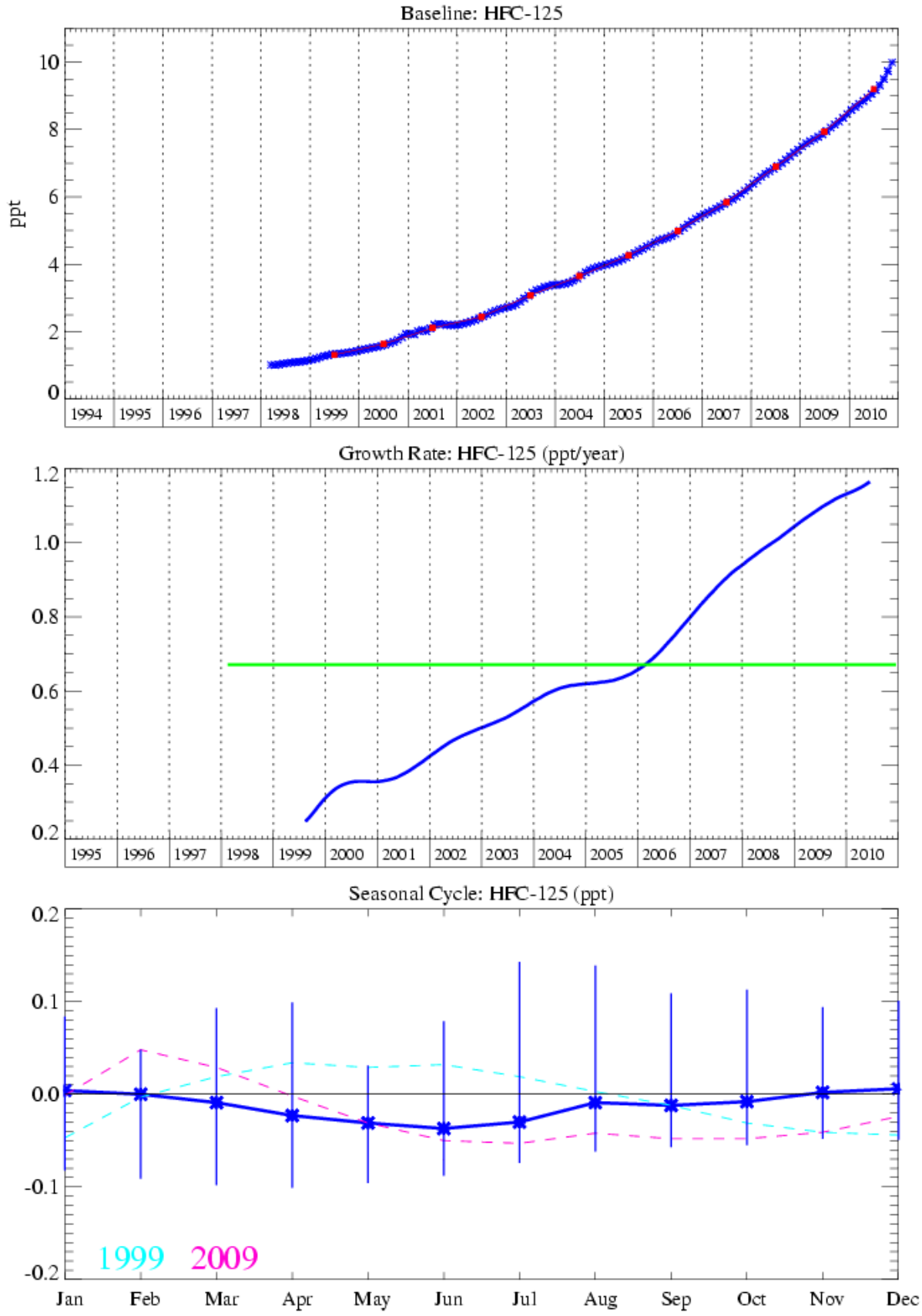

Figure 17: HFC-125: Monthly (blue) and annual (red) baseline concentrations (top plot). Annual (blue) and overall average growth rate (green) (middle plot). Seasonal cycle (de-trended) with year to year variability (lower plot).

3.3.3.2 HFC-134a

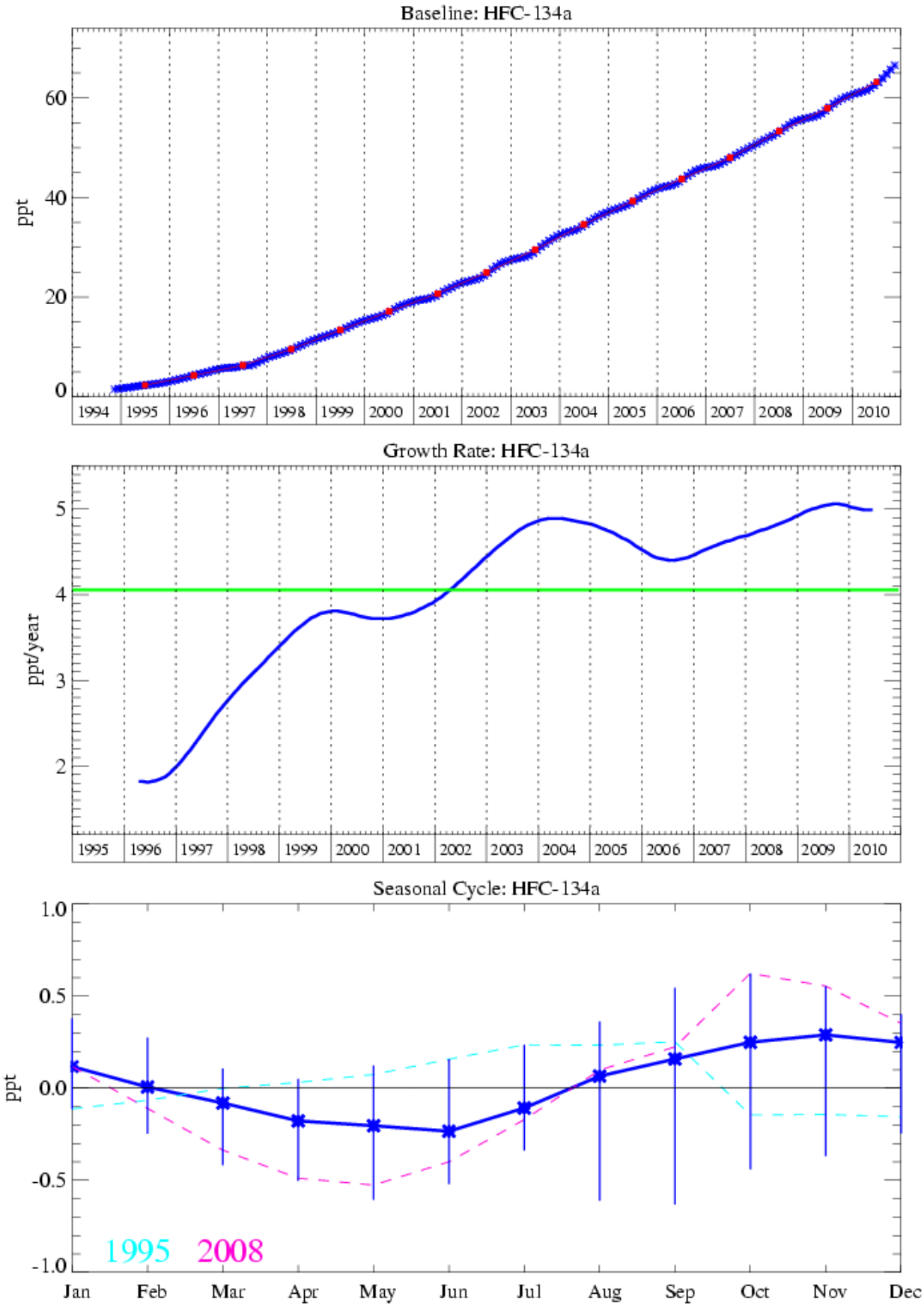

Figure 18: HFC-134a: Monthly (blue) and annual (red) baseline concentrations(top plot). Annual (blue) and overall average growth rate (green) (middle plot). Seasonal cycle (de-trended) with year to year variability (lower plot).

3.3.3.3 HFC-143a

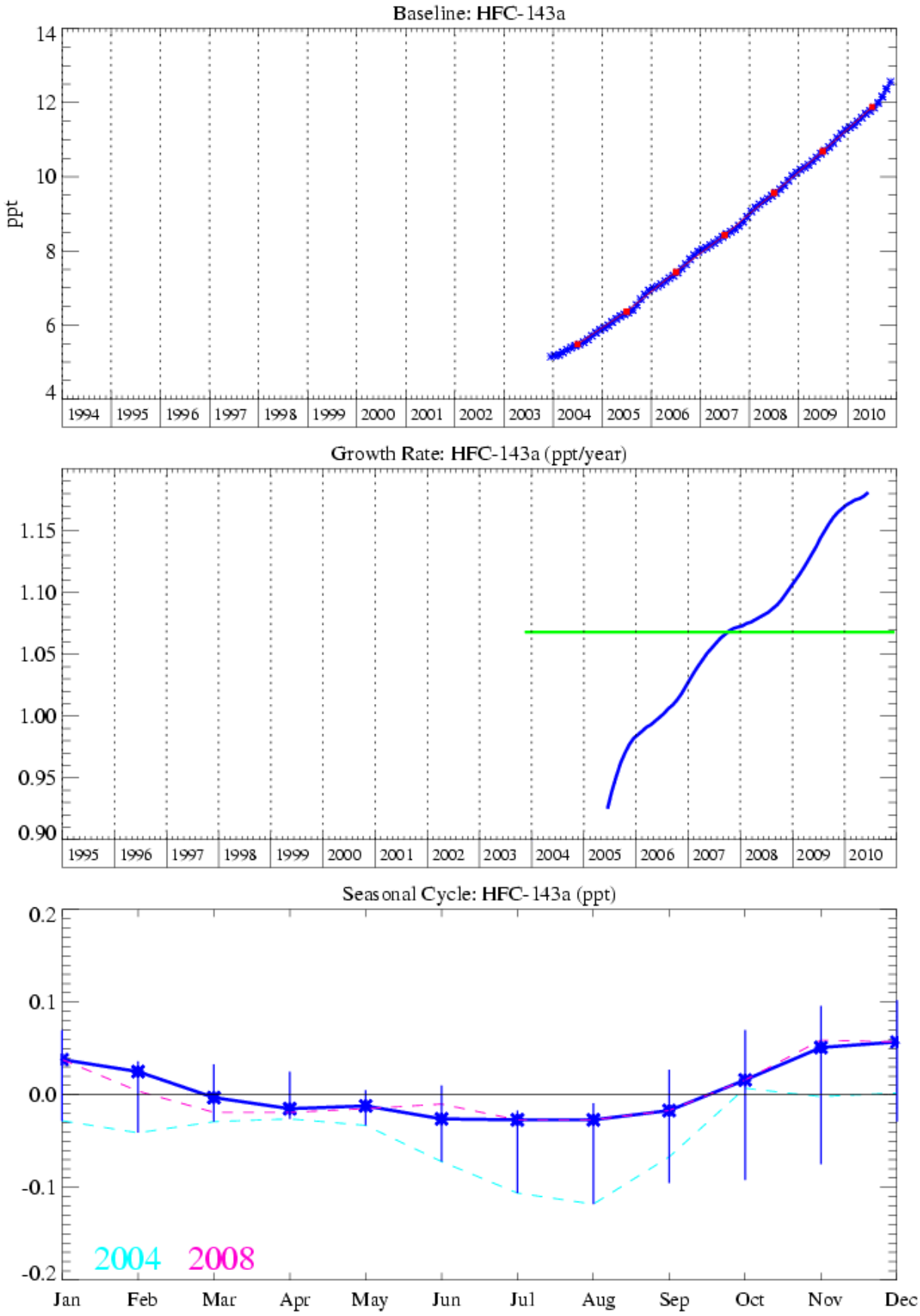

Figure 19: HFC-143a: Monthly (blue) and annual (red) baseline concentrations (top plot). Annual (blue) and overall average growth rate (green) (middle plot). Seasonal cycle (de-trended) with year to year variability (lower plot).

3.3.3.4 HFC-152a

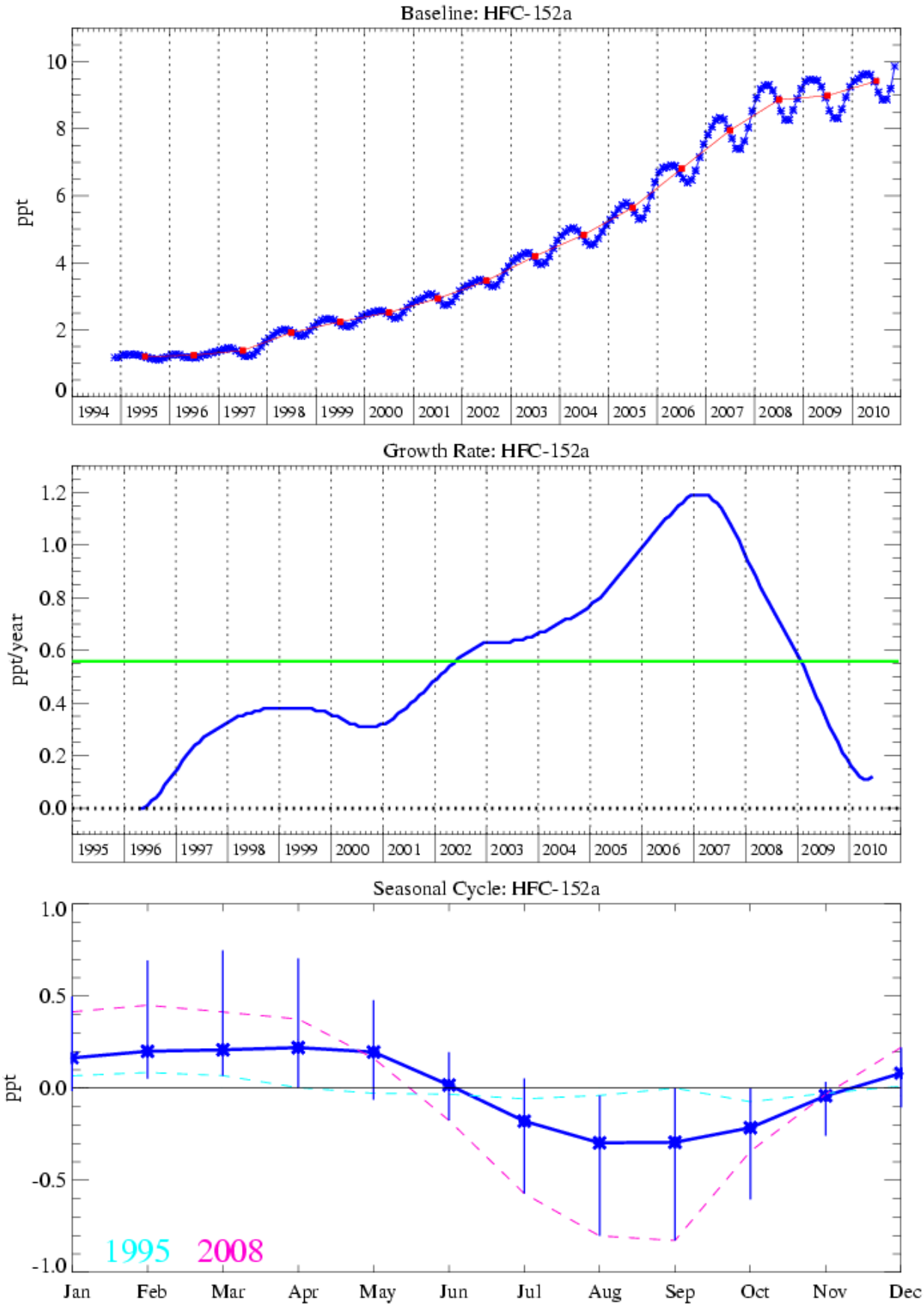

Figure 20: HFC-152a: Monthly (blue) and annual (red) baseline concentrations (top plot). Annual (blue) and overall average growth rate (green) (middle plot). Seasonal cycle (de-trended) with year to year variability (lower plot).

3.3.3.5 HFC-23

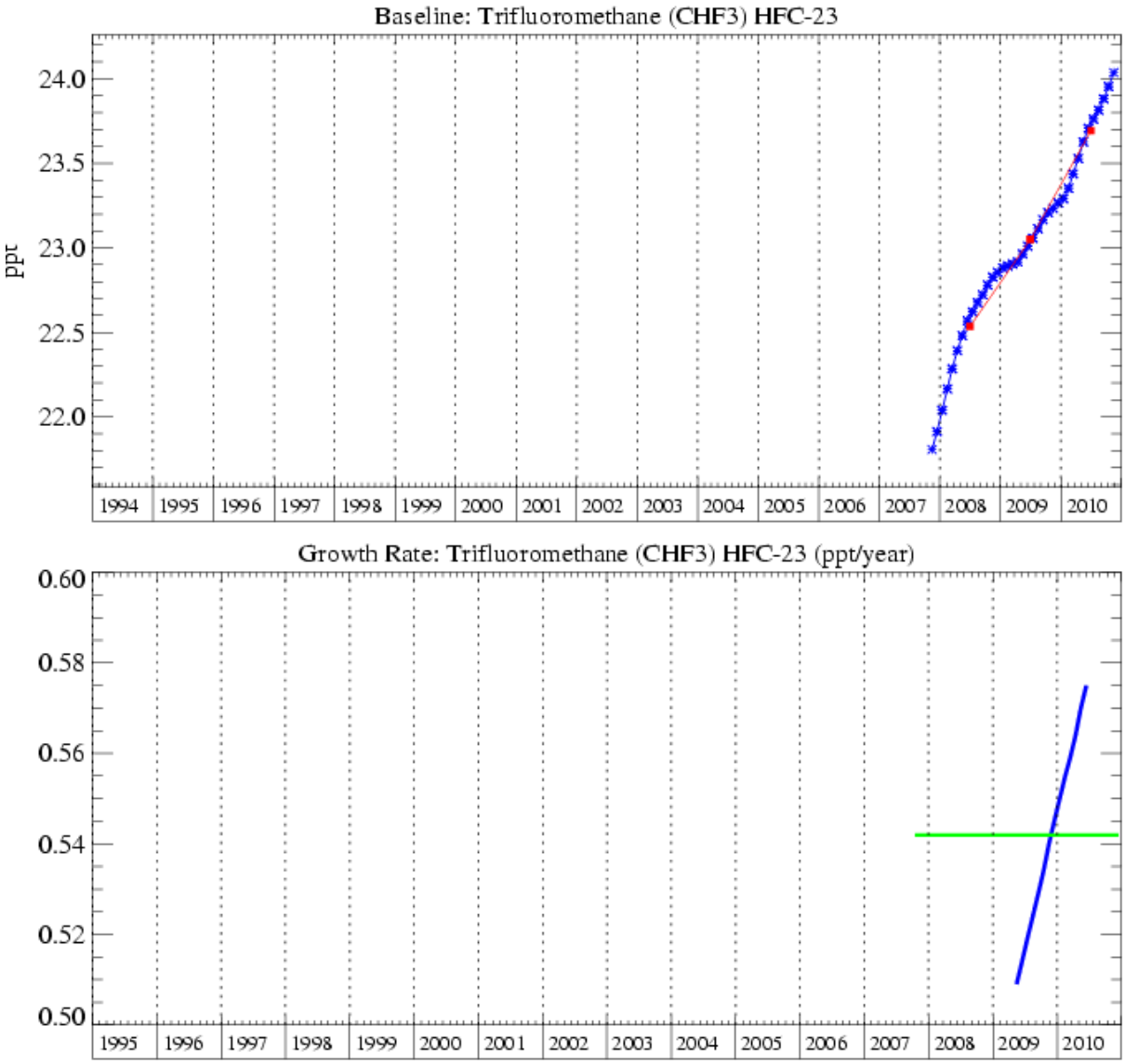

Figure 21: HFC-23: Monthly (blue) and annual (red) baseline concentrations. Annual (blue) and overall average growth rate (green) (lower plot).

3.3.3.6 HFC-32

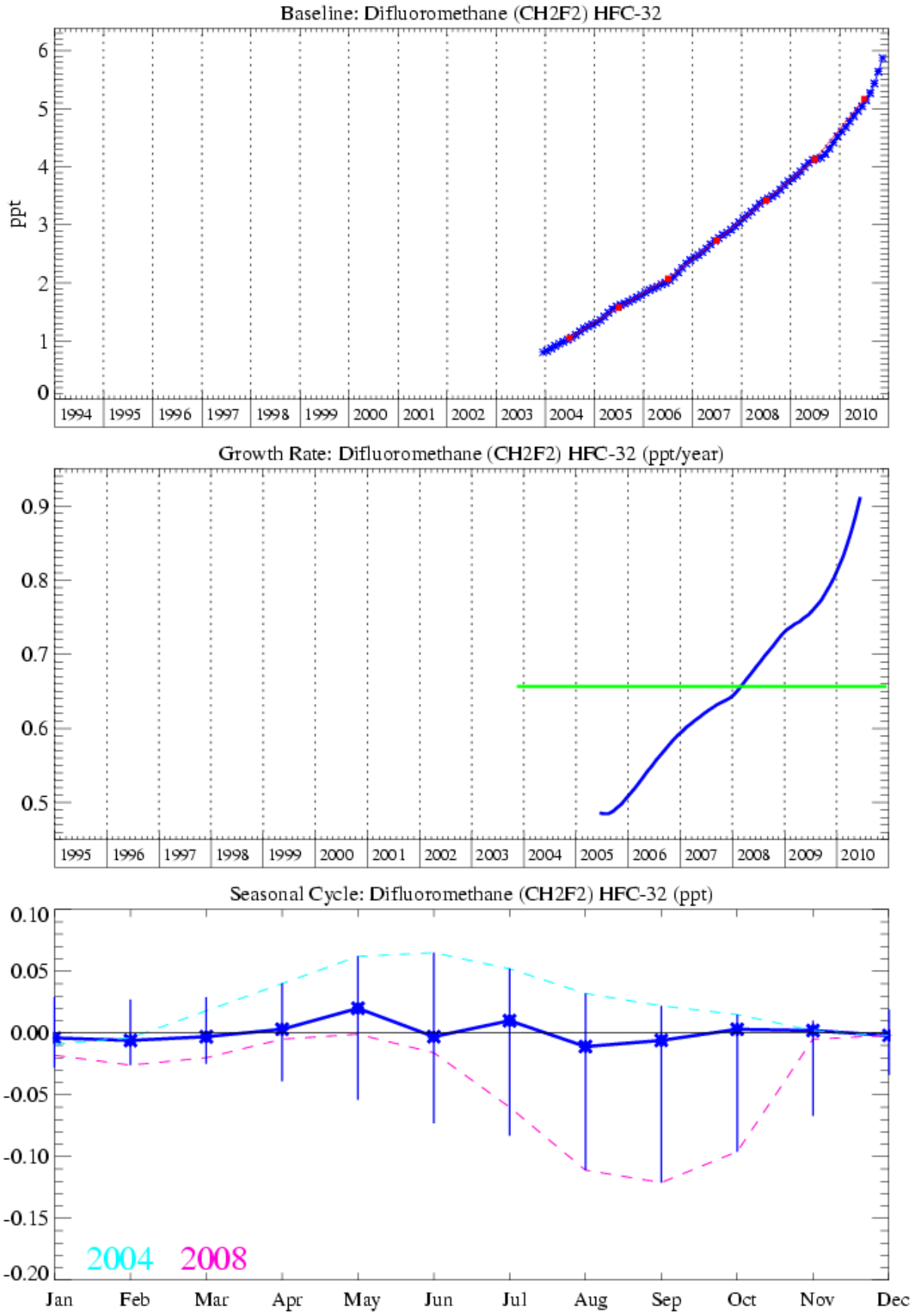

Figure 22: HFC-32: Monthly (blue) and annual (red) baseline concentrations (top plot). Annual (blue) and overall average growth rate (green) (middle plot). Seasonal cycle (de-trended) with year to year variability (lower plot).

3.3.3.7 HFC-227ea

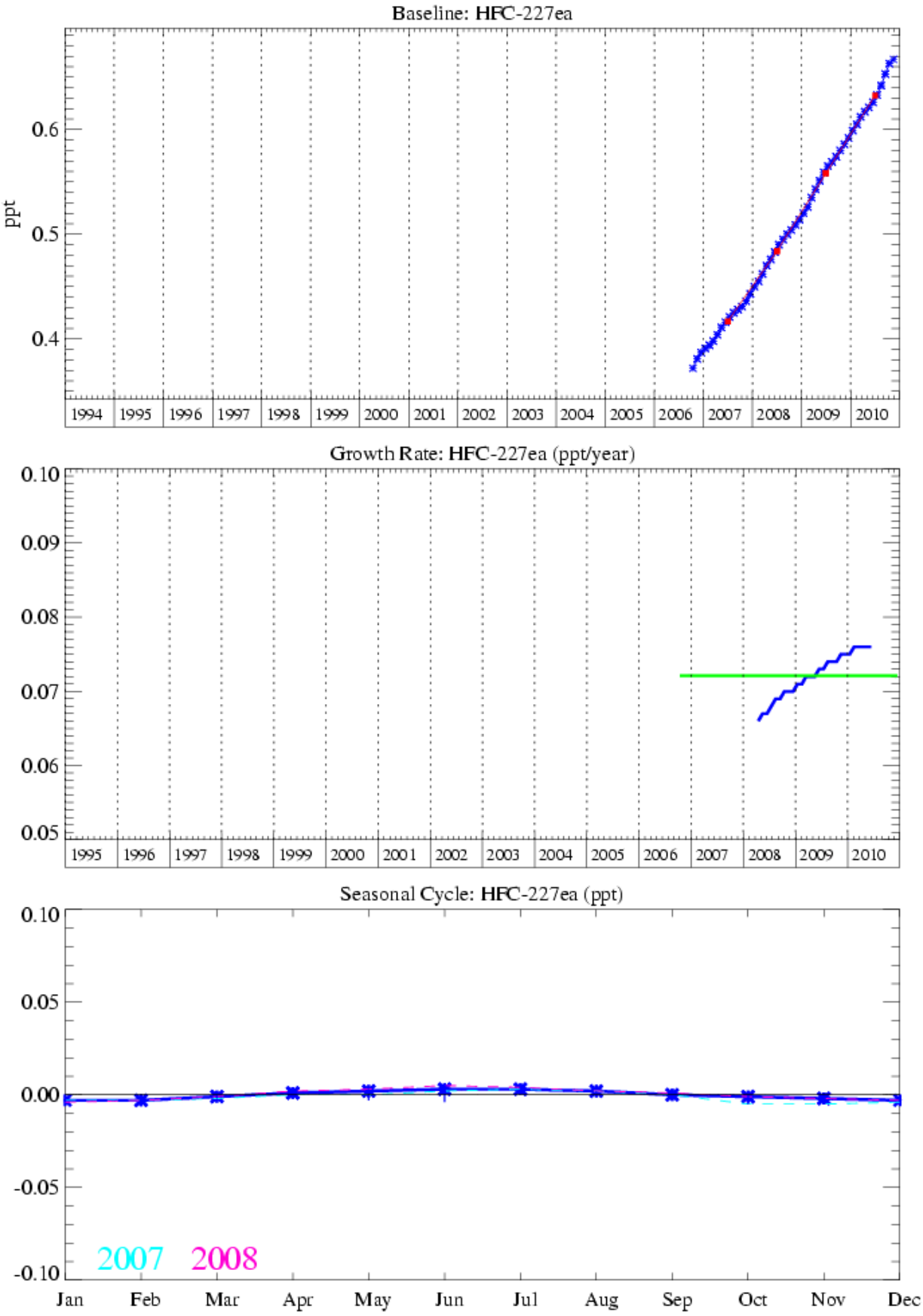

Figure 23: HFC-227ea: Monthly (blue) and annual (red) baseline concentrations (top plot). Annual (blue) and overall average growth rate (green) (middle plot). Seasonal cycle (de-trended) with year to year variability (lower plot).

3.3.3.8 HFC-236fa

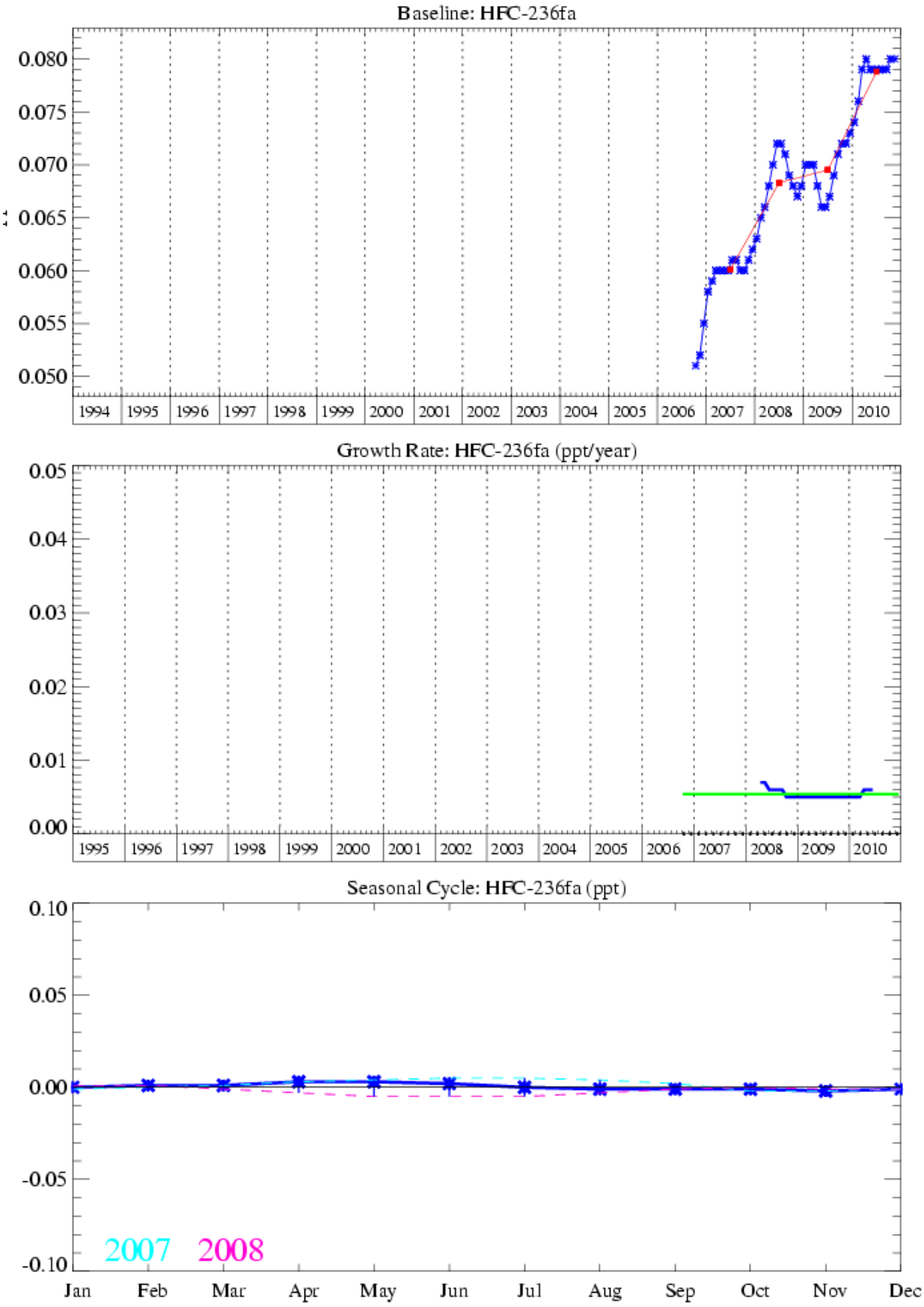

Figure 24: HFC-236fa: Monthly (blue) and annual (red) baseline concentrations (top plot). Annual (blue) and overall average growth rate (green) (middle plot). Seasonal cycle (de-trended) with year to year variability (lower plot).

3.3.3.9 HFC-245fa

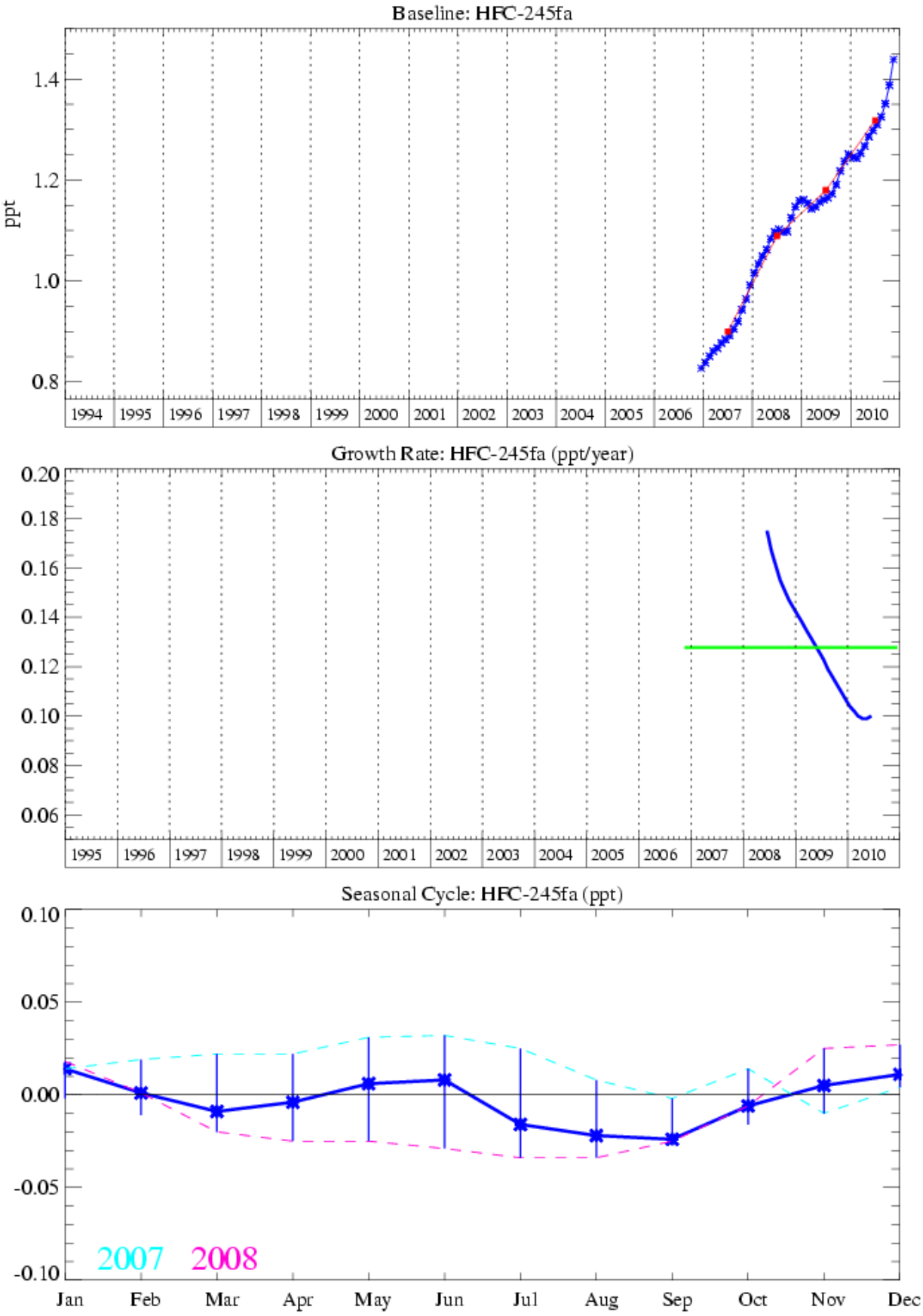

Figure 25: HFC-245fa: Monthly (blue) and annual (red) baseline concentrations (top plot). Annual (blue) and overall average growth rate (green) (middle plot). Seasonal cycle (de-trended) with year to year variability (lower plot).

3.3.3.10 HFC-365mfc

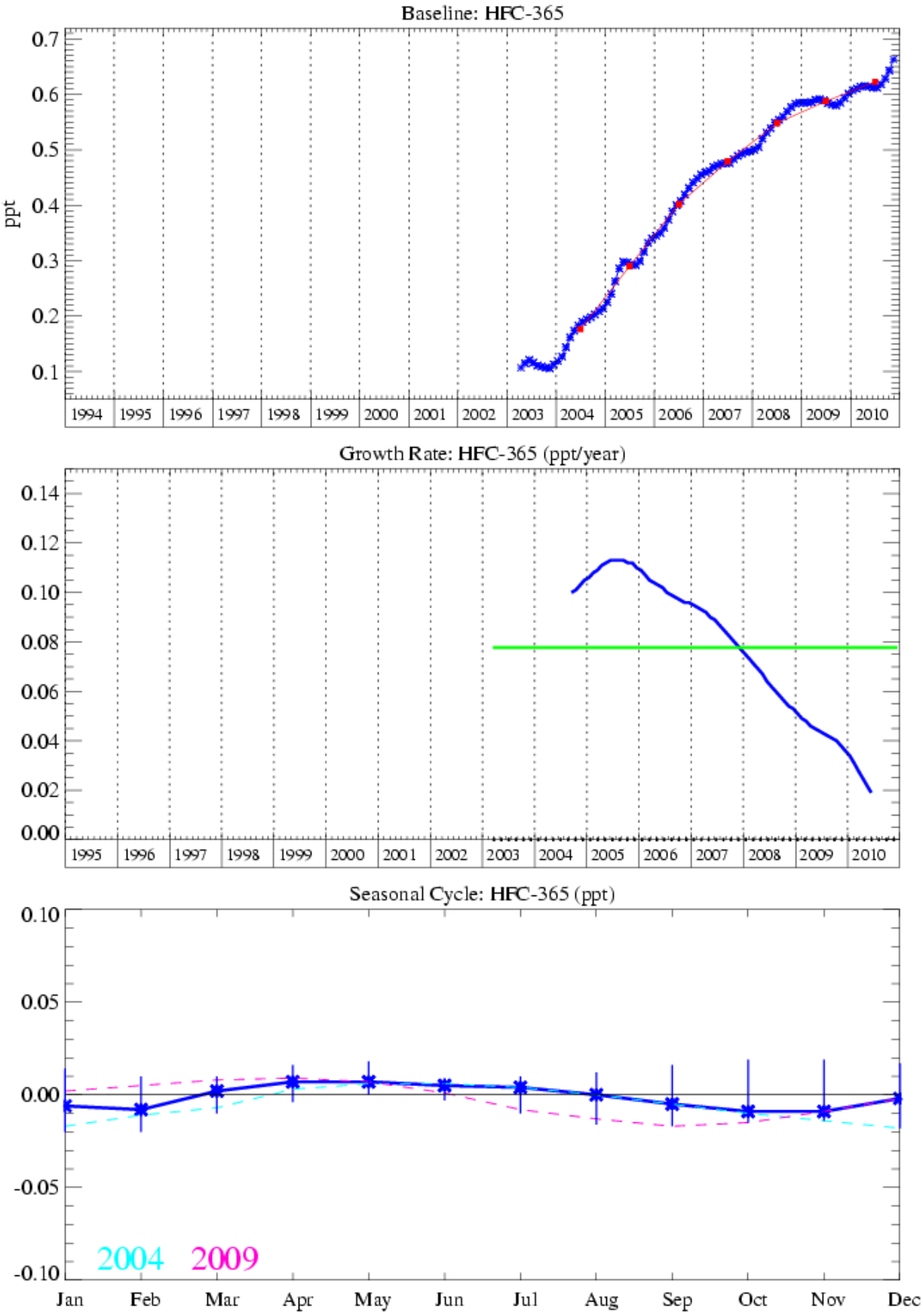

Figure 26: HFC-365mfc: Monthly (blue) and annual (red) baseline concentrations (top plot). Annual (blue) and overall average growth rate (green) (middle plot). Seasonal cycle (de-trended) with year to year variability (lower plot).

3.3.4 Fluorine compounds

CF_4 possesses the longest known lifetime of anthropogenic molecules (~50,000 yrs), which, when coupled with its high absolute radiative forcing (0.08 W m^{-2} ppb^{-1}, 6500 x eCO_2 (CO_2 equivalent, 100 yr time horizon)), can equate to upwards of 1 % of total radiative forcing. Its primary emission source is as an unwanted by-product of Aluminium smelting during a fault condition known as the Anode Effect. Thus the frequency of occurrence and duration of an Anode Effect event will determine the regional and global CF_4 emission. PFC-116 (C_2F_6) is also emitted during an Anode Effect event, but in much lesser quantities than CF_4 (~10:1 CF_4:C_2F_6). CF_4 has some additional minor applications in the semiconductor industry (as a source of F radicals), but industry has shied away from using CF_4 knowing that its GWP is so high. The Aluminium industry has recognised the CF_4 (and C_2F_6) emission problem and has been undergoing processes of replacement of older, less efficient Aluminium production cells with more efficient designs, and automated and quicker intervention policies to prevent the occurrence of these Anode Effects.

The Medusa data record for CF_4, C_2F_6, C_3F_8, and SF_6 are shown in Figures 27-31 below C_2F_6 has a common source to CF_4, this serves to help explain why all of the CF_4 above-baseline (pollution) events are usually correlated with those of C_2F_6. However, we note that there are many more frequent and greater magnitude emissions of C_2F_6 relative to CF_4. This is due to the dominant source of C_2F_6 being emitted from semiconductor industries. The gas C_3F_8 is also used in semiconductor manufacturing, but to a lesser extent to that of C_2F_6. Observations of above-baseline C_3F_8 emissions are less frequent than those of C_2F_6 but are of a higher relative magnitude. The atmospheric trends for CF_4, C_2F_6 and the minor semi-conductor component C_3F_8 are 0.5, 0.06 and 0.02 ppt/yr respectively. These compounds tend to accumulate in the atmosphere due to their very long atmospheric lifetimes, the current mixing ratio of CF_4 (50,000 year lifetime) is 79.0 ppt, C_2F_6 (10,000 year lifetime) is 4.2 ppt and C_3F_8 (2600 year lifetime) is 0.6 ppt.

SF_6, although having minor usage in the semiconductor industry, is predominantly used in heavy duty electrical switchgear. Although the units themselves are hermetically sealed, breakdown and disposal, alongside leakage from wear-and-tear will cause this sector to emit SF_6. A minor use of this gas is also reported in its use as a blanketing (i.e. oxygen inhibiting inert gas) agent during Magnesium production. Hence SF_6 will have many and more diffuse sources relative to the other perfluorinated species. Its atmospheric trend has been predicted to rise at a rate faster than linear, as older electrical switchgear is being switched to higher efficiency units

3.3.4.1 PFC-14 (CF_4)

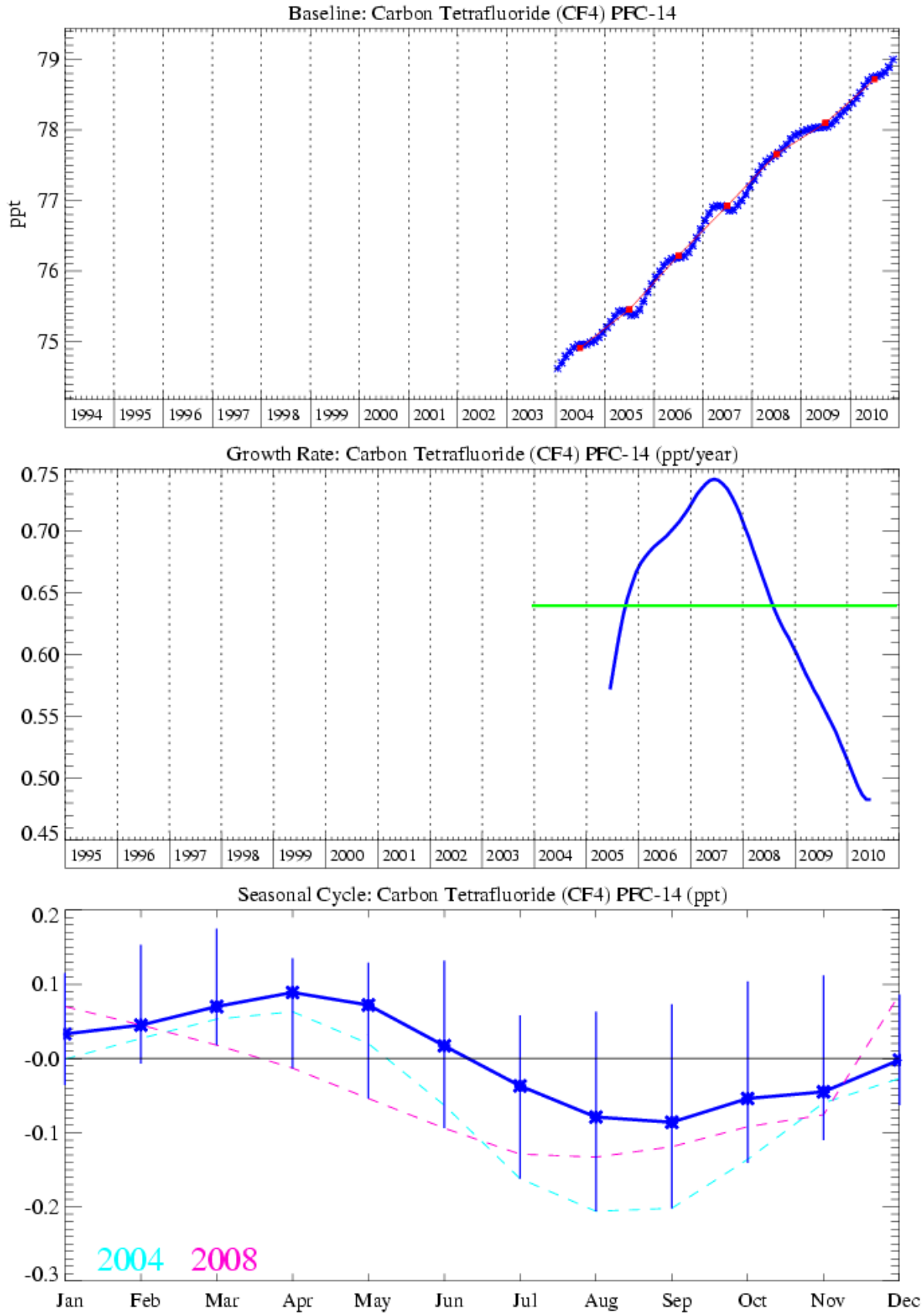

Figure 27: PFC-14: Monthly (blue) and annual (red) baseline concentrations (top plot). Annual (blue) and overall average growth rate (green) (middle plot). Seasonal cycle (de-trended) with year to year variability (lower plot).

3.3.4.2 PFC-116

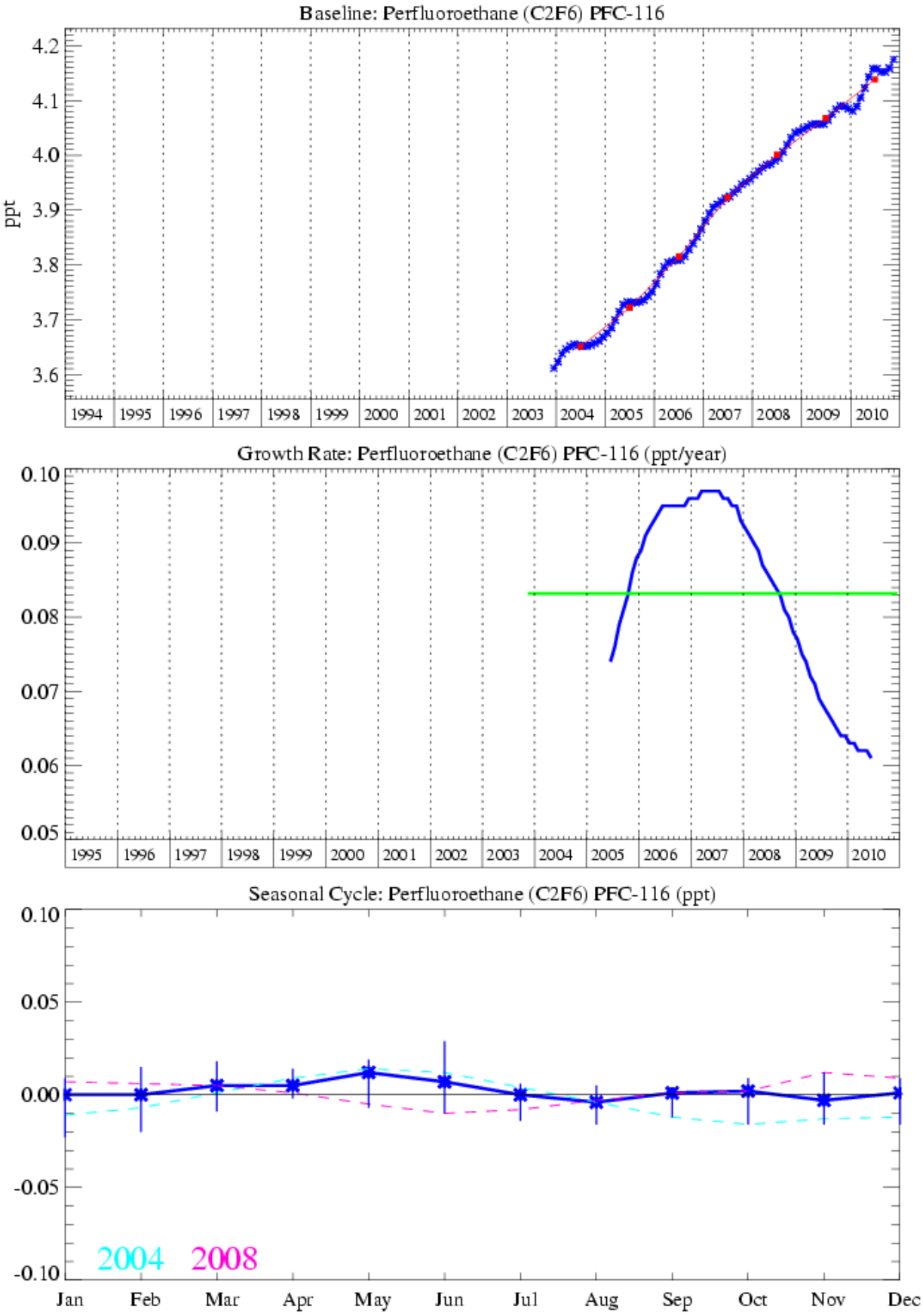

Figure 28: PFC-116: Monthly (blue) and annual (red) baseline concentrations (top plot). Annual (blue) and overall average growth rate (green) (middle plot). Seasonal cycle (de-trended) with year to year variability (lower plot).

3.3.4.3 PFC-218

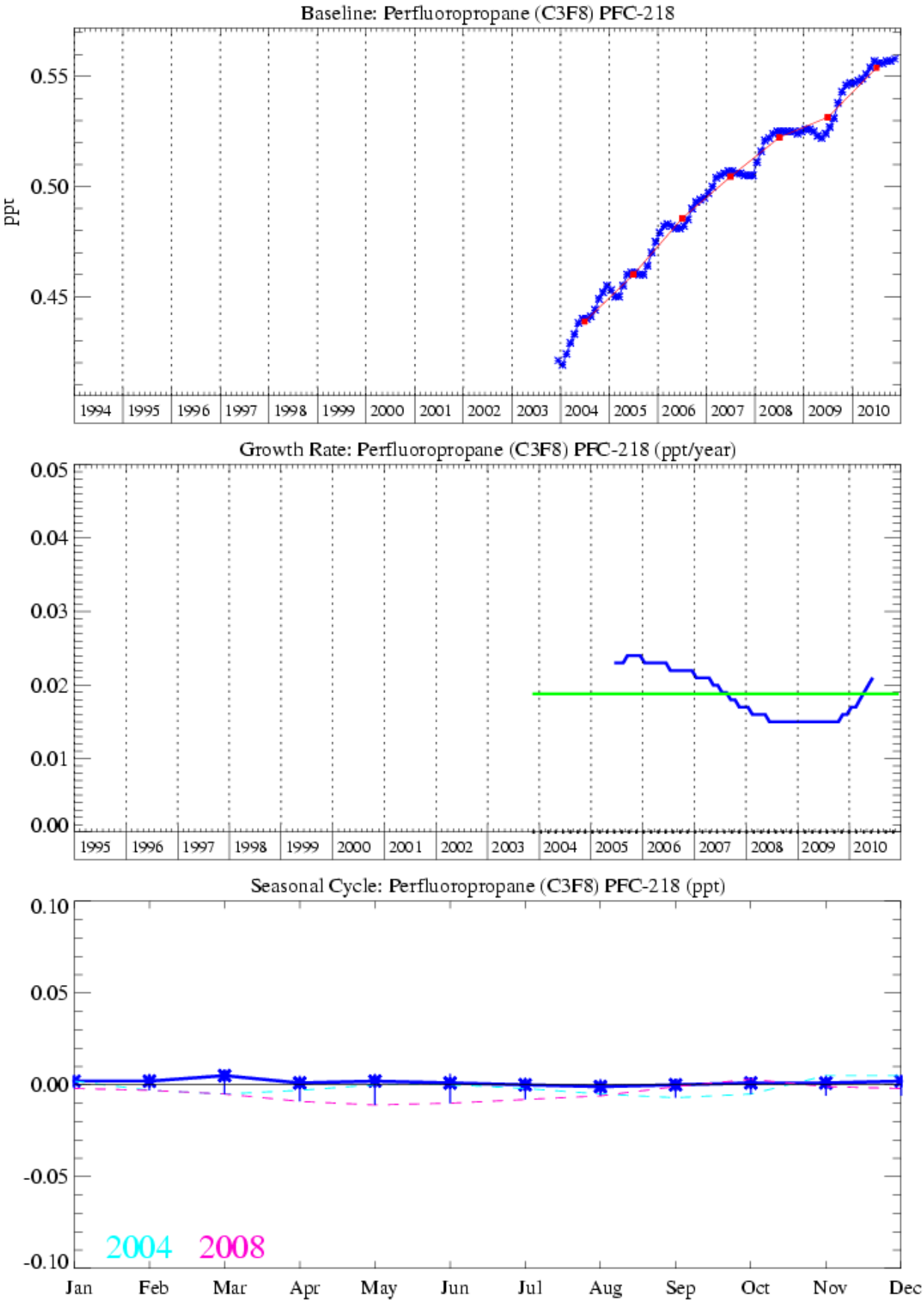

Figure 29: PFC-218: Monthly (blue) and annual (red) baseline concentrations (top plot). Annual (blue) and overall average growth rate (green) (middle plot). Seasonal cycle (de-trended) with year to year variability (lower plot).

3.3.4.4 SF_6

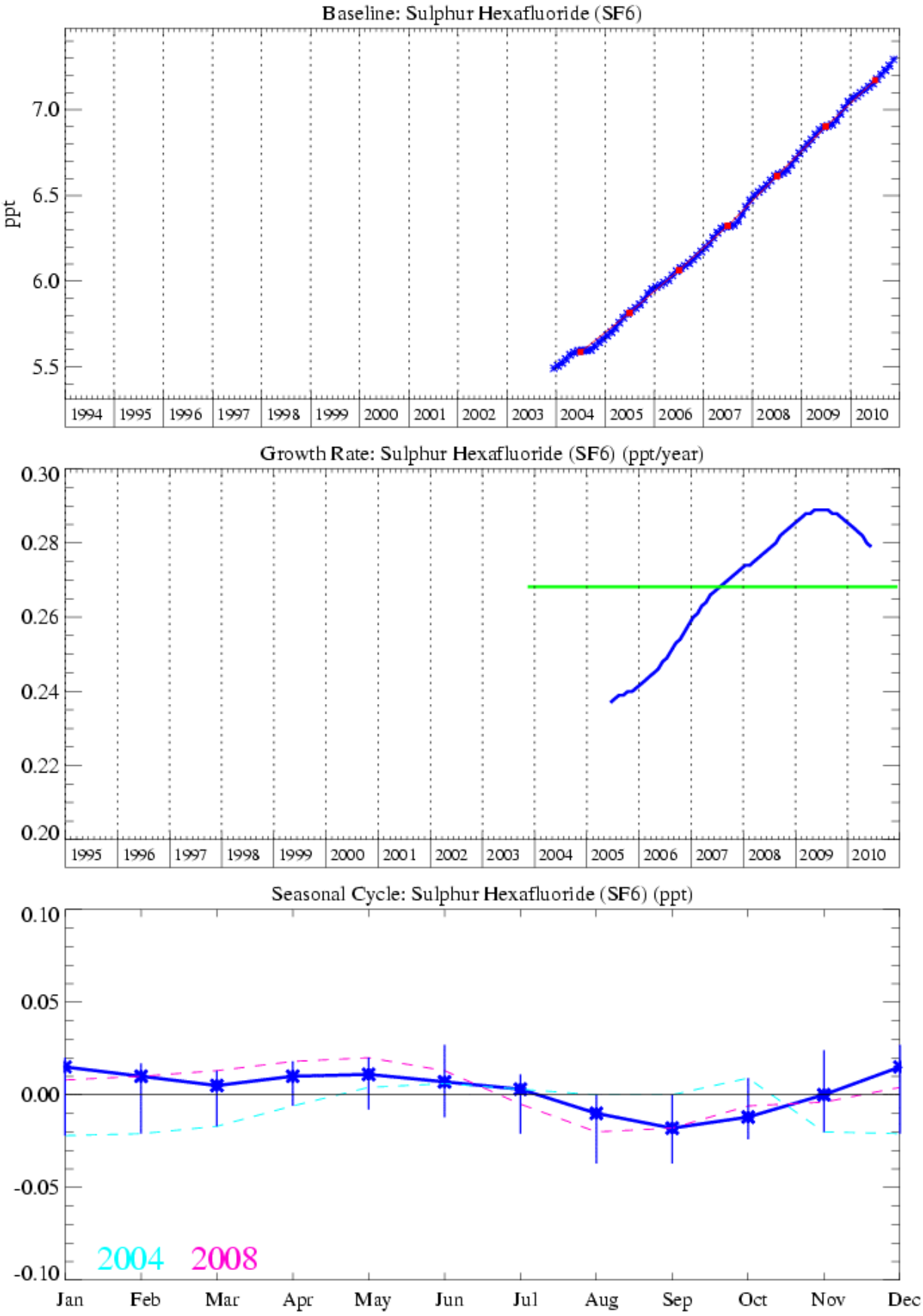

Figure 30: SF_6: Monthly (blue) and annual (red) baseline concentrations (top plot). Annual (blue) and overall average growth rate (green) (middle plot). Seasonal cycle (de-trended) with year to year variability (lower plot).

3.3.4.5 SO_2F_2

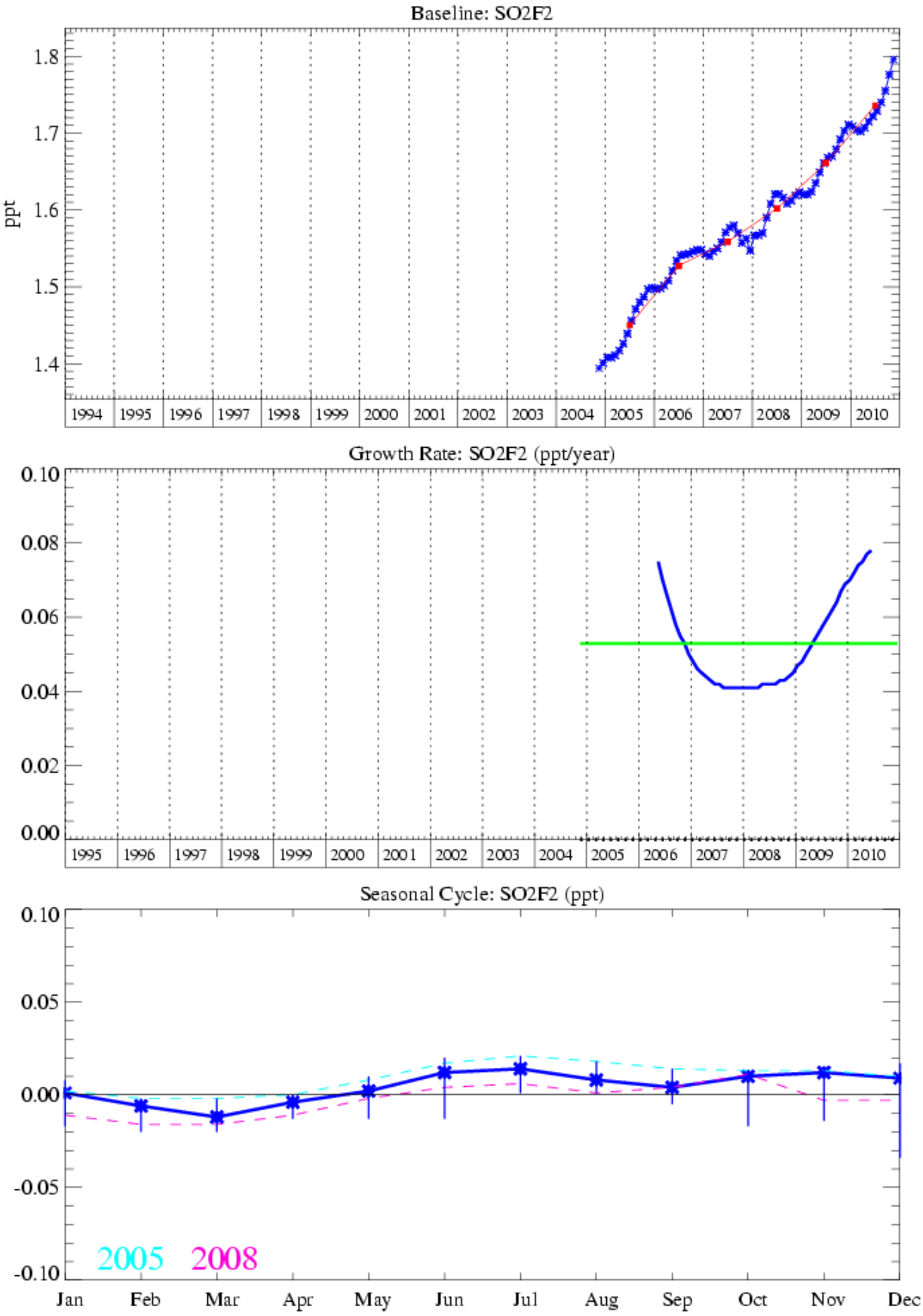

Figure 31: SO_2F_2: Monthly (blue) and annual (red) baseline concentrations (top plot). Annual (green), smoothed through 12-month running filter (red) and overall average growth rate (blue) (middle plot). Seasonal cycle (de-trended) with year to year variability (lower plot).

3.3.5 Chlorine compounds

A number of long lived and very short lived substances (VSLS) halocarbons are measured by the Medusa GC-MS. We have previously reported the recovery of CH_3Cl growth in the atmosphere, this growth has abated in January - June 2010 and the trend now shows a decline of 3.3 ppt/yr to 515.0 ppt (Figure 32). CH_2Cl_2 also showed a decline in line with a reduction in the many solvent applications for this compound, however, since around 2003, measurements at Mace Head have shown it to be accumulating in the atmosphere, shown in Figure 33, with a growth rate in January – June 2010 is 2.2 ppt/yr, it has a mixing ratio in December 2010 of 38.9 ppt. Emission totals derived using the NAME model and the industry derived inventory suggest that emissions from the NW Europe (and the UK) are decreasing, which implies a source of CH_2Cl_2 to the atmosphere from a location outside of Europe.

Figure 35 illustrates the steady downward trend of CCl_4 (26 year lifetime) of 1.2 ppt/yr January – June 2010), this compound is the second most rapidly decreasing chlorocarbon after CH_3CCl_3. The level of CCl_4 at Mace Head in December 2010 was 86.5 ppt. Its major use was as a feedstock for CFC manufacturing and unlike CH_3CCl_3 a significant inter-hemispheric CCl_4 gradient still exists in 2010, resulting from a persistence of significant NH emissions. It is interesting that atmospheric observations for this compound are decreasing less rapidly than projected in the A1 scenario of the Ozone Assessment (Daniel and Velders et al., 2007). CCl_4 emissions derived from atmospheric observations (top-down) suggest substantially smaller emissions than emissions derived from bottom-up techniques using reported production, feedstock and destruction data. The reason for this discrepancy is not yet fully understood.

The major solvent (CH_3CCl_3), is an important compound because of its use to estimate concentrations of the hydroxyl radical (OH), which is the major sink species for CH_4, HFCs and HCFCs. The global atmospheric CH_3CCl_3 concentration peaked in 1992 (Prinn et al., 2000) then declined in accordance with its short atmospheric lifetime (4.9 years). The average baseline mixing ratio of CH_3CCl_3 at Mace Head (Figure 36) has decreased by 1.5 ppt/yr (January - June 2010) to reach a mixing ratio of 7.2 ppt in December 2010.

The major source of trichloroethylene (C_2HCl_3) is from industrial usage as a degreasing agent. It is currently measured with a mole fraction of 0.7 ppt, but is decreasing in the atmosphere at a rate of 0.7 ppt/yr (Figure 37). All but about 2% of the sales are in the NH. The main removal process is with OH. It has an atmospheric lifetime of about 4-7 days.

Perchloroethylene (C_2Cl_4) is mainly used for dry cleaning and as a metal degreasing solvent. Small but significant quantities of C_2Cl_4 are emitted in the flue gas from coal-fired power plants. The atmospheric lifetime of C_2Cl_4 is 3-4 months and its primary atmospheric sink is reaction with OH. Its December 2010 atmospheric mole fraction is 3.2 with a trend decreasing at the rate of 0.2 ppt/yr (Figure 38).

3.3.5.1 CH_3Cl

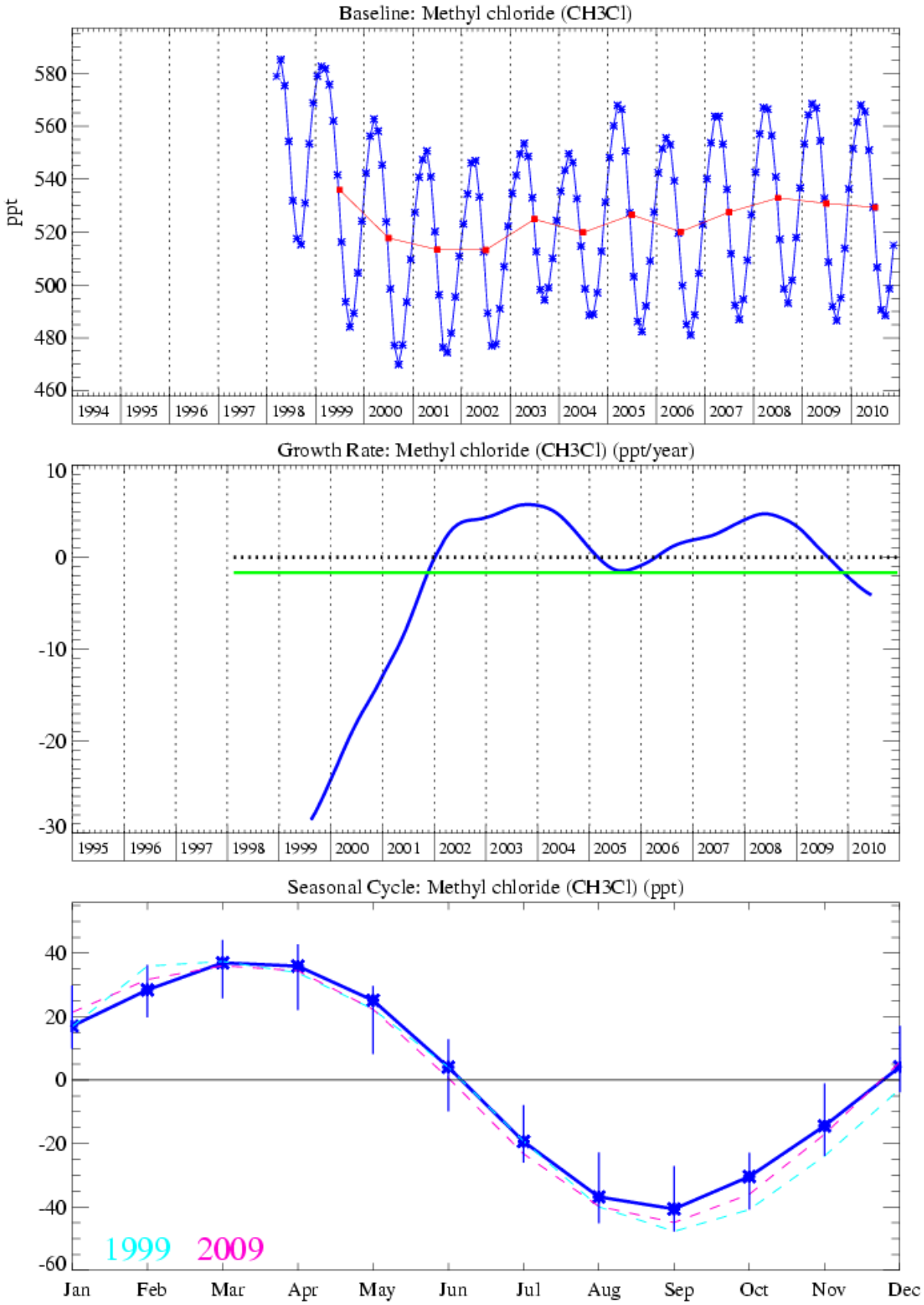

Figure 32: CH_3Cl: Monthly (blue) and annual (red) baseline concentrations (top plot). Annual (blue) and overall average growth rate (green) (middle plot). Seasonal cycle (de-trended) with year to year variability (lower plot).

3.3.5.2 CH_2Cl_2

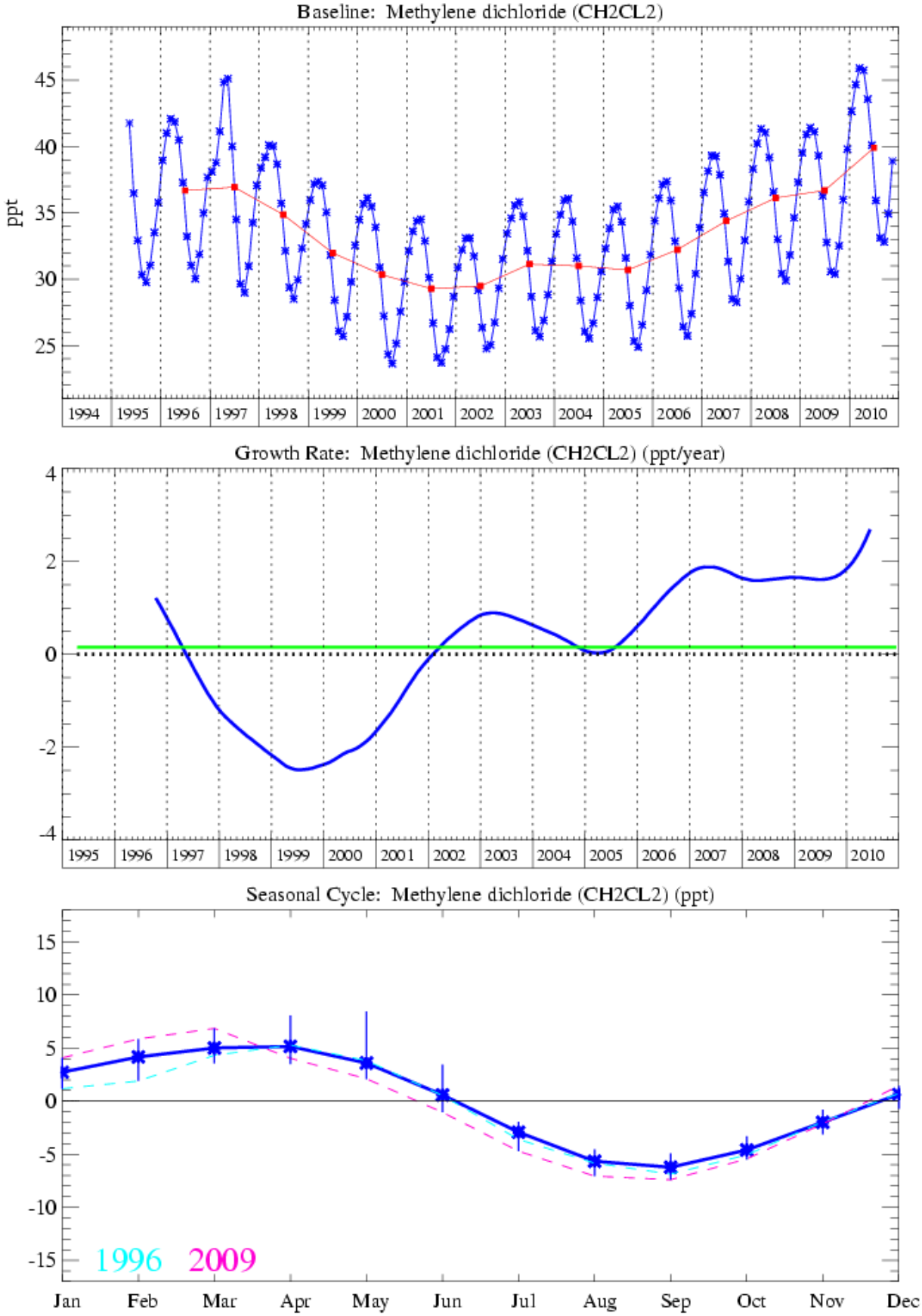

Figure 33: CH_2Cl_2: Monthly (blue) and annual (red) baseline concentrations (top plot). Annual (blue) and overall average growth rate (green) (middle plot). Seasonal cycle (de-trended) with year to year variability (lower plot).

3.3.5.3 $CHCl_3$ (chloroform)

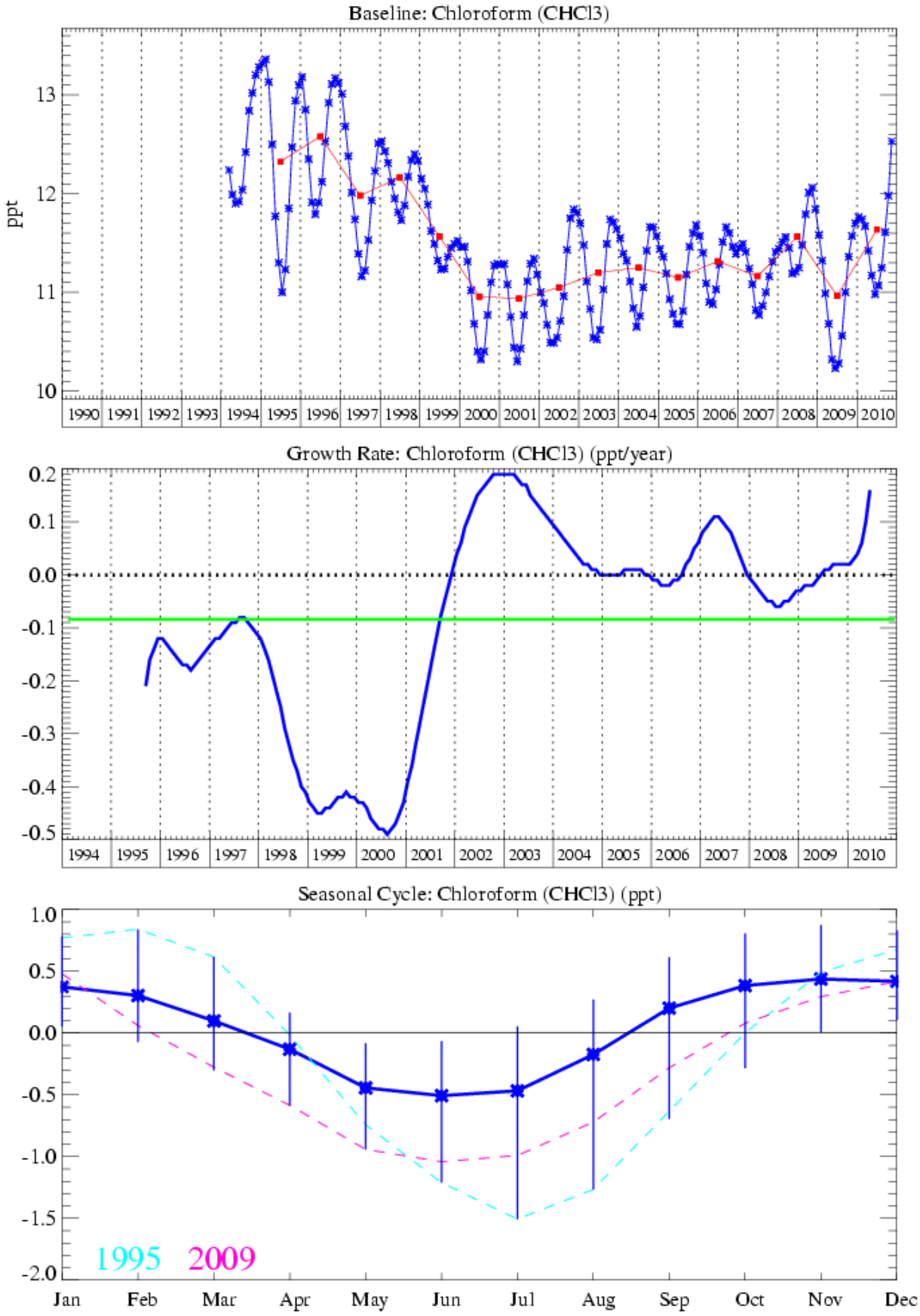

Figure 34: $CHCl_3$: Monthly (blue) and annual (red) baseline concentrations (top plot). Annual (blue) and overall average growth rate (green) (middle plot). Seasonal cycle (de-trended) with year to year variability (lower plot).

3.3.5.4 CCl_4 (carbon tetrachloride)

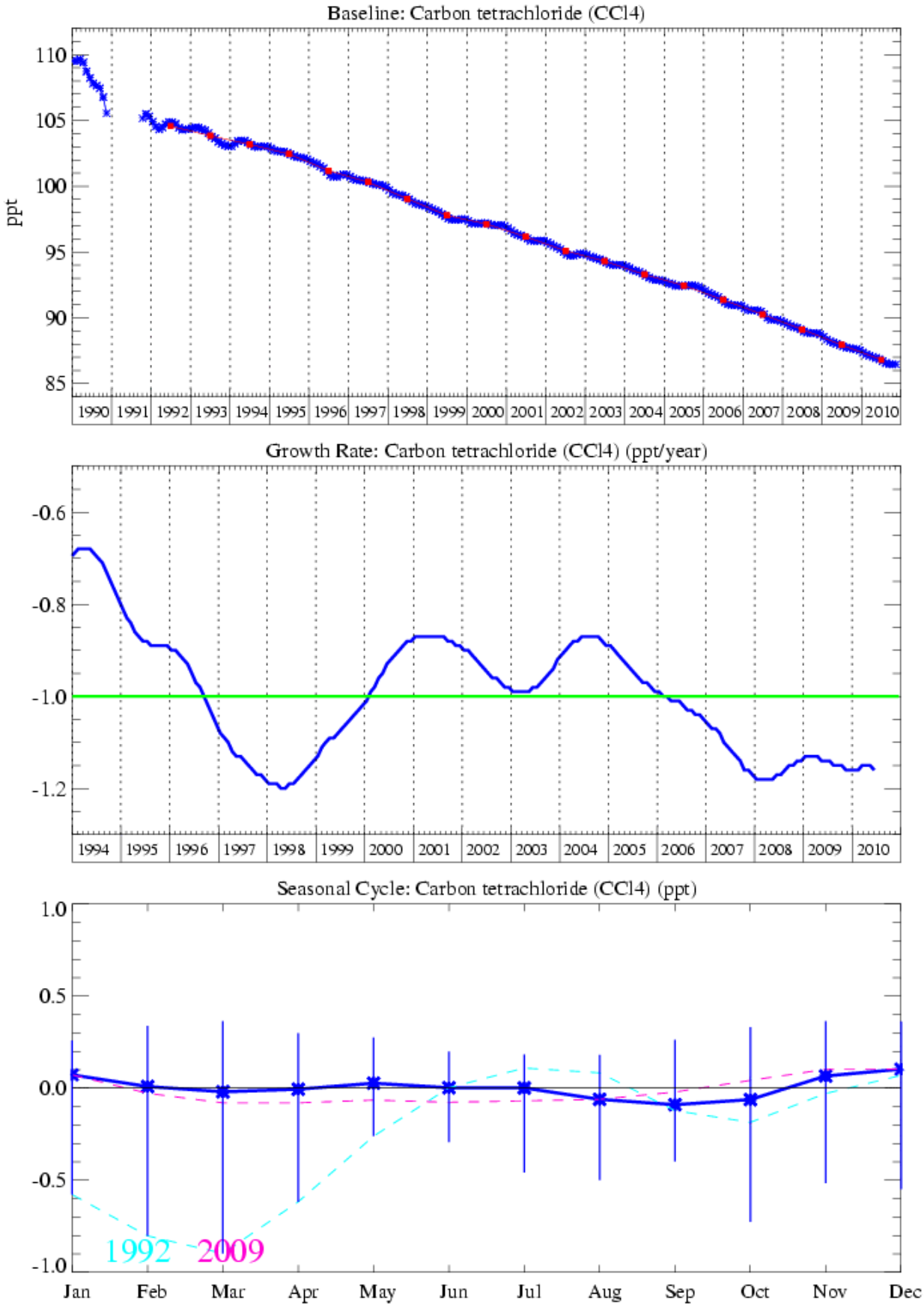

Figure 35: CCl_4: Monthly (blue) and annual (red) baseline concentrations (top plot). Annual (blue) and overall average growth rate (green) (middle plot). Seasonal cycle (de-trended) with year to year variability (lower plot).

3.3.5.5 CH_3CCl_3 (methyl chloroform)

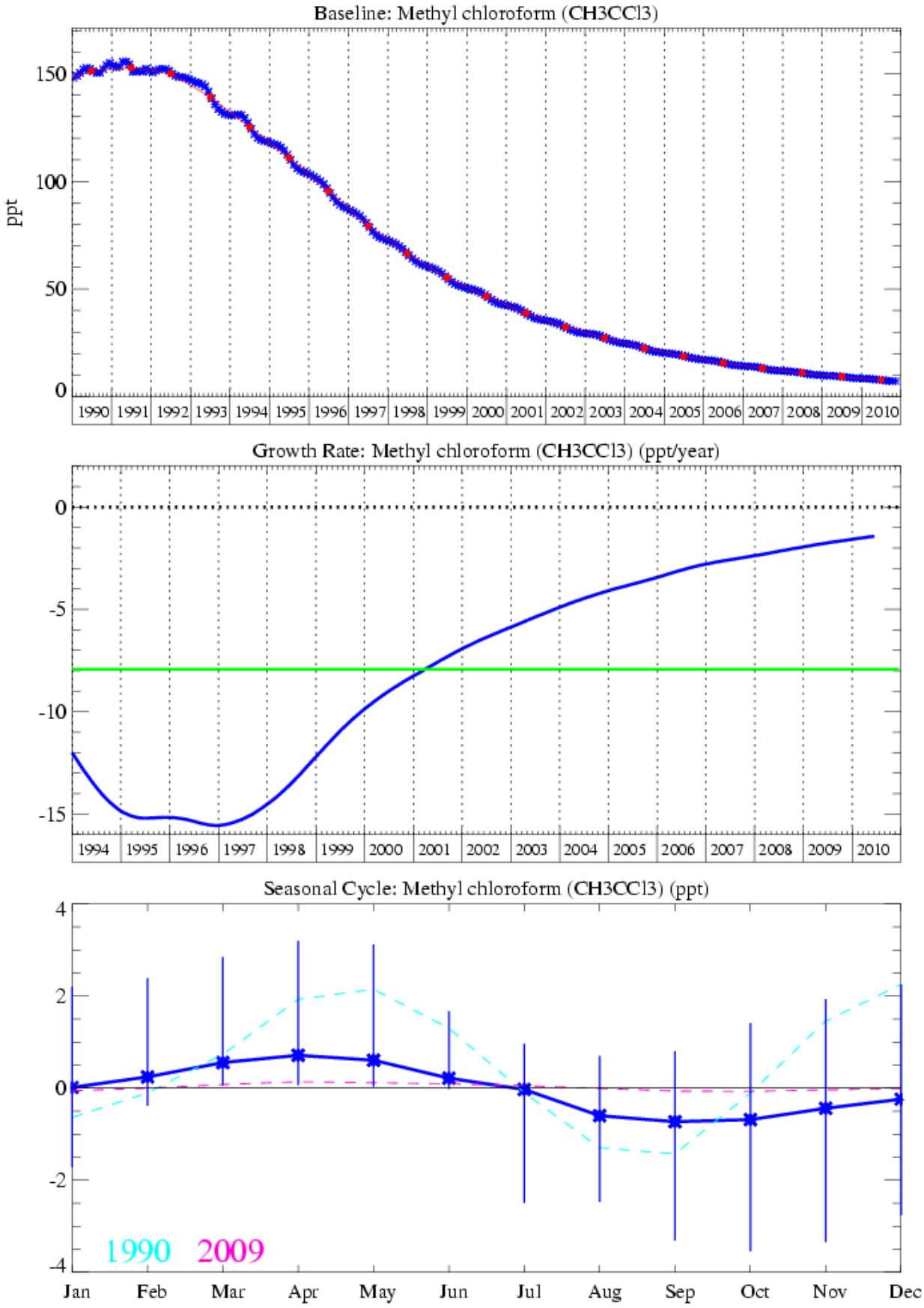

Figure 36: CH_3CCl_3: Monthly (blue) and annual (red) baseline concentrations (top plot). Annual (blue) and overall average growth rate (green) (middle plot). Seasonal cycle (de-trended) with year to year variability (lower plot).

3.3.5.6 $CHClCCl_2$

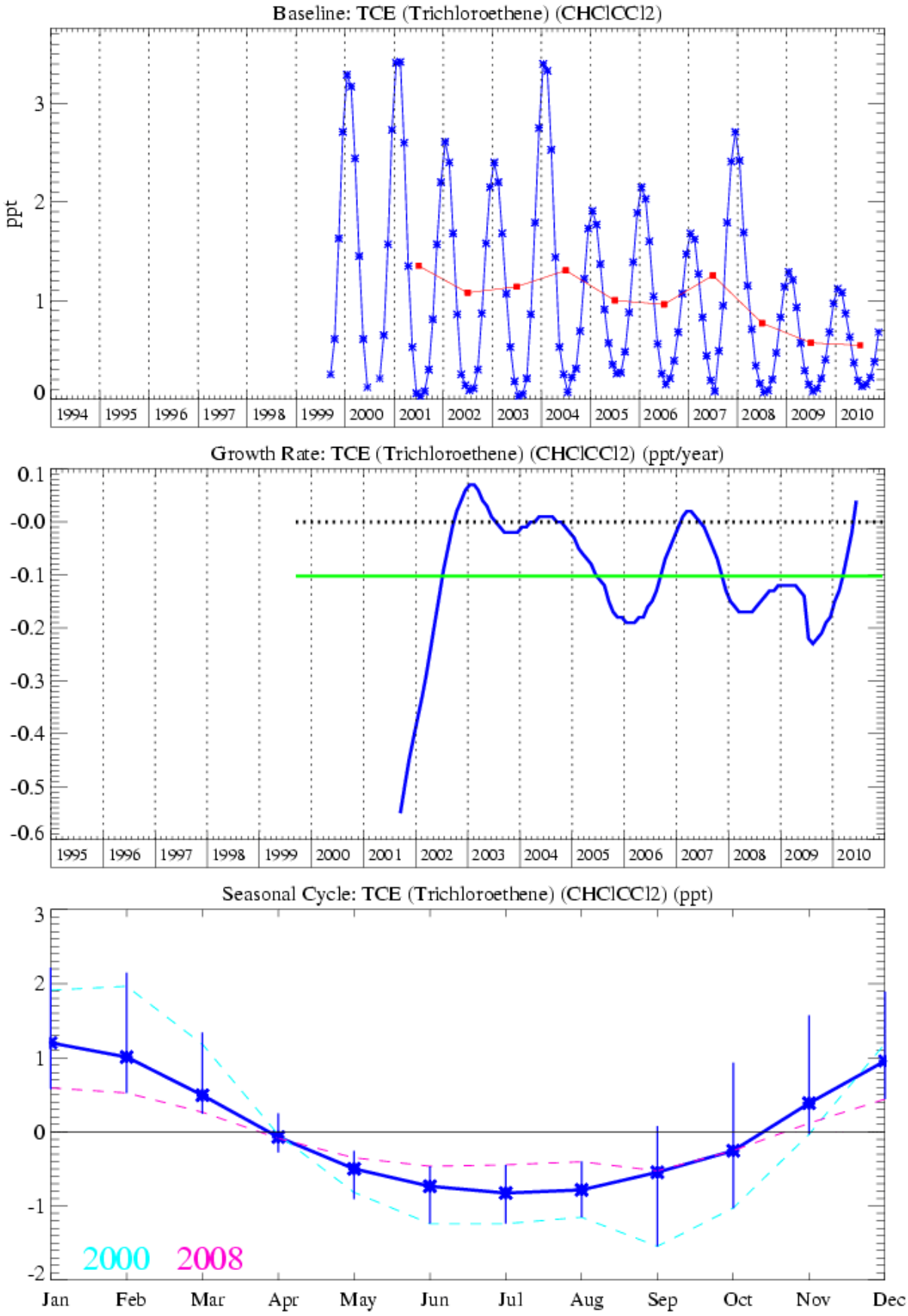

Figure 37: $CHClCCl_2$: Monthly (blue) and annual (red) baseline concentrations (top plot). Annual (blue) and overall average growth rate (green) (middle plot). Seasonal cycle (de-trended) with year to year variability (lower plot).

3.3.5.7 CCl_2CCl_2

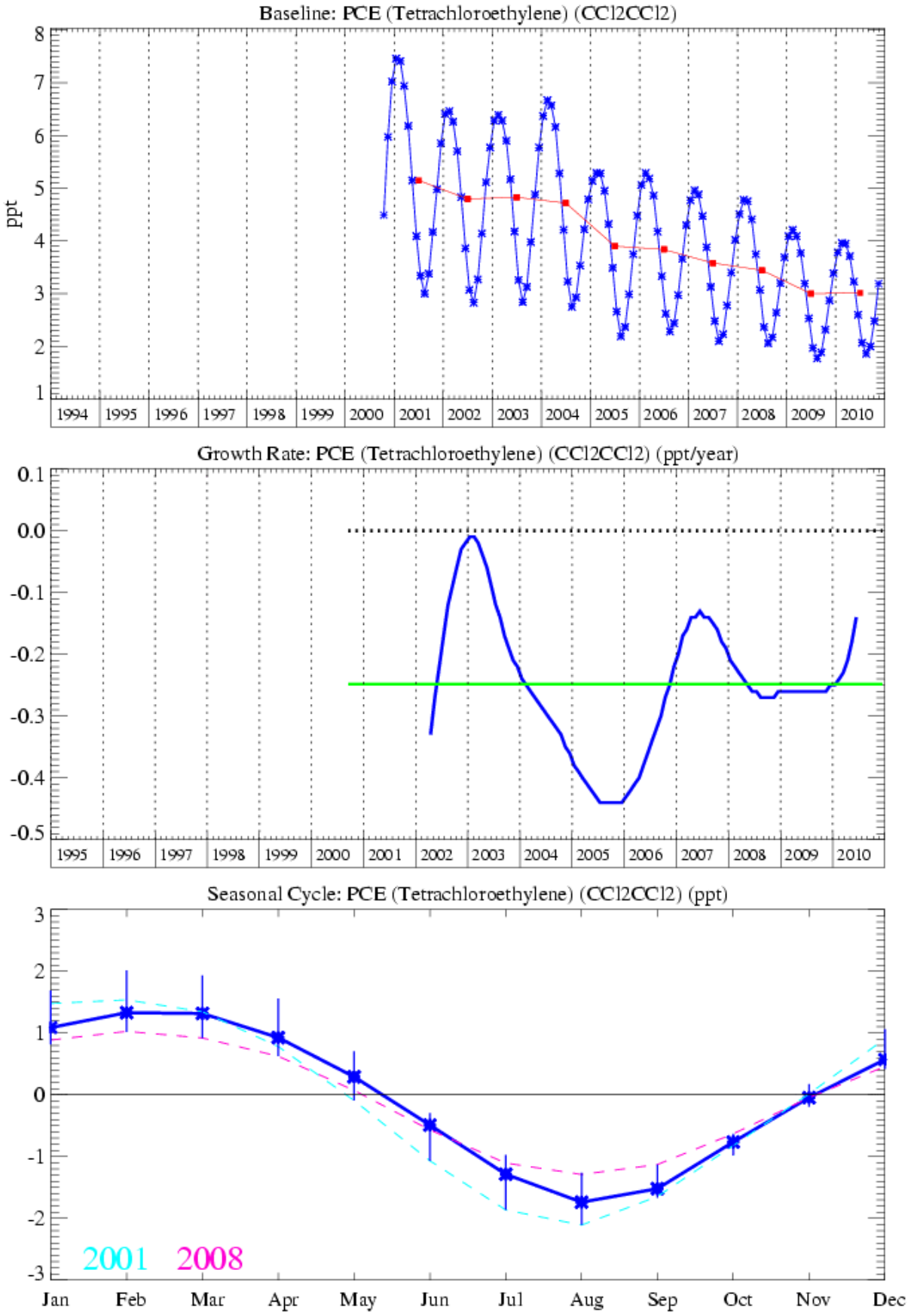

Figure 38: CCl_2CCl_2: Monthly (blue) and annual (red) baseline concentrations (top plot). Annual (blue) and overall average growth rate (green) (middle plot). Seasonal cycle (de-trended) with year to year variability (lower plot).

3.3.6 Bromine compounds

Halon-1211 (Figure 42) continues to show a slight reduction of 0.07 ppt/yr due to limits imposed on halon production in developed nations. Levels at Mace Head are 4.2 ppt for halon-1211 at the end of December 2010. The trend of halon-1301 shown in Figure 43 appears to have reached a plateau at 3.3 ppt in the background atmosphere at Mace Head. The differing rate of decline of the two halons is reflected by their different atmospheric lifetimes; 65 years for halon-1301 and 16 years for halon-1211.

We continue to report trends for the minor halon-2402 (20 year lifetime). This compound was used predominantly in the former Soviet Union. No information on the production of halon-2402 before 1986 has been found. Fraser et al., (1999) developed emission projections for halon-2402 based on atmospheric measurements. They reported that the emissions grew steadily in the 1970s and 1980s, peaking in the 1988-91 timeframe at 1.7 Gg/yr and found these results to be qualitatively consistent with the peak production of 28,000 ODP tonnes reported by the Russian Federation under Article VII of the Montreal Protocol (or assuming all production was halon-2402 and an ODP of 6, a peak production of approximately 4.650 Gg/yr). Measurements at Mace Head indicate that the levels of halon-2402 are fairly stable in the atmosphere (0.46 ppt), the trend estimates are for a reduction of 0.01 ppt/yr in January – June 2010, however the error bars associated with the measurement are large (Figure 44).

3.3.6.1 Methyl bromide (CH_3Br)

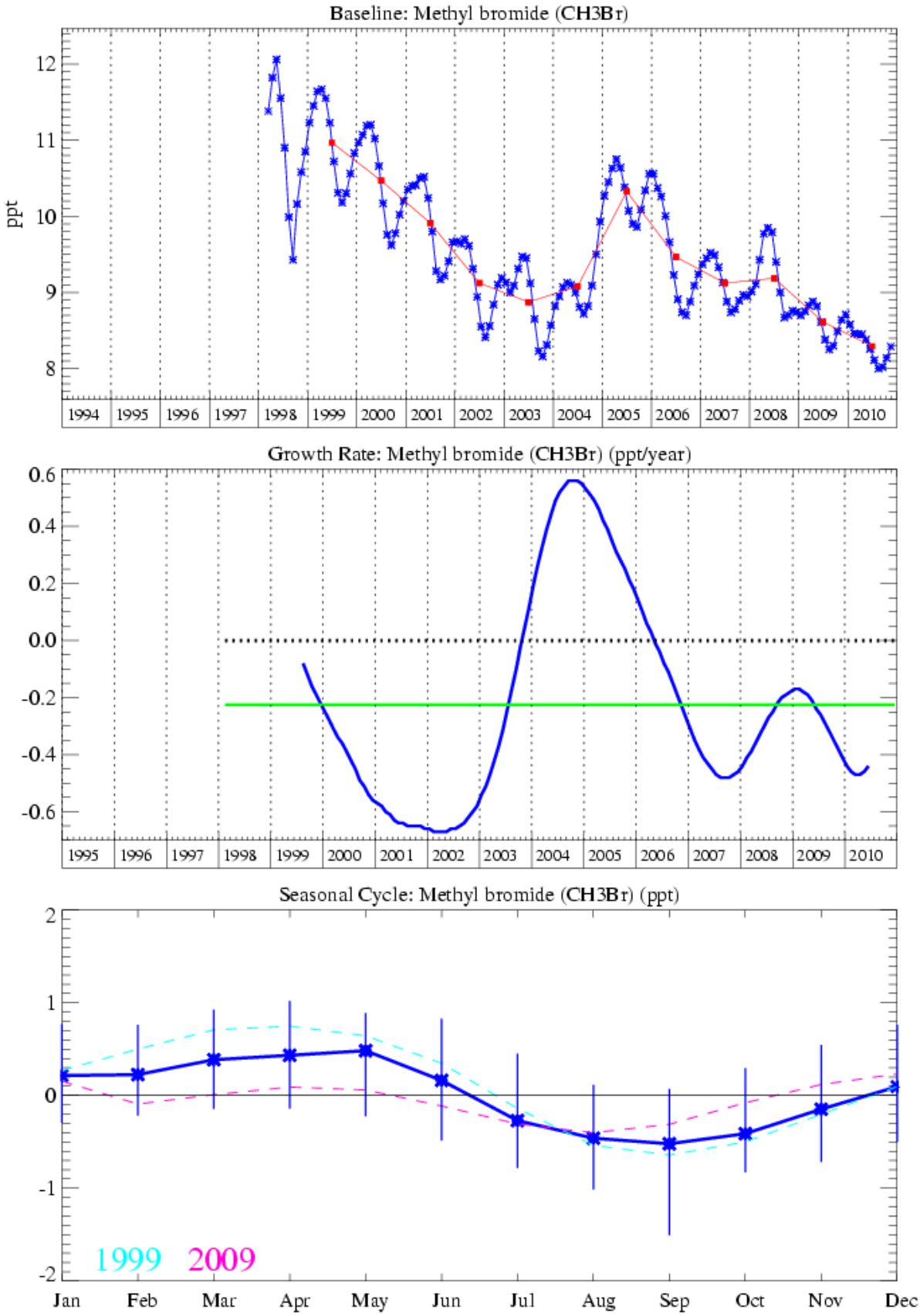

Figure 39: Methyl bromide: Monthly (blue) and annual (red) baseline concentrations (top plot). Annual (blue) and overall average growth rate (green) (middle plot). Seasonal cycle (de-trended) with year to year variability (lower plot).

3.3.6.2 CH_2Br_2

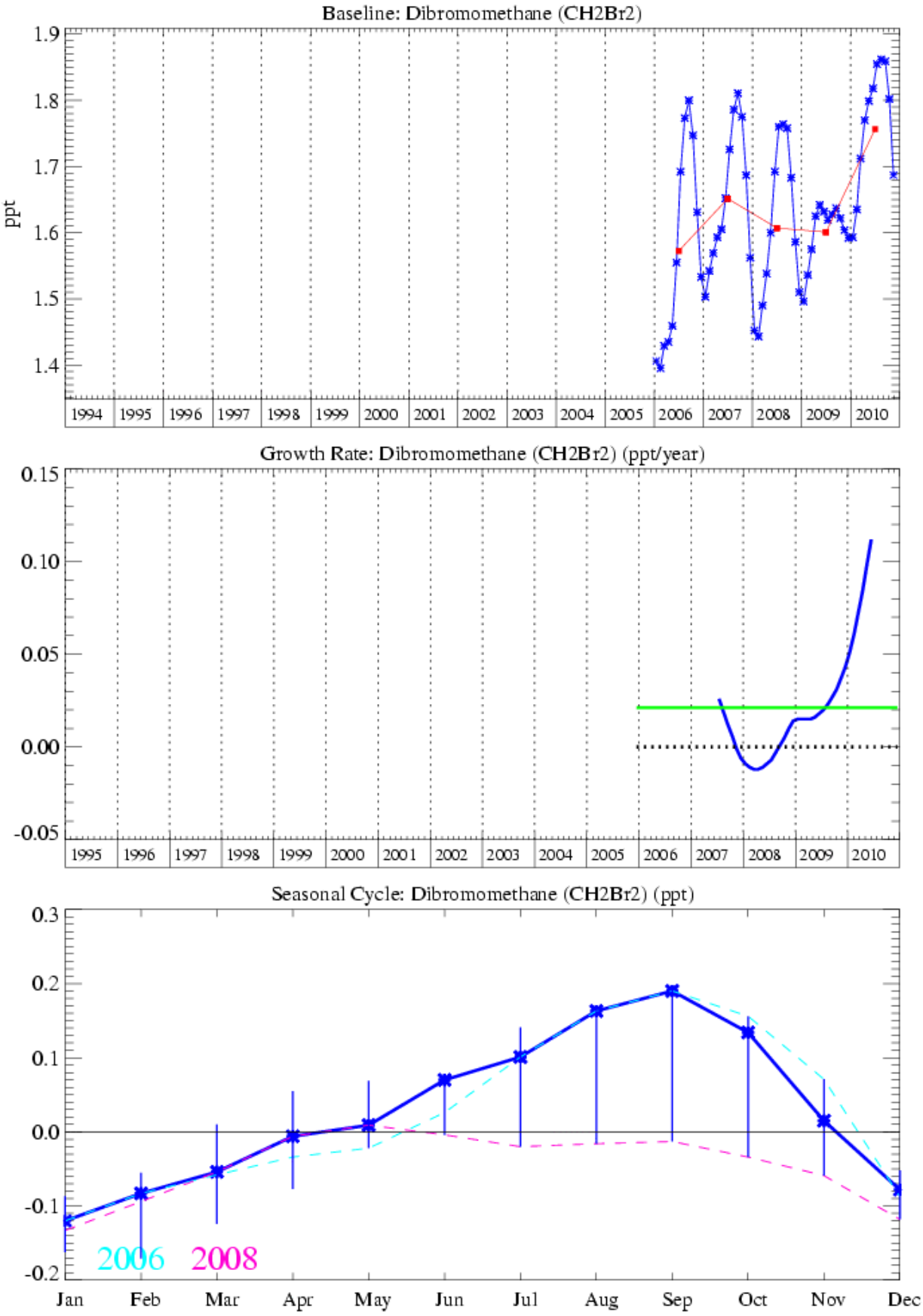

Figure 40: Dibromomethane: Monthly (blue) and annual (red) baseline concentrations (top plot). Annual (blue) and overall average growth rate (green) (middle plot). Seasonal cycle (de-trended) with year to year variability (lower plot).

3.3.6.3 Bromoform ($CHBr_3$)

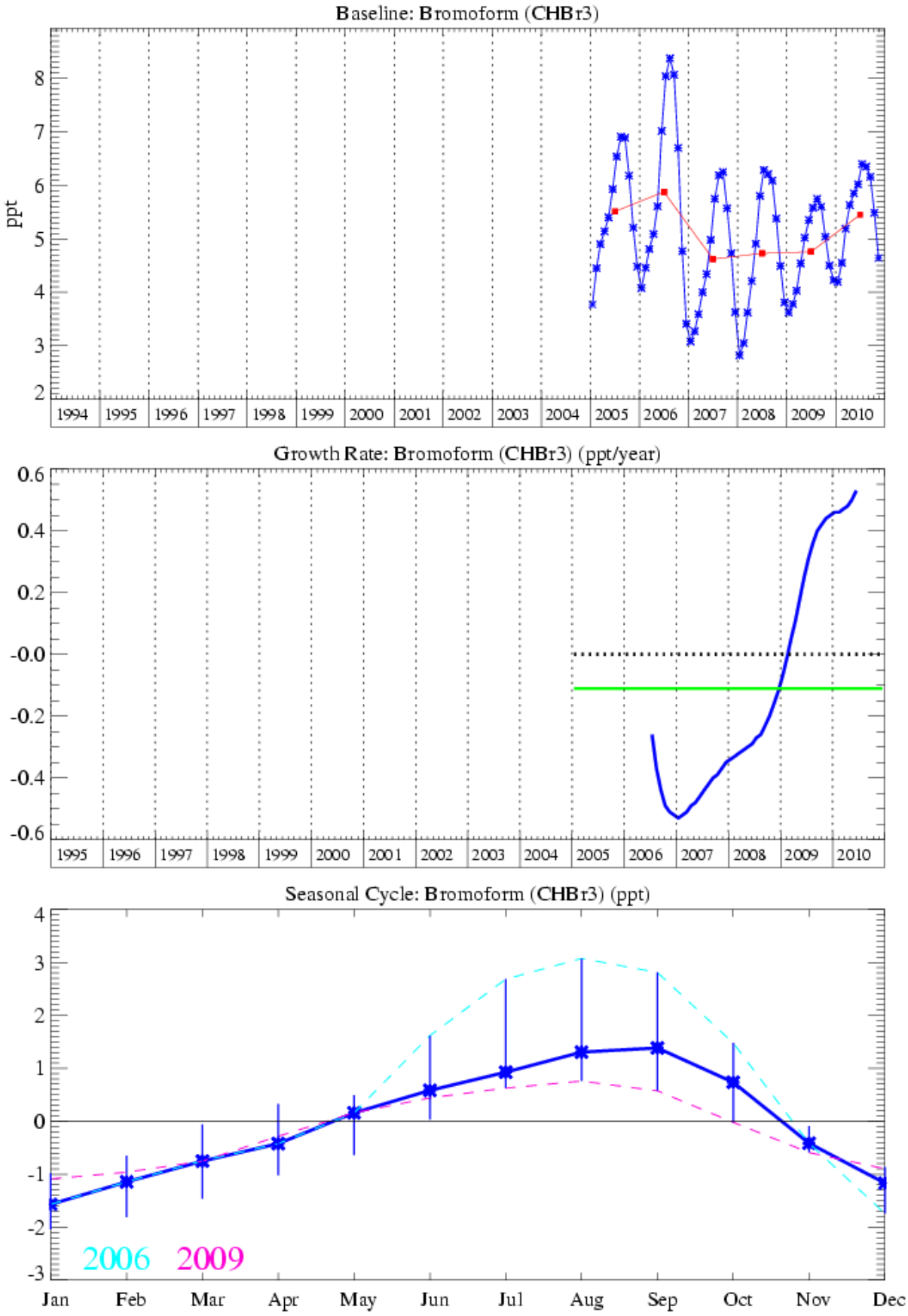

Figure 41: Bromoform: Monthly (blue) and annual (red) baseline concentrations (top plot). Annual (blue) and overall average growth rate (green) (middle plot). Seasonal cycle (de-trended) with year to year variability (lower plot).

3.3.6.4 Halon-1211

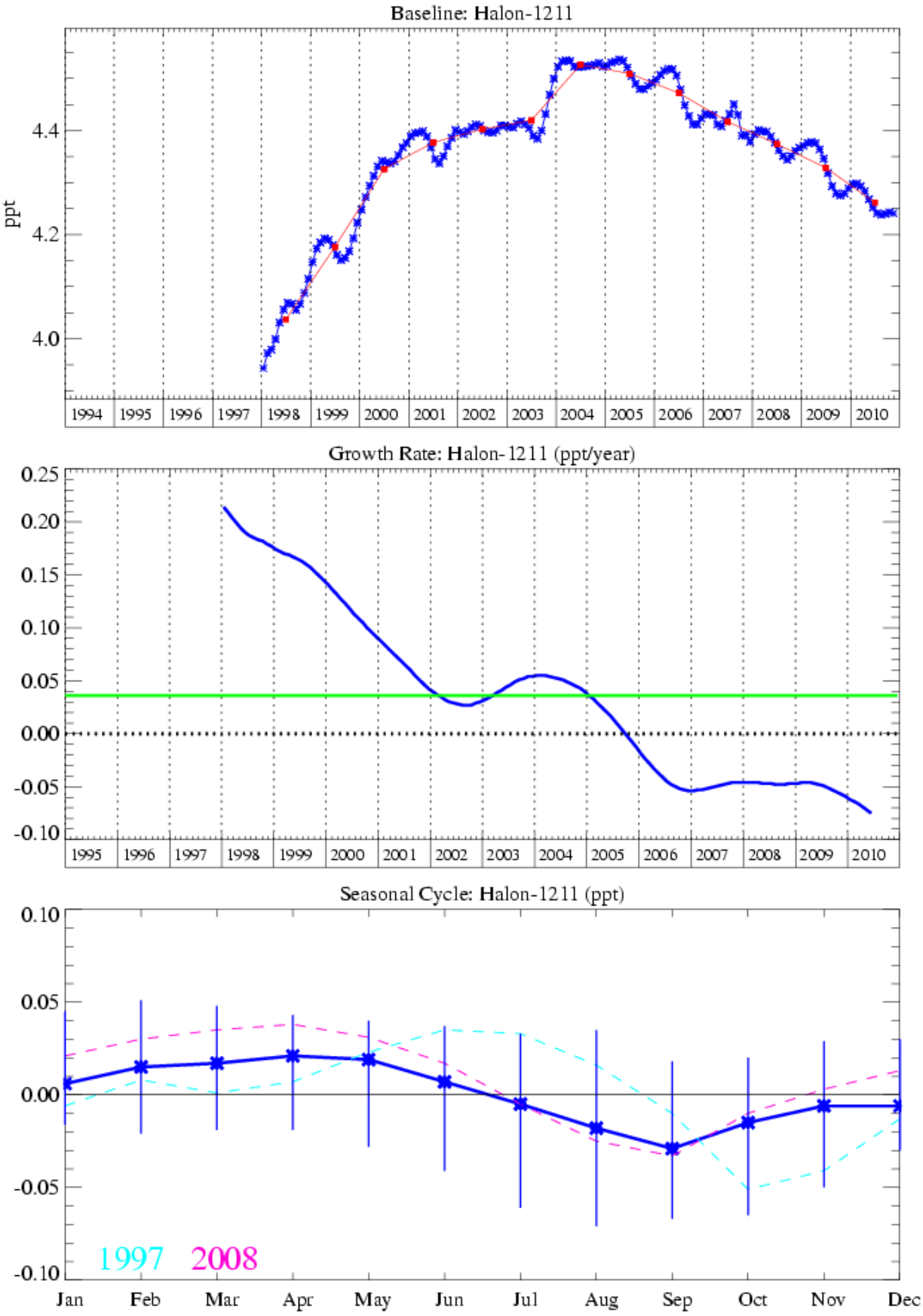

Figure 42: Halon-1211: Monthly (blue) and annual (red) baseline concentrations (top plot). Annual (blue) and overall average growth rate (green) (middle plot). Seasonal cycle (de-trended) with year to year variability (lower plot).

3.3.6.5 Halon-1301

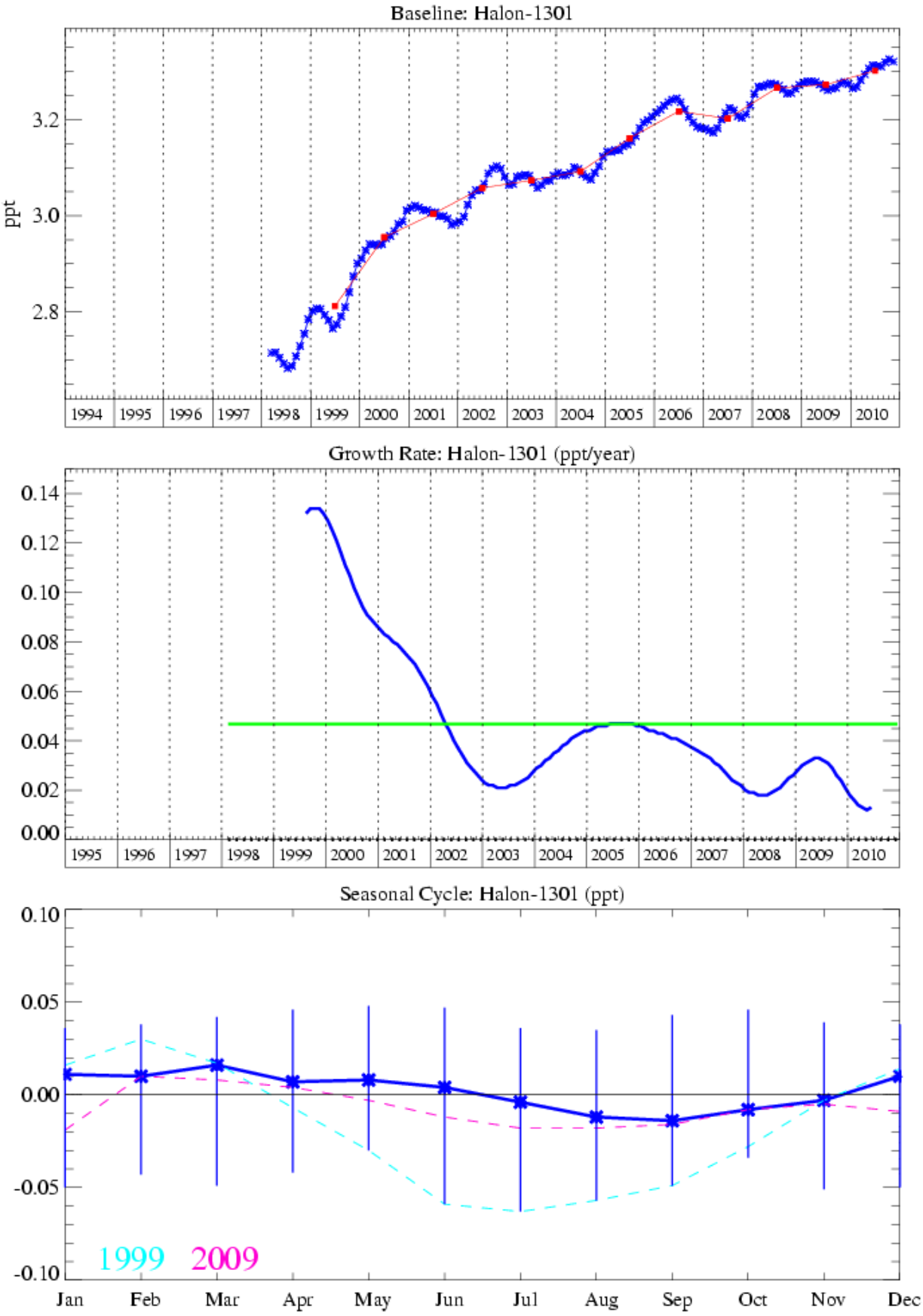

Figure 43: Halon-1301: Monthly (blue) and annual (red) baseline concentrations (top plot). Annual (blue) and overall average growth rate (green) (middle plot). Seasonal cycle (de-trended) with year to year variability (lower plot).

3.3.6.6 Halon-2402

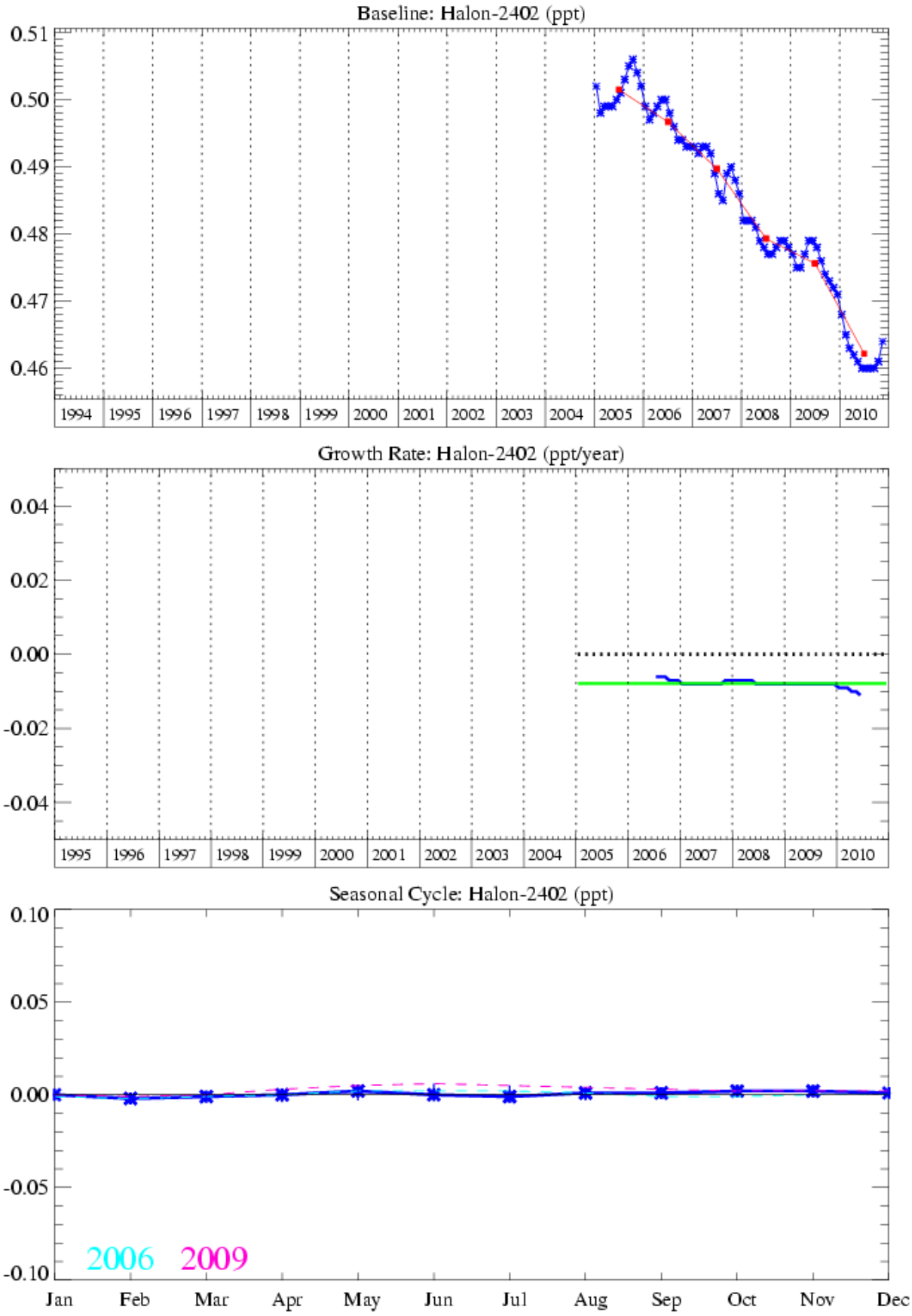

Figure 44: Halon-2402: Monthly (blue) and annual (red) baseline concentrations (top plot). Annual (blue) and overall average growth rate (green) (middle plot). Seasonal cycle (de-trended) with year to year variability (lower plot).

3.3.7 Iodine compounds

3.3.7.1 CH_3I

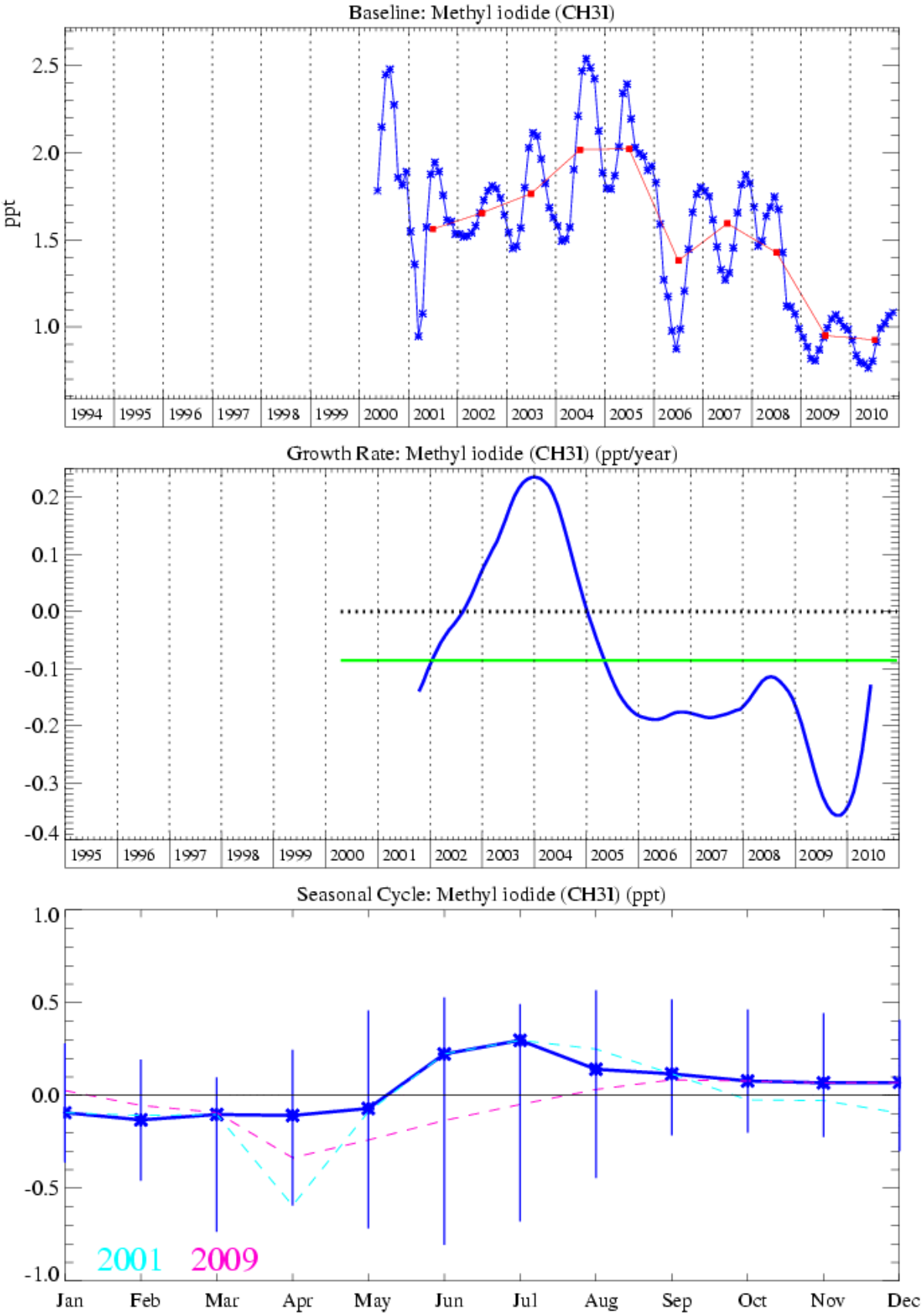

Figure 45: CH_3I: Monthly (blue) and annual (red) baseline concentrations (top plot). Annual (blue) and overall average growth rate (green) (middle plot). Seasonal cycle (de-trended) with year to year variability (lower plot).

3.3.8 Hydrocarbons

The long term trend for CH_4, shown in Figure 46 is of particular interest with a steep rise up to about 2000 followed by a flat period with almost no growth and then most recently a steep rise of 7.5 ppb/yr over the period 2008-2009, January – June 2010 showed growth of 1.2 ppb/yr with a mixing ratio of 1877.5 ppb in December 2010. This most recent growth rate anomaly is unusual in that it occurred almost simultaneously at all of the AGAGE stations in both hemispheres.

In our annual report in 2009 we discussed how the mole fraction of CH_4 in the atmosphere had been rising considerably faster than its long term average growth rate. Several theories were postulated:

(1) Increased emissions from the high latitudes in the Northern hemisphere related to wetlands and reduced permafrost/snow cover.
(2) Increased emissions in the tropics due to increased emissions from wetlands/rice production or biomass burning due to El Niňo conditions.
(3) Reduced levels of OH in the atmosphere. OH is the major sink for atmospheric CH_4.

However each of these theories in isolation does not seem to completely fit the evidence gathered so far. It was therefore our opinion that it is as yet too early to precisely pinpoint the cause for the elevated levels of CH_4 across the globe.
The inferences drawn from the observations were that the CH_4 increase are driven by wetland emissions in the boreal region (driven by a temperature anomaly) and in the tropics (possibly driven by a precipitation anomaly) with a small role for OH changes a possibility in the tropics but not statistically significant. The mole fraction of CH_4 reported from Mace Head (and other AGAGE stations) in 2009 indicate that the rise in CH_4 has now levelled out (as shown in Figure 46)

3.3.8.1 Methane (CH_4)

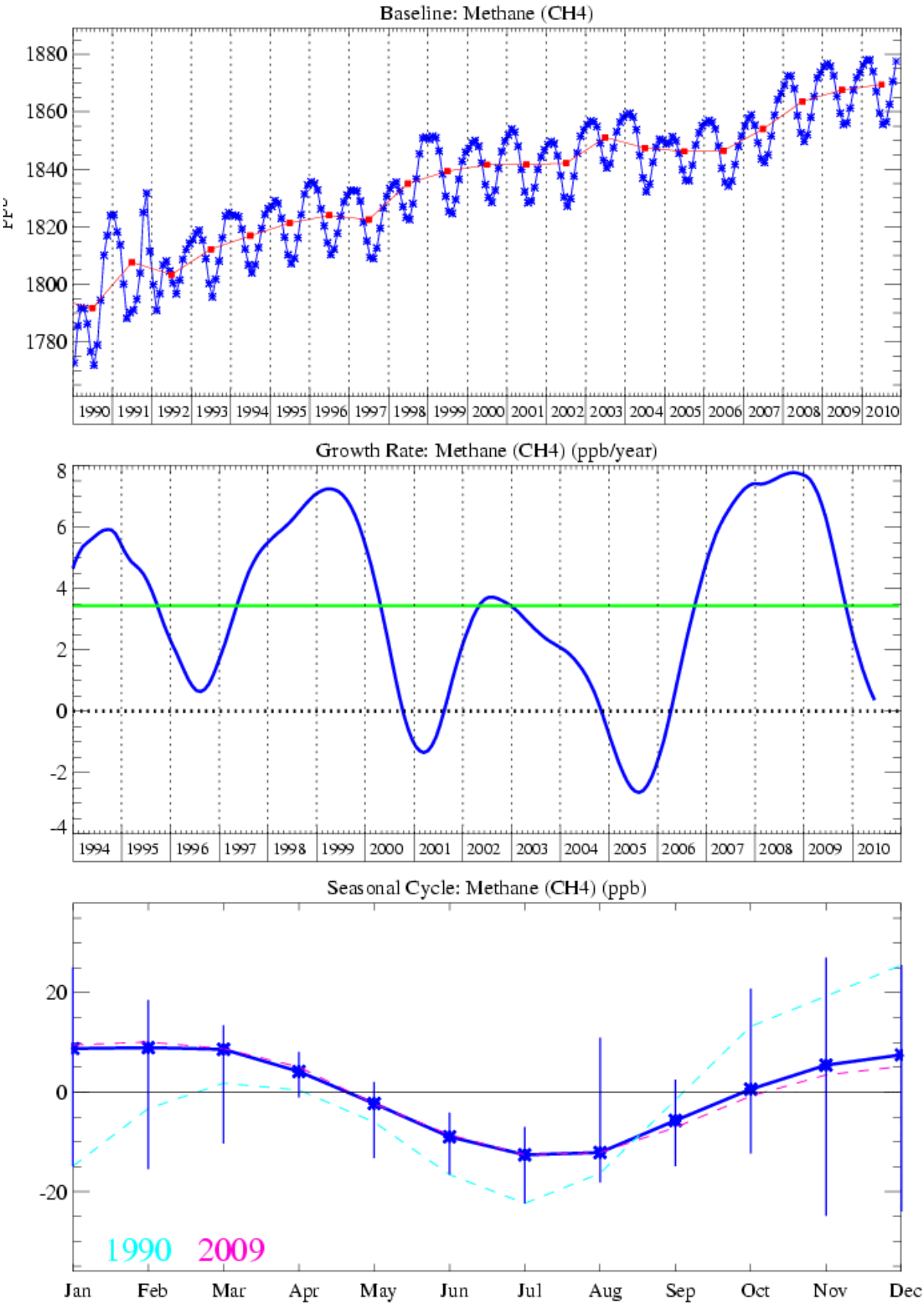

Figure 46: Methane: Monthly (blue) and annual (red) baseline concentrations (top plot). Annual (blue) and overall average growth rate (green) (middle plot). Seasonal cycle (de-trended) with year to year variability (lower plot).

3.3.8.2 Ethane (C_2H_6)

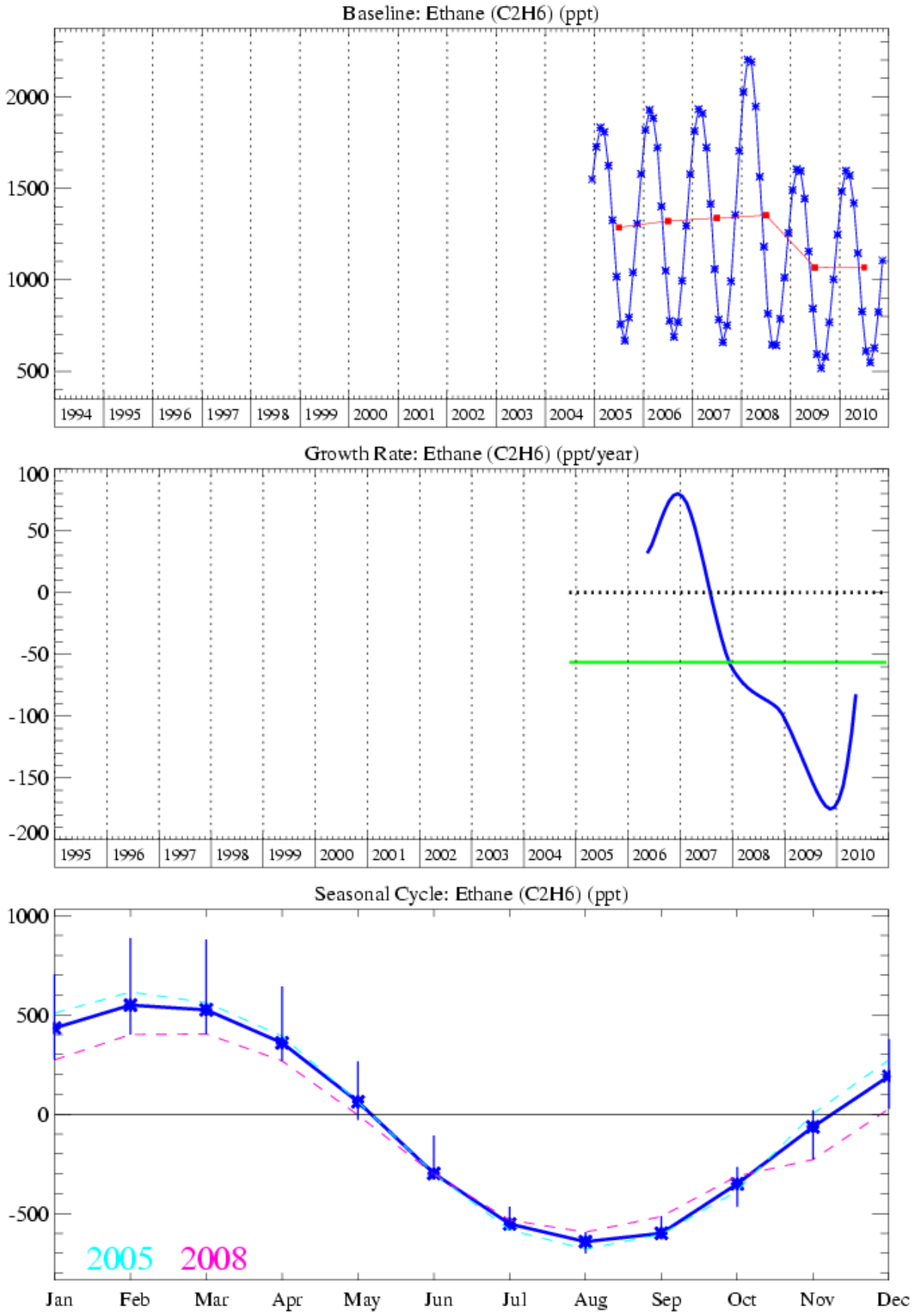

Figure 47: Ethane: Monthly (blue) and annual (red) baseline concentrations (top plot). Annual (blue) and overall average growth rate (green) (middle plot). Seasonal cycle (de-trended) with year to year variability (lower plot).

3.3.8.3 Benzene (C_6H_6)

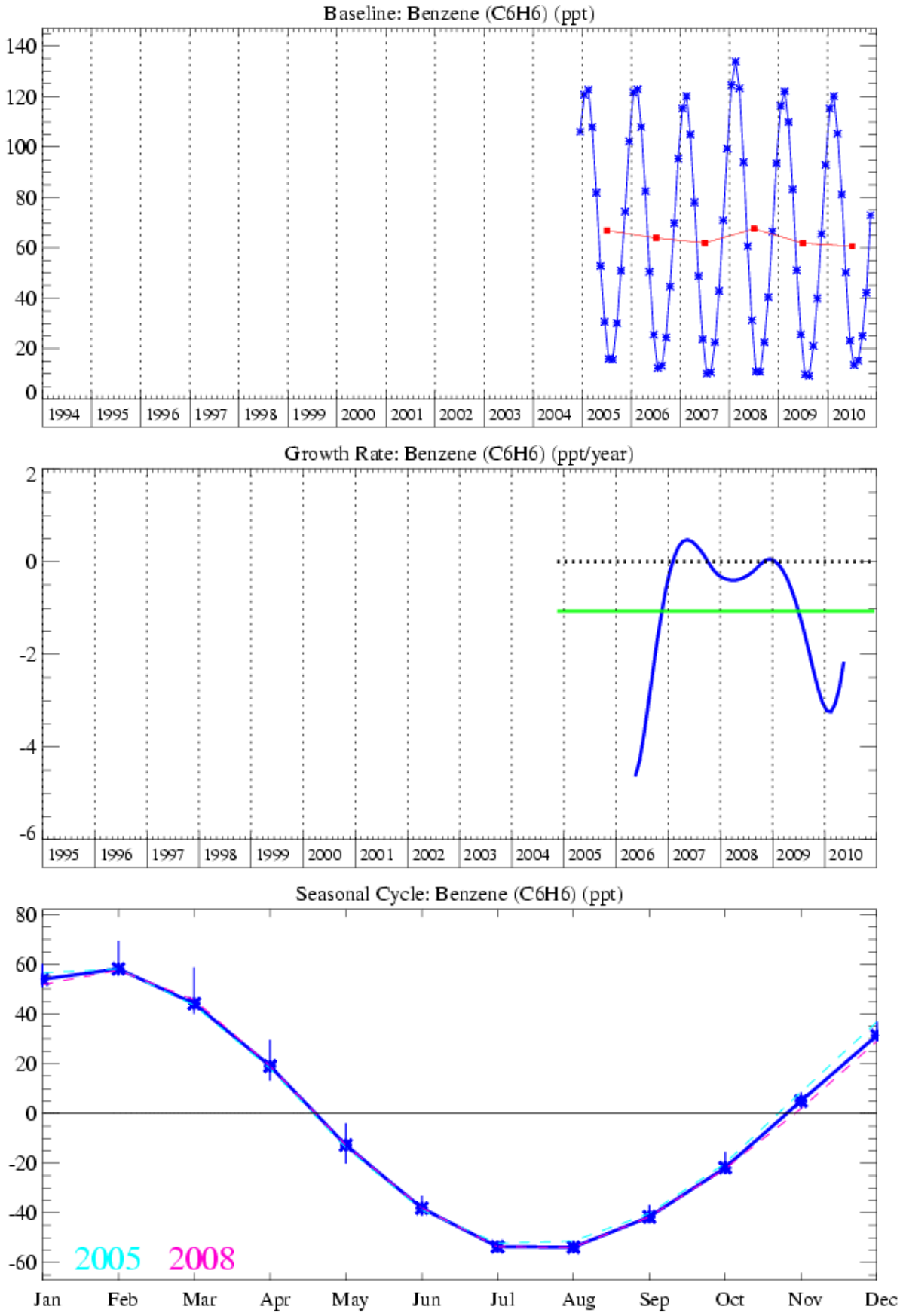

Figure 48: Benzene: Monthly (blue) and annual (red) baseline concentrations (top plot). Annual (blue) and overall average growth rate (green) (middle plot). Seasonal cycle (de-trended) with year to year variability (lower plot).

3.3.8.4 Toluene (C_7H_8)

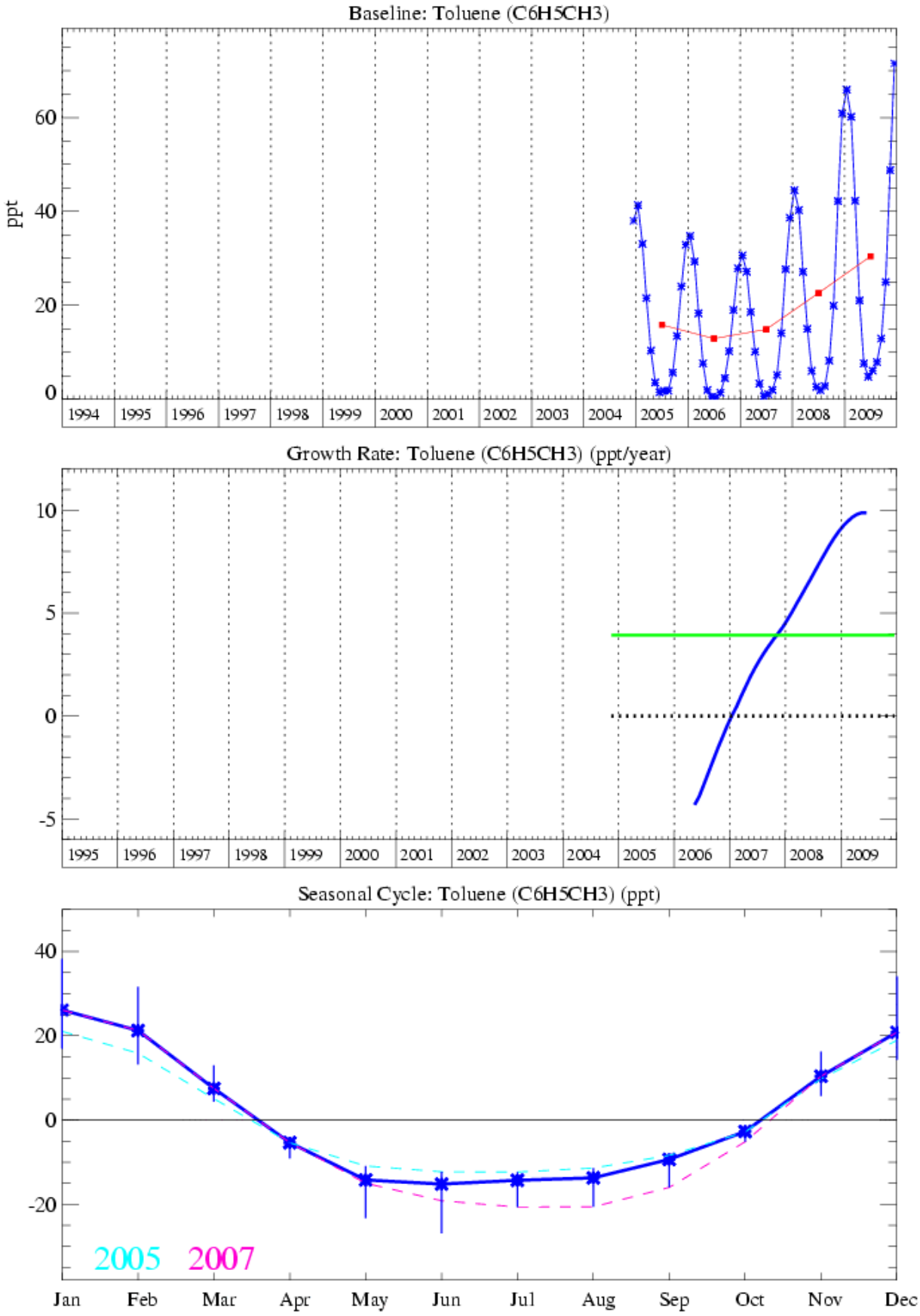

Figure 49: Toluene: Monthly (blue) and annual (red) baseline concentrations (top plot). Annual (blue) and overall average growth rate (green) (middle plot). Seasonal cycle (de-trended) with year to year variability (lower plot).

3.3.9 Oxides of carbon, nitrous oxide, ozone and hydrogen

CO (Figure 50) shows a slightly positive trend of 0.05 ppb/yr over the most recent 6-month period (January – June 2010). It mole fraction at Mace Head in December 2010 was 107.8 ppb. The annual trend in this gas is quite variable; this is attributable to the effects of biomass burning. There is evidence of a small biomass burning event in late 2007 which contrasts with the much larger biomass burning events in 1998/9 and 2003/4.

CO_2 (Figure 51) is the most important greenhouse gas, and has steadily grown at an annual average rate of 1.9 ppm/yr, calculated from the baseline-selected monthly means, it has now reached a mixing ratio of 390 ppm (2010 average) and has shown significant growth rate anomalies in 1998/99 and 2002/03, which we suggest are a result of the global biomass burning events in those years.

Figure 53 shows the baseline monthly means and trend for N_2O with an almost linear upwards trend of about 0.6 ppb/yr (January – June 2010) and a mixing ratio of 323.8 ppb in December 2010 at Mace Head. The N_2O increase is attributable to human activities, such as fertilizer use and fossil fuel burning, although is also emitted through natural processes occurring in soils and oceans. There are large uncertainties associated with the quantifying the sources of this gas.

Tropospheric O_3 measurements first started at Mace Head in 1987 and the trends derived from the baseline-selected monthly means, the growth rate and seasonal cycles are shown in Figure 55. The Mace Head O_3 measurements exhibited a positive trend (~0.49 ppb) up to about 2003. However, since then there has been no significant growth in ozone and the 12-month moving average of the baseline monthly means in 2010 if anything suggest a small decline of 0.6 ppb/yr (January – June 2010), it's mole fraction at Mace Head was 40.5 in December 2010. Assessment of the long-term trends in tropospheric ozone is difficult due to the scarcity of representative observing sites with long records. The records that do exist vary both in terms of sign and magnitude (Forster *et al.,* 2007).

H_2 (Figure 56) shows a trend which is practically flat within measurement uncertainty (-2.3 ppb/yr) over the most recent 6 month period (January – June 2010). It shows a mole fraction of 485.2 ppb in December 2010 which is in the upward phase of its seasonal cycle. Emissions of H_2 come from large scale biomass burning events which are generally responsible for the elevations in annual averages observed in 1998/99, 2002/03 and 2006.

3.3.9.1 Carbon monoxide (CO)

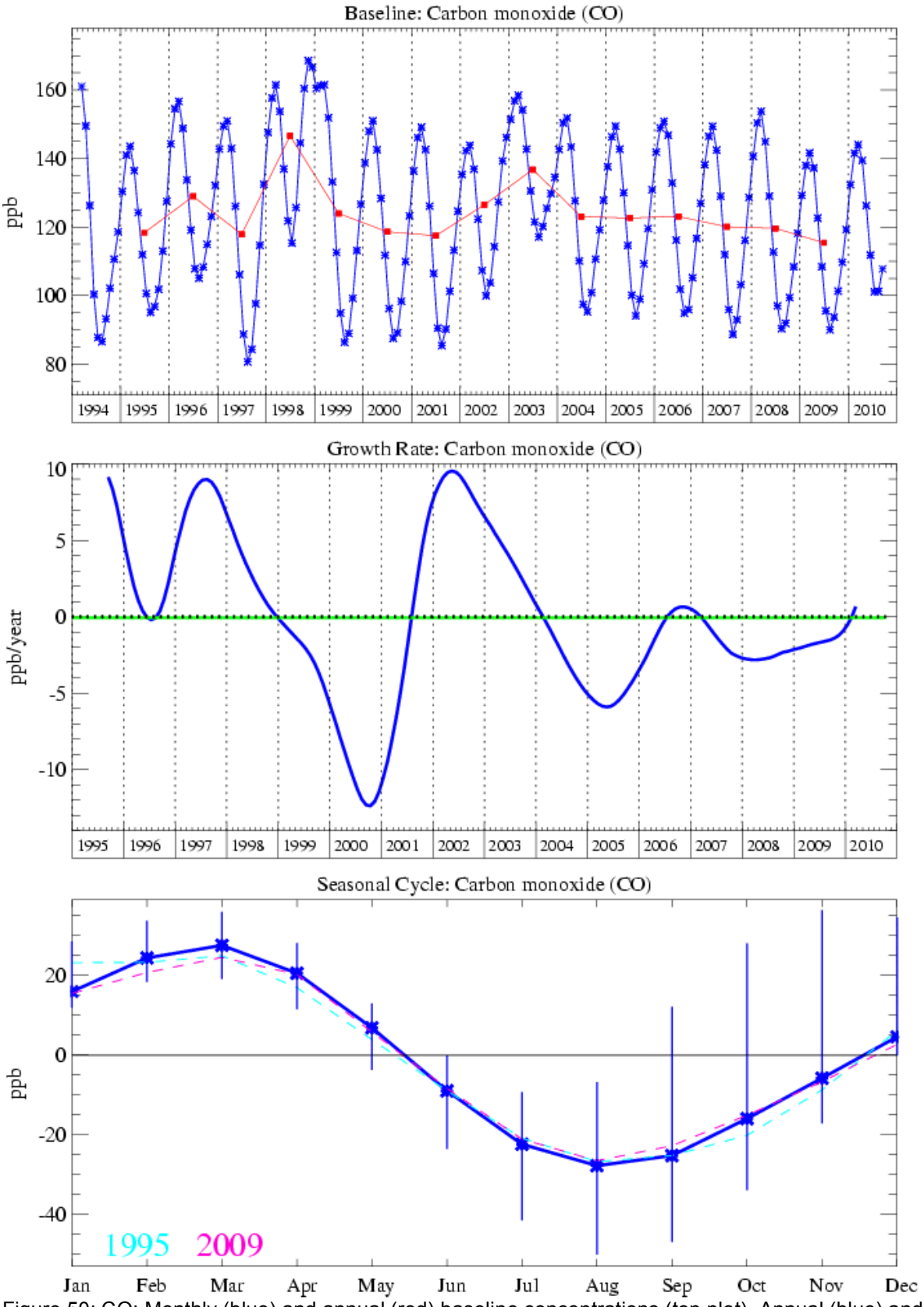

Figure 50: CO: Monthly (blue) and annual (red) baseline concentrations (top plot). Annual (blue) and overall average growth rate (green) (middle plot). Seasonal cycle (de-trended) with year to year variability (lower plot).

3.3.9.2 Carbon dioxide (CO_2)

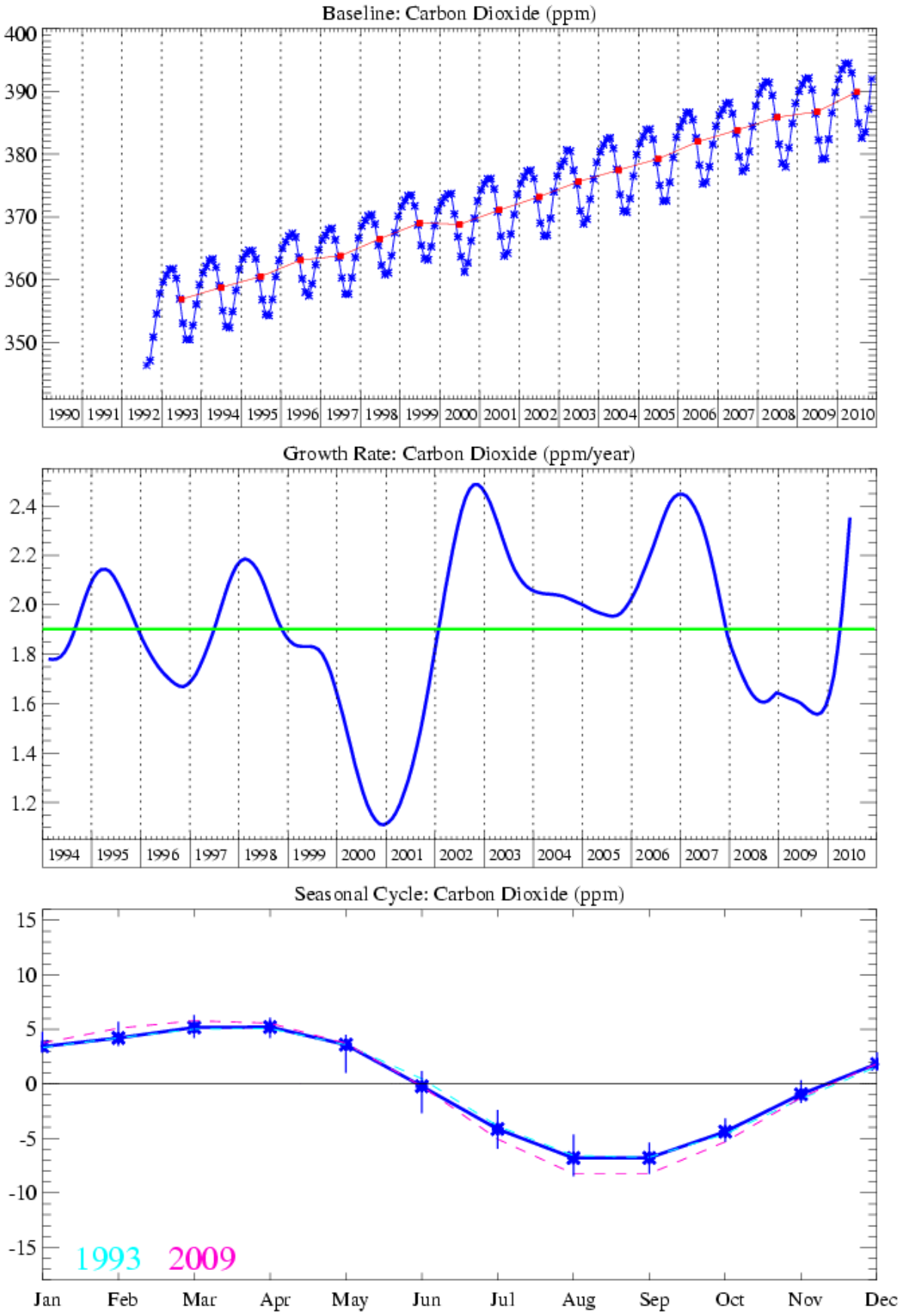

Figure 51: Carbon dioxide: Monthly (blue) and annual (red) baseline concentrations (top plot). Annual (blue) and overall average growth rate (green) (middle plot). Seasonal cycle (de-trended) with year to year variability (lower plot).

3.3.9.3 Carbonyl sulphide (COS)

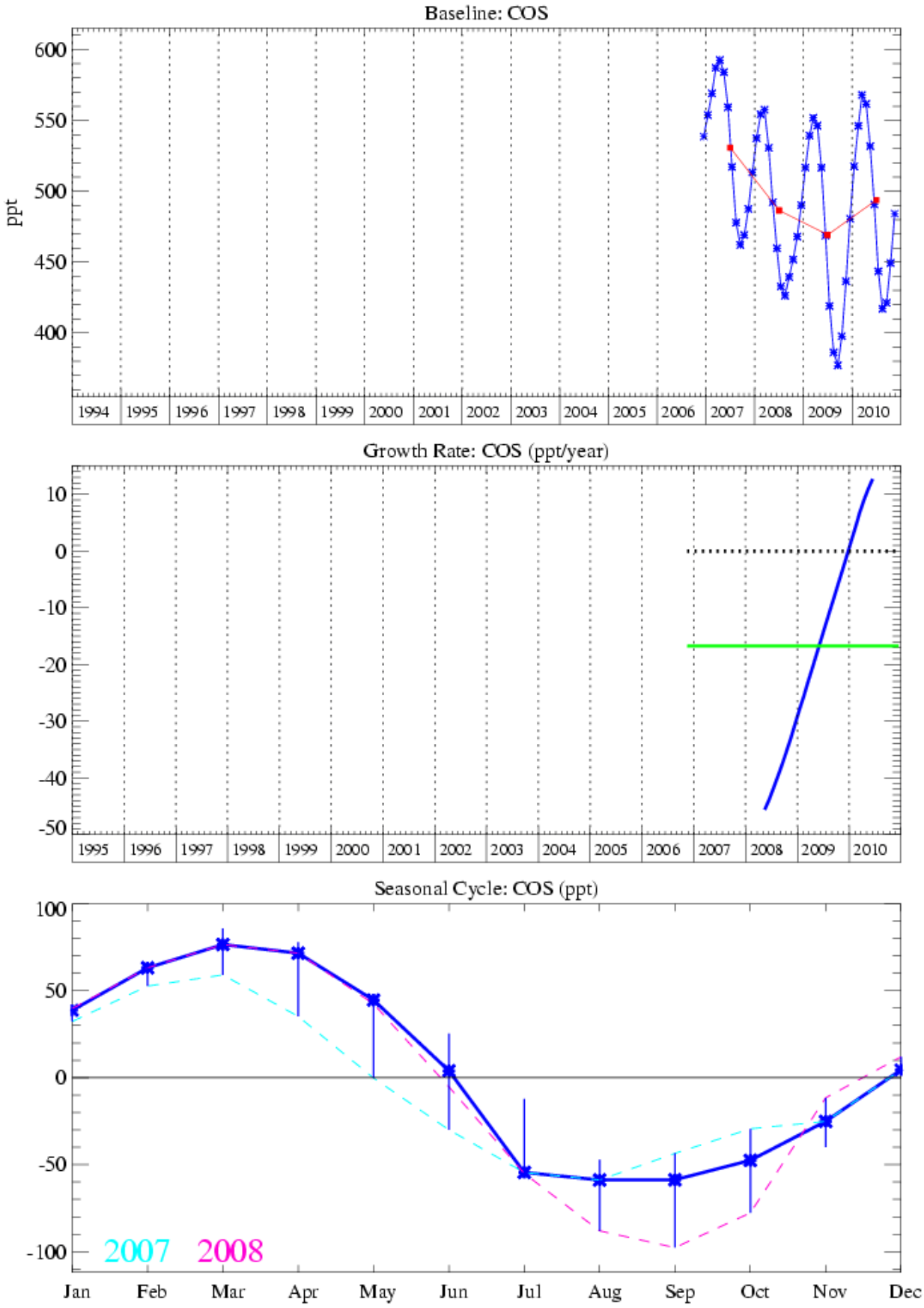

Figure 52: COS: Monthly (blue) and annual (red) baseline concentrations (top plot). Annual (blue) and overall average growth rate (green) (middle plot). Seasonal cycle (de-trended) with year to year variability (lower plot).

3.3.9.4 Nitrous oxide (N_2O)

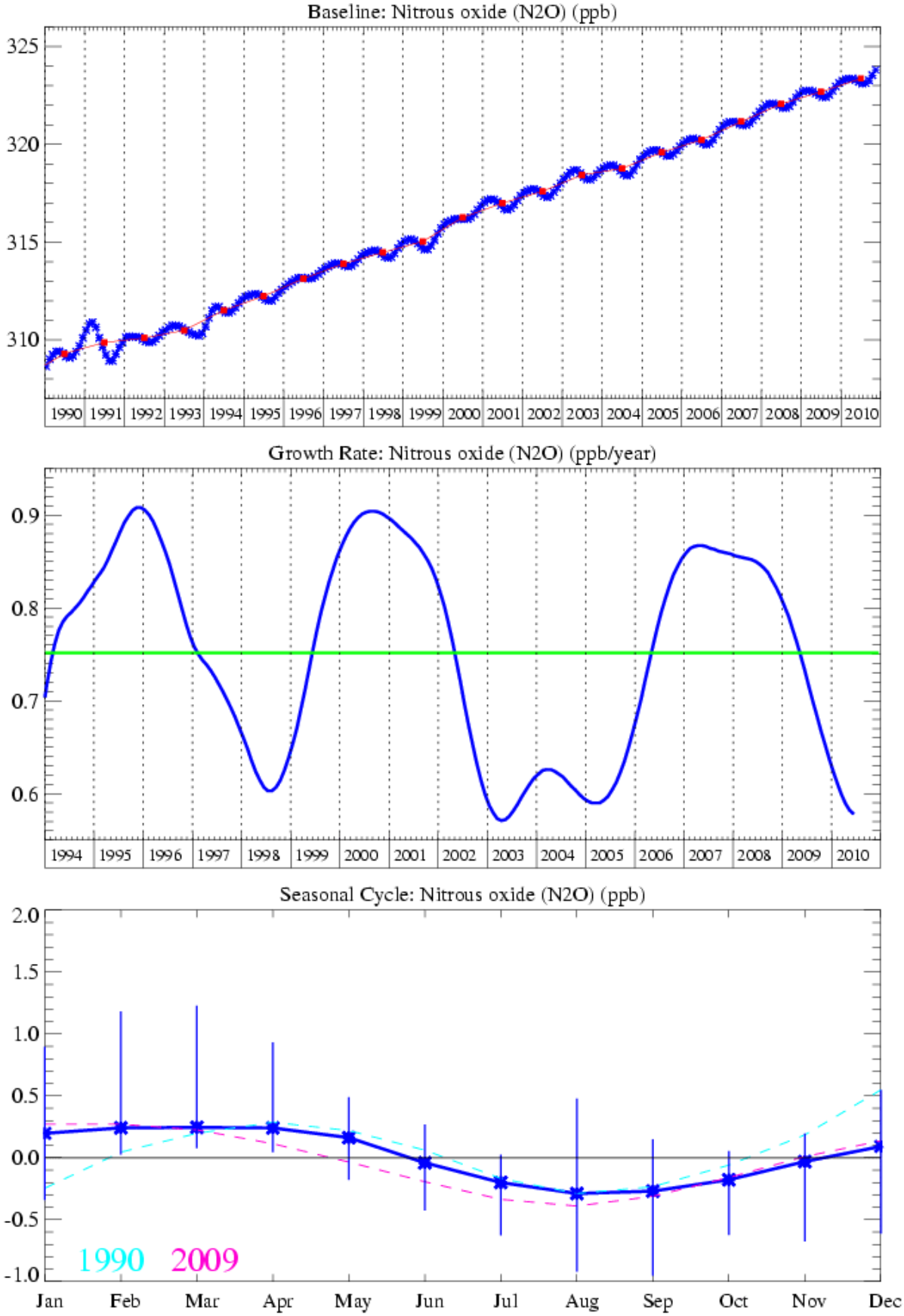

Figure 53: Nitrous oxide: Monthly (blue) and annual (red) baseline concentrations (top plot). Annual (blue) and overall average growth rate (green) (middle plot). Seasonal cycle (de-trended) with year to year variability (lower plot).

3.3.9.5 Ozone (O_3)

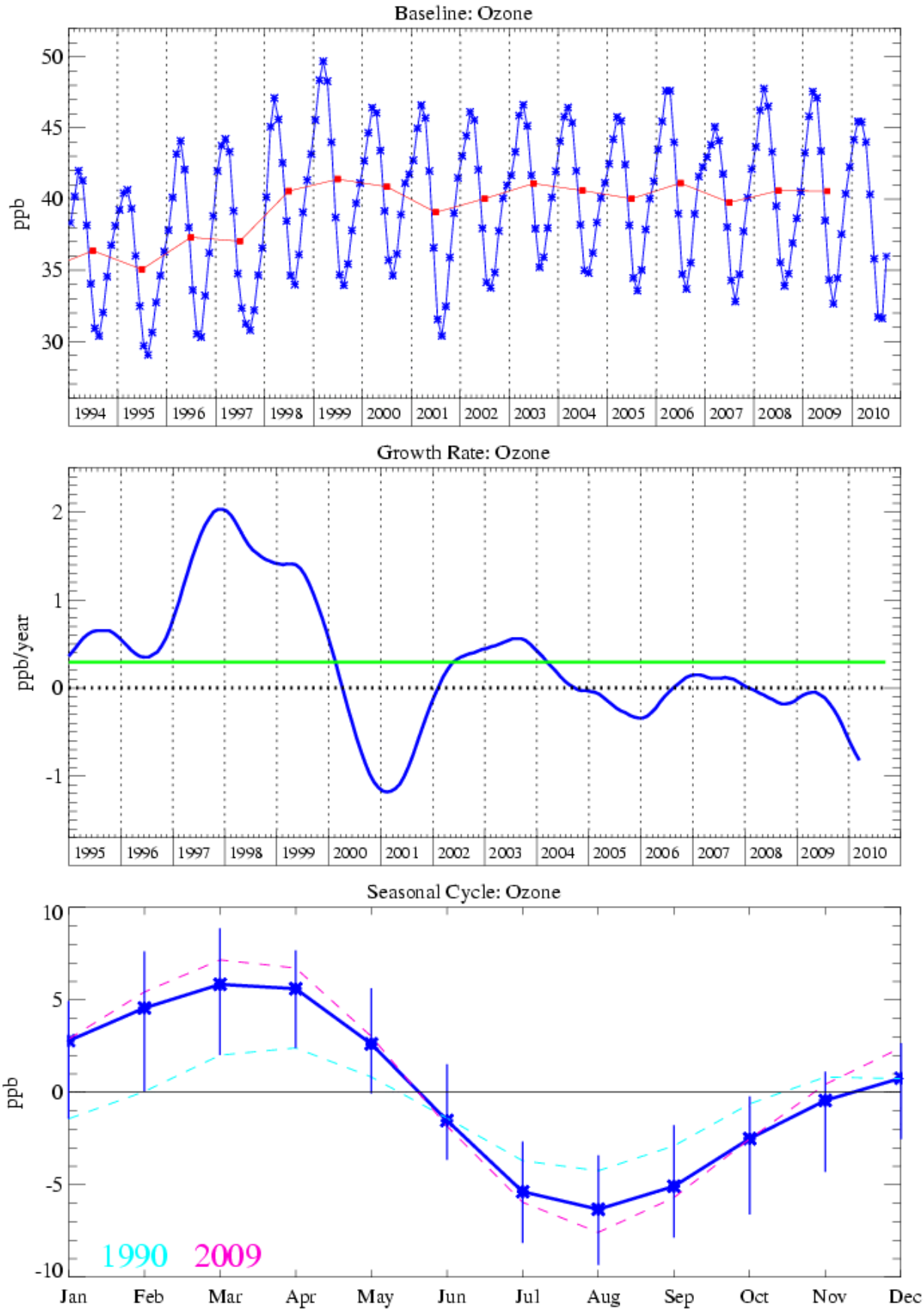

Figure 54: Ozone: Monthly (blue) and annual (red) baseline concentrations (top plot). Annual (blue) and overall average growth rate (green) (middle plot). Seasonal cycle (de-trended) with year to year variability (lower plot).

3.3.9.6 Hydrogen

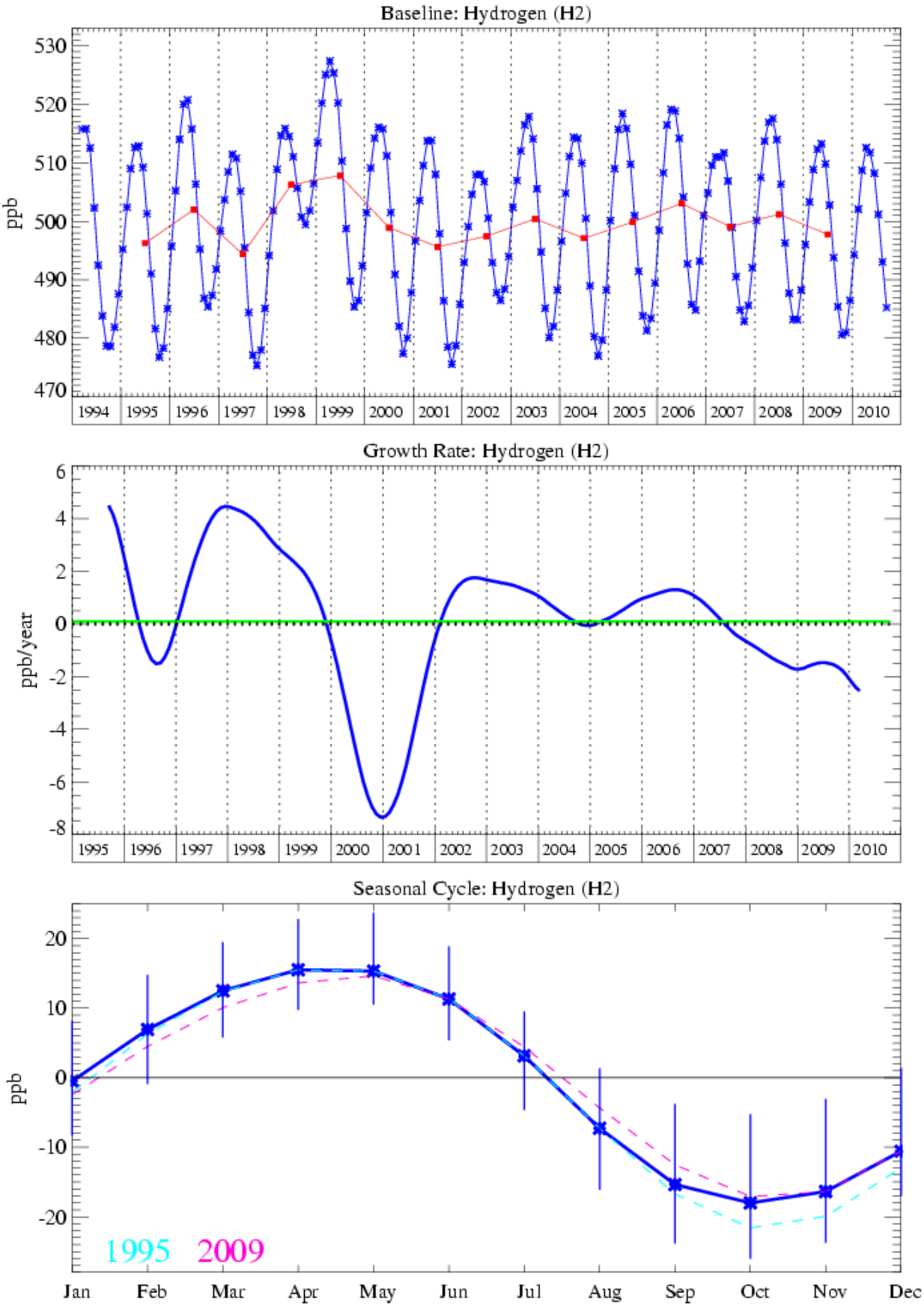

Figure 55: Hydrogen: Monthly (blue) and annual (red) baseline concentrations (top plot). Annual (blue) and overall average growth rate (green) (middle plot). Seasonal cycle (de-trended) with year to year variability (lower plot).